

QUANTUM GRAPHS AND THEIR RESONANCE PROPERTIES

J. Lipovský¹

*Department of Physics, Faculty of Science, University of Hradec Králové,
Rokitanského 62, 500 03 Hradec Králové, Czechia*

Received 31 December 2016, accepted 23 February 2017

In the current review, we study the model of quantum graphs. We focus mainly on the resonance properties of quantum graphs. We define resolvent and scattering resonances and show their equivalence. We present various results on the asymptotics of the number of resolvent resonances in both non-magnetic and magnetic quantum graphs and find bounds on the coefficient by the leading term of the asymptotics. We explain methods how to find the spectral and resonance condition. Most of the notions and theorems are illustrated in examples. We show how to find resonances numerically and, in a simple example, we find trajectories of resonances in the complex plane. We discuss Fermi's golden rule for quantum graphs and distribution of the mean intensity for the topological resonances.

PACS: 03.65.Ge, 03.65.Nk, 02.10.Ox

KEYWORDS: Quantum graphs, Resonances, Weyl asymptotics, Scattering theory, Fermi's golden rule

Contents

1	Introduction	267
2	Description of the model	272
3	Coupling conditions and their derivation	274
4	Spectrum of a quantum graph	278
4.1	Example: particle on a loop – spectrum	278
5	Resolvent resonances and external complex scaling	280
5.1	Example: a half-line with an appendix – resolvent resonances	282
5.2	Example: triangle with half-lines – resolvent resonances	283
6	Scattering resonances	285
6.1	Example: a half-line with an appendix – scattering resonances	285
6.2	Example: triangle with half-lines – scattering resonances	286

¹E-mail address: jiri.lipovsky@uhk.cz

7	The resonance condition	288
8	The equivalence of resonances	290
9	Effective coupling on a finite graph	291
10	Asymptotics of resonances for non-magnetic graphs	292
10.1	Main theorems	293
10.2	Permutation symmetric coupling	299
10.3	Example with a regular polygon	301
10.4	Size reduction	302
11	Asymptotics of the resonances for magnetic graphs	304
12	Pseudo-orbit expansion for the eigenvalue condition in compact graphs	307
12.1	Example: star graph with three edges	310
13	Pseudo-orbit expansion for the resonance condition	314
13.1	Example: triangle with attached leads – pseudo-orbit expansion	317
14	Method of simplifying the resonance condition by deleting the bonds of the directed graph	320
14.1	Example: two abscissas and two half-lines	322
15	Asymptotics of the resonances – the effective size of a non-Weyl graph	325
16	Numerically finding the resonances	329
17	Trajectories of resonances	331
18	Fermi’s golden rule	335
18.1	Example: two segments and a half-line	345
18.2	Example: five internal edges and two half-lines	347
19	Topological resonances and tails of the integrated distribution for the mean intensity	351
	Acknowledgement	354
A	Appendix: Combinatorial and metric graphs	355
B	Appendix: L^p and Sobolev spaces	356
C	Appendix: Self-adjoint extensions	357
	References	359

1 Introduction

Quantum mechanics is quite an unintuitive theory, in which experience from our common life often fails to describe the results of experiments. However, a mathematical theory based on a few simple axioms gives quite a precise explanation of experimental results. One of the most famous examples is the sequential Stern-Gerlach experiment, where particles with spin $1/2$ are by a non-homogeneous magnetic field split up into two beams with different spin components and spin in different directions is measured (see e.g. chapter 1 in [Sak94]).

Also, waveguides provide an example, where our intuition fails. If a small ball rolls in a bent groove on the table, it continues moving in after the turn. On the other hand, an electron in a bent waveguide behaves differently than the ball in this mechanical example. For certain energies, it “gets stuck” in the curve. More precisely, there are bound states in a bent infinite quantum waveguide, as proven in [EŠ89].

In the present survey, we are interested in a network build from these waveguides (or quantum wires) in the limit where their width approaches zero. This *quantum graph* is quite a simple model which studies the behaviour of a quantum particle on this network. The simplicity of this model allows to exactly solve various problems and therefore discover nontrivial phenomena and better understand them.

First attempts to place a quantum particle to a graph date back to 1930’s (Pauling [Pau36] studied diamagnetic properties of aromatic molecules) and 1950’s (work of Ruedenberg and Scherr [RS53] on π -electron behavior in aromatic molecules). There are three electrons present for each carbon atom in the molecule of naphthalene. Two of them are σ -electrons, which are responsible for bonds between the carbon atoms and they therefore form two hexagons with one joint edge. The remaining one π electron can move through the whole structure in the effective potential. In the simplified model, the π electrons move only in the edges which connect two neighbouring carbon atoms, i.e. the corresponding quantum graph. The model of quantum graphs has been developed mainly in the last thirty years. Relations to various areas of physics have been established; the quantum graphs can be used e.g. for describing photonic crystals, carbon nano-structures, thin waveguides or some problems in dynamical systems.

The metric graph is equipped with a second order differential operator (acting as $-\frac{d^2}{dx^2}$), which is the quantum Hamiltonian in a certain set of units. One can add an electric potential $V(x)$ on the internal edges of the graph (in this review we will not consider this case) or consider a magnetic Hamiltonian (acting as $-\left(\frac{d}{dx} + iA_j(x)\right)^2$) on the internal edges of the graph. One can show (see e.g. [EL11]) that the magnetic Hamiltonian is equivalent to a non-magnetic Hamiltonian with changed coupling conditions. Magnetic Hamiltonians on quantum graphs were studied e.g. in [Pan06, GG08, BW14, Ber13, EM15, Exn97, Kur11, EL11]. In this review, attention is paid to magnetic quantum graphs in Section 11.

From a mathematical point of view, the model of quantum graphs is quite simple – it is a set of ordinary differential equations. Hence, it can be used as a toy model for various notions. For instance, it has been used for the study of quantum chaos; see e.g. two pioneering articles [KS97, KS99a], the paper [GS06] or the study [BBK01], where spectral statistics of quantum graphs is compared to the previously known chaotic two-dimensional system of Šeba billiard [Šeb90].

Effects of disorder on the stability of the absolutely continuous spectra were studied e.g.

in [ASW06a, ASW06b]. This topic is closely related to so-called *Anderson localization*, where random perturbation causes that localized states arise at the edges of absolutely continuous spectra. Again, due to their relative simplicity, quantum graphs can be used to study these effects.

The coupling conditions used in this review were defined in the papers [KS99b, KS00, Har00] and previously in a more general form in the book [GG91]. For quantum graphs also the number of nodal domains can be studied (see e.g. papers [GSW04, Ban14, OB12]).

Another interesting problem is the question of isospectrality. Famous Kac's question "Can one hear a shape of a drum?" can be rephrased also for quantum graphs as "Can one hear a shape of a graph?". This means if there exist two different graphs with the same spectra or not. (It is easy to show that pairs of such graphs exist if one allows for general coupling; for a more non-trivial setting we assume standard coupling at the vertices – continuity of the functional value and sum of the outgoing derivatives being equal to zero.) It was formerly established that there exist pairs of isospectral combinatorial graphs. For quantum graphs, existence of pairs of graphs with the same spectrum was proven e.g. in [vBe01, GS01, BPB09]. On the other hand, Gutkin and Smilansky [GS01] also show that for graphs with rationally independent edges, which are strongly coupled (i.e., there are no zeros in the vertex-scattering matrices defined in Section 12) and do not have loops (edges starting and ending at one vertex) and multiple edges between a given pair of the vertices, the spectrum is unique.

For a more detailed introduction to quantum graphs and more examples of their usage, we refer the reader to the book by Berkolaiko and Kuchment [BK13], papers [Kuc04, Kuc05, Kuc08] or Chapter 17 of the book [BEH08]. There exist generalizations of quantum graphs, we mention the hedgehog manifolds, where to a Riemannian manifold half-lines are attached. The reader can find more details in the publications [BEG03, BG03, EŠ97, ETV01, Kis97, EL13]. Hamiltonians on "fat" graphs can be also considered and convergence to quantum graphs is studied. This "fat" graph is some neighbourhood of a metric graph and, of course, corresponding partial differential equations should be solved to find its spectral and resonance properties. For results on convergence of "fat" graphs to quantum graphs we refer to the book [Pos12] or a series of papers by Exner and Post [EP05, EP07, EP09, EP13]. These results show that quantum graphs are feasible approximations of graph-like structures made from quantum wires.

Another generalization of quantum graphs are so-called "leaky" graphs where tunneling between nearby edges is allowed (see review [Exn07] and references therein). In this model the spectral problem

$$-\Delta u = \alpha(x)\delta(x - \Gamma)u + \lambda u$$

is considered, where $\delta(x - \Gamma)$ is a delta distribution supported on the metric graph Γ , $\alpha(x)$ is the coefficient giving strength of the interaction, λ is the spectral parameter and u is the wavefunction in two or three dimensions.

Aside from the spectrum of quantum graphs, we can study transport properties of this model. In the current review, we define resonances and introduce some of their properties, which we illustrate in simple examples. By resonances we mean complex points in the energy plane. The resonances can be obtained by the method of external complex scaling developed in 1970's by Aguilar, Baslev and Combes, see pioneering works [AC71, BC71, Si79]. Its main idea is that functions (generalized eigenfunctions for a resonance) which were not square integrable become after transformation square integrable. Therefore, resonances may be obtained as eigenvalues of a certain non-self-adjoint operator (scaled Hamiltonian). For quantum graphs it was applied

in [EL07] to obtain equivalence of resolvent and scattering resonances, which is in a more general setting described in [EL13] and this review.

Resonances appear in various branches of physics; we can find them in acoustics, mechanics, in electrical circuits or particle physics. In quantum physics we can look at them as certain generalization of the notion of eigenvalues; the main difference is that corresponding generalized eigenfunctions are not necessarily square integrable. We may also further look at the dynamics of the states. Eigenvalues of the Hamiltonian describe bound states of the system. These states exist forever if they are not perturbed, their probability density is constant in time, only the phase of the eigenfunction may change. For a resonance $E_n = E_{nR} + iE_{nI}$ with a non-trivial imaginary part $E_{nI} < 0$ the situation is different. The time evolution of the generalized wavefunction $u_n(x, t)$ is given by

$$u_n(x, t) = e^{-itH} u_n(x, 0) = e^{-itE_n} u_n(x, 0) = e^{-it(E_{nR} + iE_{nI})} u_n(x, 0),$$

where H denotes the time-independent Hamiltonian and the second equality is given by time-independent Schrödinger equation. For another way how to obtain the time dependence of the generalized eigenfunctions see Section 6.

The probability of survival of the resonance state beyond time t is then

$$p(t) = \frac{|u_n(x, t)|^2}{|u_n(x, 0)|^2} = \frac{|e^{-itE_{nR}} e^{tE_{nI}}|^2}{1} = e^{-2|E_{nI}|t}.$$

So the resonance state exponentially decays in time and the rate of decay is bigger if the resonance is farther from the real axis. Therefore, resonances with small imaginary parts are from the physical point of view most interesting. (For result on the disappearance of the resonances close to the real axis see e.g. end of Section 19.)

The generalized wavefunction in the energy representation is obtained by the inverse Fourier transform of the generalized wavefunction in the time representation.

$$\begin{aligned} v(x, E) &= \mathcal{F}^{-1} u(x, t) = \frac{1}{\sqrt{2\pi}} \int_0^\infty e^{iEt} u(x, t) dt \\ &= \frac{1}{\sqrt{2\pi}} \int_0^\infty e^{iEt} e^{-iE_{nR}t + E_{nI}t} u(x, 0) dt = \frac{1}{\sqrt{2\pi}i} \frac{1}{E_{nR} - E + iE_{nI}}. \end{aligned}$$

Sometimes instead of E_{nI} the symbol $-\Gamma_n/2$ is used and the notion is denoted as a half-width of the resonance. We do not use this notation in order not to confuse the reader, since the notation Γ is later used for a graph. The probability density of the resonance with energy E is proportional to the square of the absolute value of $v(x, E)$ and hence we can obtain that the probability density is

$$-\frac{1}{\pi} \frac{E_{nI}}{(E - E_{nR})^2 + E_{nI}^2} dE.$$

This distribution is usually denoted as Breit-Wigner, Cauchy or Lorentz distribution and is typical for the shape of the resonance in many branches of physics. More details on this interpretation of resonances can be found e.g. in [DZ, Zwo99].

Spectral and resonance properties of quantum graphs can be directly measured; the quantum graph is simulated by a microwave network using coaxial cables. Most of the measurements were

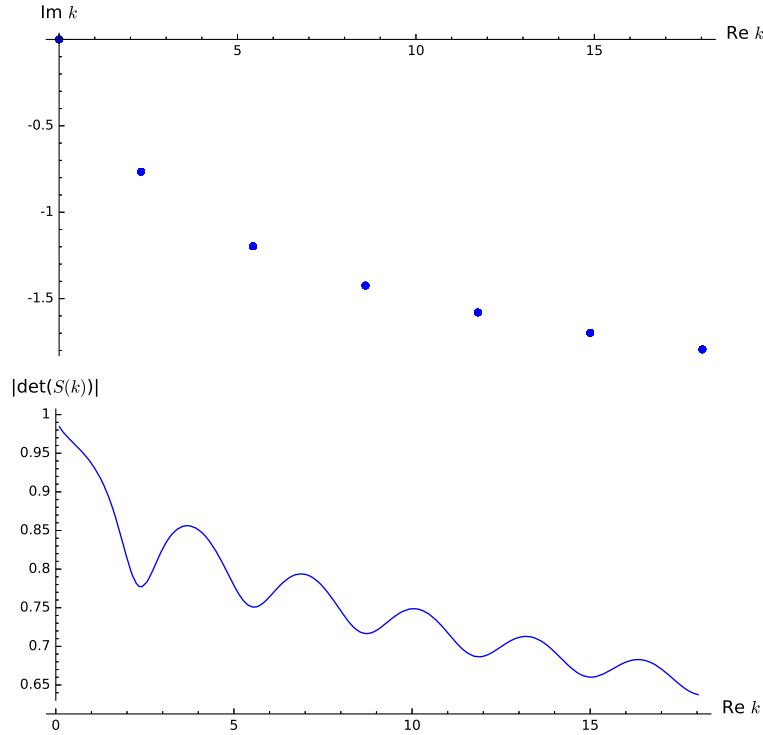


Fig. 1.1. In the upper figure several resonances for the example in Subsections 5.1 and 6.1, $l = 1$, $\alpha = 1$ are shown. In the lower figure there is the absolute value of the determinant of the scattering matrix for the curve $k = k_{\text{R}} + 0.05i\sqrt{k_{\text{R}}}$ depending on k_{R} . We can see that minima of this function approximately correspond to the real parts of the resonances. The figure is not adjusted to the actual frequency in the experiment; here speed of light is equal to 2π .

done by the group of L. Sirko from Polish Academy of Sciences (see e.g. [HBP⁺04, HTB⁺05, HŠS09, LBH⁺11, LBH⁺12, HLB⁺12, LBS⁺13, LSB⁺14]). In the measurement, the values of the coefficients of the scattering matrix can be found and therefore, its determinant can be computed. If we plot the absolute value of the determinant of the scattering matrix on the frequency (which is proportional to the real part of k , where k^2 is the energy), we can find the real parts of the resonances as valleys (local minima) of this graph of this dependence.

In Figure 1.1 we show a model which illustrates how resonances in microwave graphs are found. We consider a certain example of a quantum graph, which is in detail described in Subsections 5.1 and 6.1. In the upper figure, there are resonances plotted as blue dots in the complex plane. The lower figure shows the absolute value of the determinant of the scattering matrix (in this case determinant is not needed, since the scattering matrix is only a number) on the real part of k if losses are taken into account. It follows from the scattering theory that the scattering matrix is unitary for real k , hence its determinant is 1 in modulus. The losses are described by taking $k = k_{\text{R}} + ci\sqrt{k_{\text{R}}}$ with $c > 0$. Since in the upper half-plane there are zeros of the determinant of the scattering matrix at the positions which correspond to negatively taken poles of the scattering

matrix (resonances) and since the resonances are symmetric with respect to the imaginary axis, we find that zeros of the scattering matrix are reflections of its poles with respect to the real axis. If we choose the real part of k close to the real part of the resonance, we come closer to the zero of the scattering matrix and the determinant in modulus decreases.

The resonances in quantum graphs were studied in [CdVT, DEL10, EL07, EL10, EL11, EL, EŠ94, Exn97, Exn13, GSS13, Lip15, Lip16, LZ16]. For a general theory of resonances suitable not only for quantum graphs we refer the reader to the book in preparation by Dyatlov and Zworski [DZ]. There is a large bibliography on scattering from obstacles; without trying to list all of them we refer, e.g., to [Mel84, Chr08, DH12, LV12, FL90, Jin14].

The current review is not intended as an exhaustive summary of all results in quantum graphs; it focuses mainly on the resonance properties of graphs with attached half-lines. Most of the results for compact quantum graphs are shown (or at least mentioned) in the recent book by Berkolaiko and Kuchment [BK13]. This review can be viewed as its complement for non-compact graphs. It is intended for motivated undergraduate and postgraduate students and young researchers willing to study the resonance properties of quantum graphs. Although main concepts for quantum graphs are explained in the text (see Section 2 and the following sections or Appendices A and B), we recommend mentioned book [BK13], introductory papers [Kuc04, Kuc05, Kuc08] or Chapter 17 of the book [BEH08] for readers who are not very familiar with quantum graphs. To have a deeper understanding of studied phenomena, the reader should be familiar with the spectral theory of linear operators, see book [BEH08] or a series of four books by Reed and Simon [RS75a, RS75b, RS79, RS78]. Basics of the theory of self-adjoint extensions are summarized in Appendix C. Methods used in this review can be useful for scientists studying mathematical aspects of resonances in different systems (e.g. scattering on obstacles, resonances for point interactions, etc.). If the reader is more interested in the general theory of resonances, we recommend the book in preparation [DZ].

In this review the results of papers [KS99b, Har00, EL07, DP11, DEL10, EL10, EL11, Lip16, Lip15, LZ16, GSS13, CdVT] are presented with in many cases simplified and improved proofs. In the Section 2 the model of quantum graphs is described and in Section 3 the coupling conditions are studied (with the use of results of papers [KS99b, Har00]). In Section 4 spectrum of a graph is found in a simple example. Sections 5 and 6 introduce resolvent and scattering resonances and describe their main properties. In Sections 7 and 8 the resonance condition is found and the equivalence to the two types of resonances is established (result of [EL07], generalized in [EL13]). In Section 9 effective coupling on a finite graph is introduced, which is used in the following sections. Later, results for asymptotics of the number of resonances for non-magnetic graphs (Section 10, results of [DP11, DEL10]) and magnetic graphs (Section 11, results of [EL11]) are shown. The method of pseudo-orbit expansion is introduced in Sections 12 and 13 for finding the spectral (see [BHJ12]) or resonance condition (see [Lip16, Lip15]). This method is used in Section 15 to find more results on the asymptotics of the number of resonances (results of [Lip16]). In Sections 16 and 17 we show how to find numerically the positions and trajectories of resonances if lengths of the edges are changed (similarly to [EL10]). In Section 18 Fermi's golden rule for quantum graphs is found (the result of [LZ16], which is written with significantly more details than the original paper) and in Section 19 results of [GSS13, CdVT] on the topological resonances are introduced. The appendices introduce the definitions and summarize the main results for combinatorial and metric graphs, spaces of functions and the theory of self-adjoint extensions.

2 Description of the model

First, we consider a metric graph Γ . It consists of the set of vertices \mathcal{X}_j , the set of N internal edges \mathcal{E}_i of positive lengths ℓ_j and set of M infinite edges \mathcal{E}_e – half-lines which can be parametrized by $[0, \infty)$. The Hilbert space of our system consists of functions with components square integrable on each edge

$$\mathcal{H} = \bigoplus_{i=1}^N L^2((0, \ell_i)) \oplus \bigoplus_{i=1}^M L^2((0, \infty)).$$

The vector in this Hilbert space is

$$\psi = (\psi_1, \dots, \psi_N, \psi_{N+1}, \dots, \psi_{N+M})^T.$$

The whole structure is equipped with a second order operator, the Hamiltonian which acts as $-\frac{d^2}{dx^2} + V(x)$ with a bounded potential $V(x)$. The potential is located only on the internal edges. This Hamiltonian corresponds to a simplified Hamiltonian of a quantum particle $-\frac{\hbar^2}{2m} \frac{d^2}{dx^2} + V(x)$; we have chosen the set of units in which $\hbar = 1$ and $m = 1/2$. For the purposes of this paper, we will assume potential equal to zero. The domain of our Hamiltonian consists of functions in Sobolev space on the graph $W^{2,2}(\Gamma)$ (which is an orthogonal sum of Sobolev spaces on the edges). The function belongs to Sobolev space $W^{k,p}(e)$ on the edge e if its weak derivatives up to the order k belong to $L^p(e)$. Moreover, functions from the domain of the Hamiltonian must satisfy the coupling conditions at the vertices

$$(U_j - I)\Psi_j + i(U_j + I)\Psi'_j = 0, \quad (2.1)$$

where U_j is a $d_j \times d_j$ matrix, where d_j is degree (see Appendix A for definition) of j -th vertex, I is $d_j \times d_j$ identity matrix, Ψ_j is the vector of limits of functional values from various edges to the j -th vertex and, similarly, Ψ'_j is the vector of outgoing derivatives.

The following construction can be used to describe easily the coupling on the whole graph. One joins all the vertices into one and obtains one-vertex “flower-like” graph (see Figure 2.1). The coupling on the whole graph can be described by only one big unitary $(2N+M) \times (2N+M)$ matrix U [Kuc08, EL10] with coupling condition

$$(U - I)\Psi + i(U + I)\Psi' = 0, \quad (2.2)$$

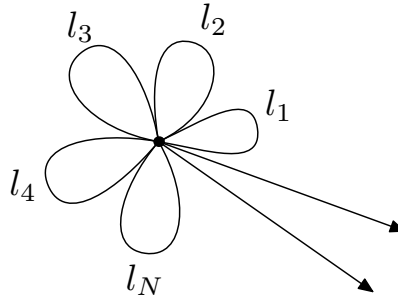


Fig. 2.1. A flower-like graph. Reproduced from [EL10].

This matrix describes not only the coupling but also the topology of the graph. The flower-like model with eq. (2.2) will be equivalent to the multivertex graph with eq. (2.1) if we choose the matrix U to be block-diagonal in the bases corresponding to the topology of the graph with blocks U_j .

3 Coupling conditions and their derivation

In this section, we prove that the equation (2.2) describes all possible self-adjoint Hamiltonians (see Appendix C) defined in the previous section.

Definition 3.1 Let L be an operator in the Hilbert space \mathcal{H} with the scalar product (\cdot, \cdot) and let its domain $D(L)$ be dense in \mathcal{H} . By its adjoint we denote the operator L^* , which acts as $L^*y = y^*$, where $(y, Lx) = (y^*, x)$ for all $x \in D(L)$. The domain of L^* consists of all y for which the above relation holds. The operator is symmetric if $(y, Lx) = (Ly, x)$ and self-adjoint if $L = L^*$, i.e. the domains of L and L^* coincide. A self-adjoint operator L_1 is called self-adjoint extension of L if $D(L) \subset D(L_1)$ and $L = L_1$ on $D(L)$.

There has been a theory developed how to construct self-adjoint extensions, but we will not reproduce it here. It can be found e.g. in the textbooks [BEH08, RS75b]. We define a symmetric operator H_0 which acts as $-\frac{d^2}{dx^2} + V_j(x)$ on the j -th edge of the flower-like graph, with the domain consisting of functions in $W^{2,2}(\Gamma)$ for which both functional value and the derivative vanish at the central vertex. The domain of its adjoint is $W^{2,2}(\Gamma)$ without any coupling conditions at the central vertex.

We study the following skew-Hermitian form

$$\Omega(\phi, \psi) = -\overline{\Omega(\psi, \phi)} = (H_0^* \phi, \psi) - (\phi, H_0^* \psi)$$

with the domain $D(H_0^*)$. Using integration by parts one can find that

$$\begin{aligned} \Omega(\phi, \psi) &= \sum_{j=1}^{N+M} \int_{e_j} \left[-\bar{\phi}_j''(x) \psi_j(x) + V_j(x) \bar{\phi}_j(x) \psi_j(x) - \right. \\ &\quad \left. - (-\bar{\phi}_j(x) \psi_j''(x) + V_j(x) \bar{\phi}_j(x) \psi_j(x)) \right] dx = \\ &= \sum_{j=1}^{N+M} \int_{e_j} \left(-\bar{\phi}_j''(x) \psi_j(x) + \bar{\phi}_j(x) \psi_j''(x) \right) dx = \\ &= \sum_{j=1}^{N+M} \left(-\bar{\phi}_j'(0) \psi_j(0) + \bar{\phi}_j(0) \psi_j'(0) \right) + \sum_{j=1}^N \left(\bar{\phi}_j'(l_j) \psi_j(l_j) - \bar{\phi}_j(l_j) \psi_j'(l_j) \right) - \\ &\quad - \sum_{j=1}^{N+M} \int_{e_j} \left(-\bar{\phi}_j'(x) \psi_j'(x) + \bar{\phi}_j(x) \psi_j'(x) \right) dx = \\ &= \Phi^* \Psi' - \Phi'^* \Psi = \omega([\Phi], [\Psi]) = ([\Phi], \mathcal{J}[\Psi])_{\mathbb{C}^{4N+2M}}. \end{aligned}$$

where e_j , $j = 1, \dots, N$ are internal edges and $j = N + 1, \dots, N + M$ are external edges, $\mathcal{J} = \begin{pmatrix} 0 & I \\ -I & 0 \end{pmatrix}$ and vectors $[\Phi] = (\Phi, \Phi')^T$, $[\Psi] = (\Psi, \Psi')^T$ contain limits of functional values and derivatives in the central vertex. The star in the last line of the equation denotes transposition and complex conjugation.

Definition 3.2 Let W be a subspace of \mathbb{C}^{4N+2M} . We denote by $W^\perp = \{[\Psi] \in \mathbb{C}^{4N+2M} : \omega([\Psi], [\Phi]) = 0, \forall [\Phi] \in W\}$. We call the subspace W maximal isotropic or a Lagrangian plane if $W^\perp = W$.

The self-adjoint extensions of a symmetric operator are closely related to Lagrangian planes of a Hermitian symplectic space. The boundary form of a symmetric operator (which is in our case $\omega([\Psi], [\Phi])$) is a Hermitian symplectic form (i.e. satisfies $\omega([\Psi], [\Phi]) = -\omega([\Phi], [\Psi])$) and the extensions of a symmetric operator can be identified with the isotropic subspaces (these are the subspaces for which $W \subset W^\perp$ holds) in the associated Hermitian symplectic space (it is a vector space over \mathbb{C} which has defined on it a non-degenerate Hermitian symplectic form). Hence maximal isotropic subspaces (Lagrangian planes) can be identified with domains of self-adjoint extensions of a symmetric operator.

Now we prove the theorem on the coupling conditions. It has been independently proven by Kostykin and Schrader [KS99b] and Harmer [Har00]. In the proof of the theorem, we use the simple argument from [FT00] originally based on physical reasons.

Theorem 3.3 *All self-adjoint extensions of the operator H_0 can be uniquely parametrized by the set of unitary matrices U of rank $(2N + M) \times (2N + M)$ by the equation (2.2).*

Proof: We will prove that the subspace is a Lagrangian plane if and only if it is parametrized by the equation (2.2). First, we prove that every Lagrangian plane is parametrized by equation (2.2). Necessary condition for $\omega([\Phi], [\Psi]) = 0$ for all $[\Phi], [\Psi] \in W$ is $\omega([\Phi], [\Phi]) = 0$ for all $[\Phi] \in W$. Let us now compute the following expression

$$\begin{aligned} & \|\Phi + i\Phi'\|_{\mathbb{C}^{2N+M}}^2 - \|\Phi - i\Phi'\|_{\mathbb{C}^{2N+M}}^2 = \\ & = (\Phi + i\Phi', \Phi + i\Phi')_{\mathbb{C}^{2N+M}} - (\Phi - i\Phi', \Phi - i\Phi')_{\mathbb{C}^{2N+M}} = \\ & = \Phi^*\Phi - i\Phi'^*\Phi + i\Phi^*\Phi' + \Phi'^*\Phi' - \Phi^*\Phi - i\Phi'^*\Phi + i\Phi^*\Phi' - \Phi'^*\Phi' = \\ & = 2i[\Phi^*\Phi' - \Phi'^*\Phi] = 2i\omega([\Phi], [\Phi]) = 0. \end{aligned}$$

Hence the norm of the vectors $\Phi + i\Phi'$ and $\Phi - i\Phi'$ must be the same and therefore these vectors must be related by a unitary matrix U . From the equation $U(\Phi + i\Phi') = \Phi - i\Phi'$ the equation (2.2) follows.

Now we prove that every subspace parametrized by (2.2) is a Lagrangian plane. We notice that the form ω can be rewritten as

$$\begin{aligned} \omega([\Phi], [\Psi]) &= (\Phi^*, \Phi'^*) \begin{pmatrix} 0 & I \\ -I & 0 \end{pmatrix} \begin{pmatrix} \Psi \\ \Psi' \end{pmatrix} = \\ &= (\Phi^*, \Phi'^*) \begin{pmatrix} V^{-1} & 0 \\ 0 & V^{-1} \end{pmatrix} \begin{pmatrix} V & 0 \\ 0 & V \end{pmatrix} \begin{pmatrix} 0 & I \\ -I & 0 \end{pmatrix} \cdot \\ &\quad \cdot \begin{pmatrix} V^{-1} & 0 \\ 0 & V^{-1} \end{pmatrix} \begin{pmatrix} V & 0 \\ 0 & V \end{pmatrix} \begin{pmatrix} \Psi \\ \Psi' \end{pmatrix} = \\ &= ((V\Phi)^*, (V\Phi')^*) \begin{pmatrix} 0 & I \\ -I & 0 \end{pmatrix} \begin{pmatrix} V\Psi \\ V\Psi' \end{pmatrix}, \end{aligned}$$

where V is a $(2N + M) \times (2N + M)$ unitary matrix. Since we can rewrite the equation (2.2) as

$$V^{-1}(D - I)V\Psi + iV^{-1}(D + I)V\Psi' = 0,$$

where D is a $(2N + M) \times (2N + M)$ diagonal unitary matrix, it suffices to prove it only for diagonal matrices. If D does not have eigenvalues -1 , we obtain from the previous equation $V\Psi' = i(D + I)^{-1}(D - I)V\Psi$, $(V\Phi')^* = (V\Phi)^*(-i)(D^* - I)(D^* + I)^{-1}$ and consequently

$$\omega([\Phi], [\Psi]) = ((V\Phi)^*, (V\Phi)^*) \begin{pmatrix} 0 & i(D + I)^{-1}(D - I) \\ i(D^* - I)(D^* + I)^{-1} & 0 \end{pmatrix} \begin{pmatrix} V\Psi \\ V\Psi \end{pmatrix}.$$

From the unitary properties of D we have

$$(D + I)(D^* - I) + (D - I)(D^* + I) = DD^* - D + D^* - I + DD^* - D^* + D - I = 0$$

and hence for no eigenvalue -1

$$(D^* - I)(D^* + I)^{-1} + (D + I)^{-1}(D - I) = 0.$$

Therefore, the form ω vanishes

$$\omega([\Phi], [\Psi]) = iV\Phi^*[(D^* - I)(D^* + I)^{-1} + (D + I)^{-1}(D - I)]V\Psi = 0$$

for every $[\Phi], [\Psi]$ satisfying (2.2). If D has eigenvalues -1 , from the coupling condition follows that entries of $V\Psi$ and $V\Phi$ corresponding to these eigenvalues vanish. In the subspace corresponding to other eigenvalues, previous argument can be used. Q.E.D.

Remark 3.4 Condition $\omega([\Phi], [\Phi]) = \Phi^*\Phi' - \Phi'^*\Phi = 0$ has a simple physical interpretation. It means that the probability current $j = \frac{\hbar}{2mi}(\bar{\phi}\phi' - \bar{\phi}'\phi)$ through the central vertex is conserved. We could have used in the difference $\|\Phi + i\ell\Phi'\|^2 - \|\Phi - i\ell\Phi'\|^2$ with $\ell \in \mathbb{R}$ in the proof and obtain the coupling condition $(U - I)\Psi + i\ell(U + I)\Psi' = 0$, but this equation can be related to an equivalent form $(U_1 - I)\Psi + i(U_1 + I)\Psi' = 0$ and hence does not add any degree of freedom. The choice of ℓ just fixes the length scale.

Remark 3.5 If we start from the flower-like graph and obtain coupling condition (2.2), we have for the corresponding multivertex graph coupling conditions which allow for “hopping” particle between vertices. If we want to get rid of it, we need to choose the coupling matrix U block diagonal with respect to the topology of the graph.

Now we describe the most common coupling conditions.

- **permutation symmetric coupling conditions**

This type of the condition is symmetric to the change of any two leads emanating from the vertex. The unitary matrix is $U = aJ + bI$, where J has all entries equal to one and a and b are complex constants. Using $J^2 = nJ$ (n is a degree of a vertex) and $JJ = IJ = J$ and unitarity of the coupling matrix we have

$$|a|^2nJ + b\bar{a}J + a\bar{b}J + |b|^2I = I. \tag{3.1}$$

From this we can obtain that $|b| = 1$ and $|an + b| = 1$. The first relation obviously follows from the previous equation, the proof of the second one is following

$$|an + b|^2 = |a|^2n^2 + \bar{a}bn + a\bar{b}n + |b|^2 = n(|a|^2n + \bar{a}b + a\bar{b}) + 1 = 1,$$

the term in the parentheses is zero, since the term by J in eq. (3.1) must be zero.

- **δ -coupling**

It is a special case of permutation symmetric coupling, with the conditions

$$f(\mathcal{X}) \equiv f_i(\mathcal{X}) = f_j(\mathcal{X}), \quad \text{for all } i, j \in \{1, \dots, n\}$$

$$\sum_{j=1}^n f'_j(\mathcal{X}) = \alpha f(\mathcal{X}),$$

where f denotes the wavefunction at the vertex \mathcal{X} and f' its outgoing derivative. The unitary matrix is $U = \frac{2}{n+i\alpha}J - I$.

- **standard (Kirchhoff, free, Neumann) conditions**

This condition is the special kind of δ -condition for $\alpha = 0$, i.e. functional value is continuous in the vertex and sum of outgoing derivatives is equal to 0. It is the most physical one since the particle moves freely through the vertex. The name Kirchhoff is not a good choice since for all self-adjoint coupling conditions the probability current is conserved. The unitary matrix is $U = \frac{2}{n}J - I$.

- **Dirichlet conditions**

In this case all functional values are zero. The unitary matrix is $U = -I$.

- **Neumann conditions**

For this condition all the derivatives are zero. The unitary matrix is $U = I$.

4 Spectrum of a quantum graph

First, we recall some definitions from the spectral theory of linear operators, more details can be found in the standard textbooks, e.g. [BEH08, RS75a].

Definition 4.1 *Let T be a closed linear operator from a Banach space \mathcal{X} to itself. Then the resolvent set $\rho(T)$ is a set of those $\lambda \in \mathbb{C}$ for which $T - \lambda \text{id}$, where id is identity operator, is a bijection with bounded inverse. If T is a closed operator in a Hilbert space \mathcal{H} , we define the resolvent set as the set of those $\lambda \in \mathbb{C}$ for which $T - \lambda \text{id}$ is a bijection of $D(T)$ onto \mathcal{H} with a bounded inverse. The set $\sigma(T) = \mathbb{C} \setminus \rho(T)$ is called the spectrum of T . Such v for which $Tv = \lambda v$ for some $\lambda \in \mathbb{C}$ is called eigenvector and the corresponding λ is eigenvalue. The set of all eigenvalues is called the point spectrum σ_p . For the rest of the spectrum holds that $T - \lambda \text{id}$ is injective but $\text{Ran}(T - \lambda \text{id}) \neq \mathcal{X}$. This set can be divided into two parts. If $\text{Ran}(T - \lambda \text{id})$ is dense, λ belongs to the continuous spectrum $\sigma_c(T)$. If $\text{Ran}(T - \lambda \text{id})$ is not dense, λ belongs to the residual spectrum $\sigma_r(T)$. It holds $\sigma(T) = \sigma_c(T) \cup \sigma_r(T) \cup \sigma_p(T)$.*

If T is a Hilbert-space operator, we can define essential spectrum $\sigma_{\text{ess}}(T)$; it consists of such $\lambda \in \mathbb{C}$ for which there is a sequence of unit vectors $v_n \in D(T)$ which has no convergent subsequence and satisfies $(T - \lambda)v_n \rightarrow 0$. Its complement $\sigma_d = \sigma \setminus \sigma_{\text{ess}}$ is called discrete spectrum and it consists of isolated eigenvalues of finite multiplicity.

4.1 Example: particle on a loop – spectrum

Now we show an example, how to find the point spectrum of a simple graph. We assume a graph without half-lines with only one edge starting and ending at one vertex (see Figure 4.1). The loop has length ℓ .

We will find the eigenvalues of this problem. The wavefunction on the loop $f(x)$ must satisfy the eigenvalue equation

$$-\frac{d^2}{dx^2}f(x) = \lambda f(x) = k^2 f(x)$$

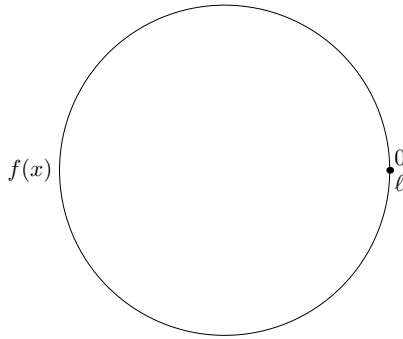


Fig. 4.1. Figure to Subsection 4.1 – loop.

for the eigenvalue $\lambda = k^2$. From the theory of ordinary differential equations we know that the fundamental system of this equation consists of functions $\{e^{ikx}, e^{-ikx}\}$ and the general form of the solutions is therefore the linear combination of the functions in the fundamental system

$$f(x) = a \sin kx + b \cos kx.$$

We must bear in mind that the function must satisfy the coupling condition. If we introduce a vertex on the loop (in Figure 4.1 on the right), both functional value and the derivative must be continuous at this vertex, in other words, we assume standard condition (see Section 3 for definition). Hence we have the conditions

$$\begin{aligned} f(0) = f(\ell) &\Rightarrow b = a \sin k\ell + b \cos k\ell, \\ f'(0) - f'(\ell) = 0 &\Rightarrow ka - ka \cos k\ell + kb \sin k\ell = 0. \end{aligned}$$

The system of these two equations can be written as

$$\begin{pmatrix} \sin k\ell & -(1 - \cos k\ell) \\ k(1 - \cos k\ell) & k \sin k\ell \end{pmatrix} \begin{pmatrix} a \\ b \end{pmatrix} = 0.$$

It is solvable if the determinant of the above matrix is zero. The condition gives

$$0 = k(\sin^2 k\ell + (1 - \cos k\ell)^2) = k(2 - 2 \cos k\ell).$$

Hence we have eigenvalues $\lambda = k^2$ with $k = \frac{2n\pi}{\ell}$, $n \in \mathbb{N}_0$. Eigenvalues have multiplicity two with eigenfunctions $\sin \frac{2n\pi x}{\ell}$, $\cos \frac{2n\pi x}{\ell}$, the only exception is $k = 0$ for which there is only one constant eigenfunction.

5 Resolvent resonances and external complex scaling

In the current and following section, we are interested in defining the resonances properly. By a resonance, we understand a complex number. The physical meaning of this number is following. If the resonance is close to the real axis, the particle sent with the energy corresponding to its real part stays in the central part of the graph longer than for other energies. Its life time is longer, the closer the resonance to the real axis is. There are two main definitions of resonances, resolvent resonances and scattering resonances. Resolvent resonances are poles of the meromorphic continuation of the resolvent $(H - \lambda \text{id})^{-1}$ to the second (unphysical) Riemann sheet. It is more convenient to study the whole problem in the k -plane, where $k^2 = \lambda$. The expression $k = \sqrt{\lambda}$ defines function analytic in the complex plane in λ (energy) with the exception of the cut $(0, \infty)$. To the upper half-plane in k the first (physical) sheet of λ corresponds, while the second (unphysical) sheet corresponds to the lower half-plane in k . The upper edge of the cut of the first sheet is connected to the lower edge of the cut of the second sheet and *vice versa*. The scattering resonances are poles of the continuation of the determinant of the scattering matrix to the second Riemann sheet. The physical meaning of these poles is described in Section 1.

Definition 5.1 *There is a resolvent resonance at k^2 if there is a pole of the meromorphic continuation of the resolvent $(H - k^2 \text{id})^{-1}$ to the second Riemann sheet across the positive real axis. For the operator described in section 2 one can define a resolvent resonance as such k^2 , for which there exists solution of the Schrödinger equation which fulfills the coupling conditions and has the asymptotics $\alpha_j e^{ikx}$ for all half-lines.*

Theorem 5.2 *There are resolvent resonances only for $\text{Im } k \leq 0$ or for $\text{Re } k = 0$ (see figure 5.1).*

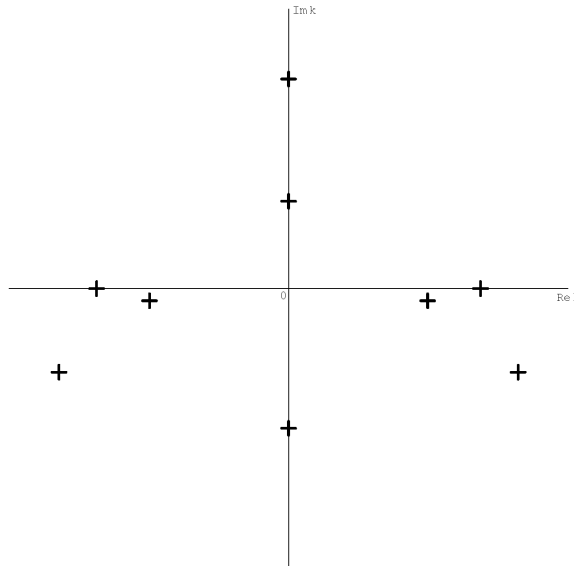


Fig. 5.1. Resolvent resonances are only in the lower halfplane or on the imaginary axis.

Proof: We know that the wavefunction components on the half-lines are $g_j(x) = \alpha_j e^{ikx}$. Let there be a resolvent resonance for $k = k_r + ik_i$ with $k_i > 0$. Then there exists a solution of the Schrödinger equation on the graph with the above behaviour on the half-lines. But the function $g_j(x) = \alpha_j e^{ik_r x} e^{-k_i x}$ is square integrable $\int_0^\infty |g_j(x)|^2 dx < \infty$ and this means that k^2 is an eigenvalue of the Hamiltonian H . This contradicts the fact that the Hamiltonian is self-adjoint, since a self-adjoint Hamiltonian has only real eigenvalues (which corresponds to real or purely imaginary k). Q.E.D.

Resolvent resonances can be effectively studied by the method developed in 1970's by Aguilar, Baslev and Combes [AC71, BC71] called *external complex scaling*. The idea is to perform the transformation

$$U_\theta g(x) = e^{\theta/2} g(e^\theta x).$$

on the external edges, while the internal edges are not scaled. For real θ this transformation is unitary, but it has the desired behaviour for θ with a nontrivial imaginary part. We transform the Hamiltonian H to a non-self-adjoint one and then prove that resolvent resonances are eigenvalues of this non-self-adjoint operator.

Theorem 5.3 *Let $H_\theta = U_\theta H U_{-\theta}$ and f_j be the wavefunction components on the internal edges, g_j wavefunction components on the external edges. Then it acts as*

$$H_\theta \begin{pmatrix} f_j(x) \\ g_j(x) \end{pmatrix} = U_\theta H U_{-\theta} \begin{pmatrix} f_j(x) \\ g_j(x) \end{pmatrix} = \begin{pmatrix} -f_j''(x) + V_j(x)f_j(x) \\ -e^{-2\theta x} g_j''(x) \end{pmatrix}$$

Proof: Clearly, the internal edges are not scaled, for the external edges we obtain

$$\begin{aligned} U_\theta (-d^2/dx^2) U_{-\theta} g_{j\theta}(x) &= U_\theta (-d^2/dx^2) e^{-\theta/2} g_{j\theta}(e^{-\theta} x) = \\ &= -U_\theta e^{-2\theta} e^{-\theta/2} g_{j\theta}''(e^{-\theta} x) = -e^{-2\theta} e^{-\theta/2} e^{\theta/2} g_{j\theta}''(x) = -e^{-2\theta} g_{j\theta}''(x), \end{aligned}$$

where $g_{j\theta}$ is the scaled component of the generalized wavefunction on the j -th half-line. Q.E.D.

Now we state a theorem on the spectrum of the scaled operator. The main idea of the external complex scaling is to obtain resonances as eigenvalues of this non-self-adjoint operator. As stated in the previous section, the spectrum $\sigma(T)$ of the operator T can be divided into two parts – *discrete spectrum* and *essential spectrum*. The discrete spectrum $\sigma_d(T)$ is the set of eigenvalues with finite multiplicity which are isolated points of $\sigma(T)$; the essential spectrum is its complement in $\sigma(T)$. We will show the idea of the proof of the essential spectrum of the operator H_θ and complete proof of the fact that resolvent resonances are for imaginary part of θ large enough eigenvalues of H_θ .

Theorem 5.4 *The essential spectrum of H_θ is $e^{-2\theta}[0, \infty)$. The resonances of H can be obtained as eigenvalues of H_θ for $\text{Im } \theta$ large enough.*

Proof: Let $H_{D\theta}$ be operator acting as H_θ with the coupling conditions changed to Dirichlet. Using Krein formula (which states that two self-adjoint extension of the same operator differ only by a compact operator) and Weyl's theorem (which states that if two operators differ by a compact operator, then their essential spectra are the same) one can prove that essential spectra of operators $H_{D\theta}$ and H_θ are the same. Since the essential spectrum of minus second derivative

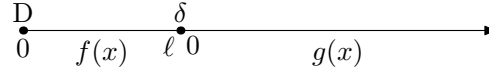


Fig. 5.2. Example: a half-line with an appendix.

on the half-line with Dirichlet coupling is $[0, \infty)$, the essential spectrum of the operator $H_{D\theta}$ and hence H_θ is $e^{-2\theta}[0, \infty)$.

Let k^2 with $k = k_r + ik_i$ be a resolvent resonance with $k_i < 0$ and $k_r > 0$. Then the corresponding solution of the Schrödinger equation with the Hamiltonian H has half-line components not square integrable. Let for simplicity be $\theta = i\vartheta$, $\vartheta \in \mathbb{R}$ and large enough $-\vartheta < \arg k < 0$. The component on the j -th edge is $g_{j\theta}(x) = \alpha_j e^{i\vartheta/2} \exp(ik e^{i\vartheta} x)$. Since $-\vartheta < \arg k$, is $\text{Im}(k e^{i\vartheta}) > 0$ and therefore $g_{j\theta}(x)$ is square integrable. Therefore, the solutions of the Schrödinger equation for H are after the scaling the eigenvalues of H_θ . Q.E.D.

Now we present examples, which show how to compute resolvent resonances for simple graphs.

5.1 Example: a half-line with an appendix – resolvent resonances

Let us consider a graph consisting of an abscissa of length ℓ and a half-line (see figure 5.2). There is a Dirichlet coupling at one end of the abscissa and δ -coupling of strength α between the abscissa and the half-line. We assume the potential on the abscissa and the half-line to be zero. We parametrize the abscissa by the interval $(0, \ell)$ and the half-line by $(0, \infty)$ and describe the wavefunction components by f and g , respectively. The coupling conditions can be written as

$$f(0) = 0, \quad f(\ell) = g(0), \quad -f'(\ell) + g'(0) = \alpha g(0).$$

We take a general ansatz for solutions of the Schrödinger equation as

$$f(x) = ae^{-ikx} + be^{ikx}, \quad g(x) = ce^{-ikx} + de^{ikx}.$$

Now we perform the scaling transformation $g_\theta(x) = U_\theta g(x) = e^{\theta/2} g(e^\theta x)$ with $\text{Im } \theta > 0$ large enough and search for eigenvalues of operator H_θ . Hence one can take $c = 0$ since the scaled function $ce^{\theta/2} e^{-ikxe^\theta}$ is not square integrable. We have

$$g(0) = e^{-\theta/2} g_\theta(0), \quad g'(0) = ik g(0) = ike^{-\theta/2} g_\theta(0).$$

The coupling conditions can be rewritten as

$$\begin{aligned} a + b &= 0, & ae^{-ik\ell} + be^{ik\ell} &= e^{-\theta/2} g_\theta(0), \\ ik(ae^{-ik\ell} - be^{ik\ell}) &= (\alpha - ik) e^{-\theta/2} g_\theta(0). \end{aligned}$$

Using $b = -a$ we have

$$\begin{aligned} a(e^{-ik\ell} - e^{ik\ell}) &= e^{-\theta/2} g_\theta(0), \\ ika(e^{-ik\ell} + e^{ik\ell}) &= (\alpha - ik) e^{-\theta/2} g_\theta(0). \end{aligned}$$

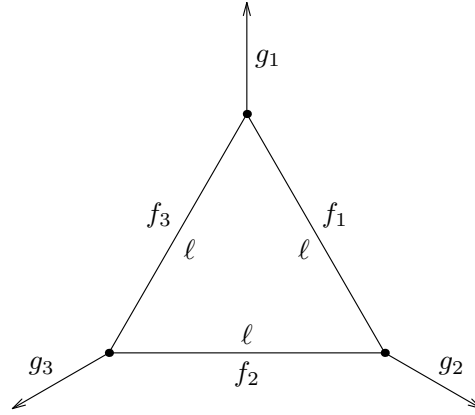


Fig. 5.3. Triangle with attached half-lines – illustration to Subsections 5.2 and 6.2.

Now substituting from the first equation for $e^{-\theta/2}g_\theta(0)$ to the second one and dividing the second equation by $(-2i)$ we obtain

$$-ak \frac{e^{ik\ell} + e^{-ik\ell}}{2} = (\alpha - ik)a \frac{e^{ik\ell} - e^{-ik\ell}}{2i}$$

which leads to the resonance condition

$$(\alpha - ik) \sin k\ell + k \cos k\ell = 0.$$

5.2 Example: triangle with half-lines – resolvent resonances

Let us study more complicated example, where we will show how to compute the resonance condition. The internal part of the graph is an equilateral triangle (all the edges have lengths ℓ). At all vertices one half-line is attached (see Figure 5.3). We assume standard coupling at all the vertices.

We assume ansatz on the internal edges $f_j(x) = a_j \sin kx + b_j \cos kx$. On the half-lines we use the ansatz $g_j(x) = d_j e^{ikx}$; we use only the outgoing edge according to the definition 5.1 because only this function is square integrable after the complex scaling with positive θ . The coupling conditions at the vertices give the following set of equations.

$$\begin{aligned} b_1 &= a_3 \sin k\ell + b_3 \cos k\ell = d_1, \\ k(a_1 - a_3 \cos k\ell + b_3 \sin k\ell + id_1) &= 0, \\ b_2 &= a_1 \sin k\ell + b_1 \cos k\ell = d_2, \\ k(a_2 - a_1 \cos k\ell + b_1 \sin k\ell + id_2) &= 0, \\ b_3 &= a_2 \sin k\ell + b_2 \cos k\ell = d_3, \\ k(a_3 - a_2 \cos k\ell + b_2 \sin k\ell + id_3) &= 0. \end{aligned}$$

This set of equations can be in the matrix form written (using $d_j = b_j$, $j = 1, 2, 3$) as

$$\begin{pmatrix} 0 & -1 & 0 & 0 & \sin k\ell & \cos k\ell \\ k & ik & 0 & 0 & -k \cos k\ell & k \sin k\ell \\ \sin k\ell & \cos k\ell & 0 & -1 & 0 & 0 \\ -k \cos k\ell & k \sin k\ell & k & ik & 0 & 0 \\ 0 & 0 & \sin k\ell & \cos k\ell & 0 & -1 \\ 0 & 0 & -k \cos k\ell & k \sin k\ell & k & ik \end{pmatrix} \begin{pmatrix} a_1 \\ b_1 \\ a_2 \\ b_2 \\ a_3 \\ b_3 \end{pmatrix} = 0.$$

Condition of the solvability of this system (determinant of this matrix is equal to zero) is our desired resonance condition. After rearrangements one obtains

$$\begin{aligned} 0 &= -k^3(-2 + 2 \cos k\ell - i \sin k\ell)(1 + 2 \cos k\ell - i \sin k\ell)^2 = \\ &= -k^3(-2i) \sin \frac{k\ell}{2} \left(\cos \frac{k\ell}{2} - 2i \sin \frac{k\ell}{2} \right) (1 + 2 \cos k\ell - i \sin k\ell)^2 = \\ &= 2ik^3 \sin \frac{k\ell}{2} \left(\frac{1}{2}e^{\frac{ik\ell}{2}} + \frac{1}{2}e^{-\frac{ik\ell}{2}} - e^{\frac{ik\ell}{2}} + e^{-\frac{ik\ell}{2}} \right) \left(1 + e^{ik\ell} + e^{-ik\ell} - \frac{1}{2}e^{ik\ell} + \frac{1}{2}e^{-ik\ell} \right)^2 = \\ &= 2ik^3 \frac{1}{2}e^{-\frac{ik\ell}{2}} \left(\frac{1}{2}e^{-ik\ell} \right)^2 \sin \frac{k\ell}{2} (3 - e^{ik\ell}) (3 + 2e^{ik\ell} + e^{2ik\ell})^2. \end{aligned}$$

The resonance condition therefore is

$$0 = k^3 \sin \frac{k\ell}{2} (3 - e^{ik\ell}) (3 + 2e^{ik\ell} + e^{2ik\ell})^2 \quad (5.1)$$

6 Scattering resonances

The second possibility how to define resonances is as poles of the meromorphic continuation of the determinant of the scattering matrix. In this view, the compact part of the graph is a scattering center and the half-lines are the leads. Since we consider zero potential on the half-lines, the solution on the semiinfinite leads can be expressed as a linear combination of e^{-ikx} and e^{ikx} . The first one we call the incoming wave and the second one the outgoing wave.

To elucidate why we have used this notation, let us for a while consider a time dependent Schrödinger equation on the half-line $(-\partial_x^2 - i\partial_t)u_j(x, t) = 0$. Its solution can be after separating the variables found in the form $u_j(x, t) = e^{-itk^2}g_j(x)$, where $g_j(x)$ is the solution of time independent Schrödinger equation. Substituting the combination of e^{-ikx} and e^{ikx} we obtain $u_j(x) = c_j e^{-ik(x+kt)} + d_j e^{ik(x-kt)}$. The first wave is incoming (for growing t the x must be smaller to get the same exponent), the second one is outgoing.

The scattering matrix $S = S(k)$ is the operator, which maps the vector of amplitudes of the incoming waves into the vector of amplitudes of the outgoing waves. The complex energies, for which its determinant diverges, are called scattering resonances.

6.1 Example: a half-line with an appendix – scattering resonances

Let us now study the same example as in the subsection 5.1 in the case of resolvent resonances. We again assume an abscissa of length ℓ and a half-line in figure 5.2 with Dirichlet coupling at one end of the segment and δ -coupling between the abscissa and the half-line.

$$f(0) = 0, \quad f(\ell) = g(0), \quad -f'(\ell) + g'(0) = \alpha g(0).$$

We use the ansatz $f(x) = ae^{-ikx} + be^{ikx}$ and $g(x) = ce^{-ikx} + de^{ikx}$ and obtain

$$\begin{aligned} a + b &= 0, & ae^{-ik\ell} + be^{ik\ell} &= c + d, \\ ik(d - c) + ik(ae^{-ik\ell} - be^{ik\ell}) &= \alpha(c + d). \end{aligned}$$

Substituting $b = -a$ we obtain

$$\begin{aligned} a(e^{-ik\ell} - e^{ik\ell}) &= c + d, \\ ik(d - c) + ika(e^{-ik\ell} + e^{ik\ell}) &= \alpha(c + d). \end{aligned}$$

Using definitions of sine and cosine and substituting now for a from the first equation to the second we get

$$\begin{aligned} ik(d - c) \sin k\ell - k \cos k\ell(c + d) &= \alpha(c + d) \sin k\ell, \\ [(\alpha - ik) \sin k\ell + k \cos k\ell] d &= -[(\alpha + ik) \sin k\ell + k \cos k\ell] c. \end{aligned}$$

We finally obtain

$$S(k) = \frac{d}{c} = -\frac{(\alpha + ik) \sin k\ell + k \cos k\ell}{(\alpha - ik) \sin k\ell + k \cos k\ell}.$$

The scattering matrix is in this case only a number (we have one half-line) and its poles give the same resonance condition as resolvent resonances.

6.2 Example: triangle with half-lines – scattering resonances

Let us consider the same graph as in the Subsection 5.2 (see Figure 5.3) and let us find the scattering matrix and scattering resonances. We use the ansatz $f_j(x) = a_j \sin kx + b_j \cos kx$ on the internal edges and $g_j(x) = c_j e^{-ikx} + d_j e^{ikx}$.

The coupling conditions at the vertices lead to the set of equations

$$\begin{aligned} b_1 &= a_3 \sin k\ell + b_3 \cos k\ell = c_1 + d_1, \\ k[a_1 - a_3 \cos k\ell + b_3 \sin k\ell + i(d_1 - c_1)] &= 0, \\ b_2 &= a_1 \sin k\ell + b_1 \cos k\ell = c_2 + d_2, \\ k[a_2 - a_1 \cos k\ell + b_1 \sin k\ell + i(d_2 - c_2)] &= 0, \\ b_3 &= a_2 \sin k\ell + b_2 \cos k\ell = c_3 + d_3, \\ k[a_3 - a_2 \cos k\ell + b_2 \sin k\ell + i(d_3 - c_3)] &= 0. \end{aligned}$$

Substituting for $b_j = c_j + d_j$, $j = 1, 2, 3$ we obtain the following set of equations

$$\begin{aligned} a_3 \sin k\ell + (c_3 + d_3) \cos k\ell - c_1 - d_1 &= 0, \\ a_1 - a_3 \cos k\ell + (c_3 + d_3) \sin k\ell + id_1 - ic_1 &= 0, \\ a_1 \sin k\ell + (c_1 + d_1) \cos k\ell - c_2 - d_2 &= 0, \\ a_2 - a_1 \cos k\ell + (c_1 + d_1) \sin k\ell + id_2 - ic_2 &= 0, \\ a_2 \sin k\ell + (c_2 + d_2) \cos k\ell - c_3 - d_3 &= 0, \\ a_3 - a_2 \cos k\ell + (c_2 + d_2) \sin k\ell + id_3 - ic_3 &= 0. \end{aligned}$$

This can be written in the form

$$\begin{pmatrix} A & C & D \\ E & F & G \end{pmatrix} \begin{pmatrix} \mathbf{a} \\ \mathbf{c} \\ \mathbf{d} \end{pmatrix} = 0, \quad (6.1)$$

where

$$\begin{aligned} A &= \begin{pmatrix} 0 & 0 & \sin k\ell \\ 1 & 0 & -\cos k\ell \\ -\cos k\ell & 1 & 0 \end{pmatrix}, & C &= \begin{pmatrix} -1 & 0 & \cos k\ell \\ -i & 0 & \sin k\ell \\ \sin k\ell & -i & 0 \end{pmatrix}, \\ D &= \begin{pmatrix} -1 & 0 & \cos k\ell \\ i & 0 & \sin k\ell \\ \sin k\ell & i & 0 \end{pmatrix}, & E &= \begin{pmatrix} \sin k\ell & 0 & 0 \\ 0 & \sin k\ell & 0 \\ 0 & -\cos k\ell & 1 \end{pmatrix}, \\ F &= \begin{pmatrix} \cos k\ell & -1 & 0 \\ 0 & \cos k\ell & -1 \\ 0 & \sin k\ell & -i \end{pmatrix}, & G &= \begin{pmatrix} \cos k\ell & -1 & 0 \\ 0 & \cos k\ell & -1 \\ 0 & \sin k\ell & i \end{pmatrix}, \end{aligned}$$

the vectors are $\mathbf{a} = (a_1, a_2, a_3)^T$, $\mathbf{c} = (c_1, c_2, c_3)^T$ and $\mathbf{d} = (d_1, d_2, d_3)^T$. Notice that we switched third and fourth equation in definition of the matrices to obtain matrix A which is invertible.

The upper equation in (6.1) gives

$$\mathbf{a} = -(A^{-1}C\mathbf{c} + A^{-1}D\mathbf{d})$$

and substituting it for \mathbf{a} in the lower equation we obtain

$$-EA^{-1}C\mathbf{c} - EA^{-1}D\mathbf{d} + F\mathbf{c} + G\mathbf{d} = 0,$$

from which we have

$$\mathbf{d} = -(G - EA^{-1}D)^{-1}(F - EA^{-1}C)\mathbf{c}$$

and the scattering matrix

$$S(k) = -(G - EA^{-1}D)^{-1}(F - EA^{-1}C).$$

We can express this equation in the numerical software and find

$$S_{ii} = -\frac{2 \cos \frac{k\ell}{2} + i \left(\sin \frac{k\ell}{2} - 3 \sin \frac{3k\ell}{2} \right)}{2 \left(\cos \frac{k\ell}{2} - 2i \sin \frac{k\ell}{2} \right) (1 + 2 \cos k\ell - i \sin k\ell)}, \quad i = 1, 2, 3,$$

$$S_{ij} = -\frac{2 \cos \frac{k\ell}{2}}{\left(\cos \frac{k\ell}{2} - 2i \sin \frac{k\ell}{2} \right) (1 + 2 \cos k\ell - i \sin k\ell)}, \quad i \neq j.$$

The determinant of the scattering matrix is

$$\det S(k) = \frac{(-1 + 3e^{ik\ell})(1 + 2e^{ik\ell} + 3e^{2ik\ell})^2}{(3 - e^{ik\ell})(3 + 2e^{ik\ell} + e^{2ik\ell})^2}$$

and hence comparing with (5.1) we find that the set of resolvent resonances is the union of the set of the scattering resonances, eigenvalues $k^2 = \left(\frac{2n\pi}{\ell}\right)^2$ (obtained from $\sin \frac{k\ell}{2} = 0$) and resonance at zero with multiplicity 3.

7 The resonance condition

In this section we express the resonance condition for finding resolvent resonances for a general graph. We will use the flower-like model (Figure 2.1). On the internal edges we use the ansatz $f_j(x) = a_j \sin kx + b_j \cos kx$, and on the external edges $g_j(x) = d_j e^{ikx}$. Using this ansatz we have

$$\begin{aligned} f_j(0) &= b_j, & f_j(\ell_j) &= a_j \sin k\ell_j + b_j \cos k\ell_j, \\ f_j'(0) &= ka_j, & -f_j'(\ell_j) &= -ka_j \cos k\ell_j + kb_j \sin k\ell_j, \end{aligned}$$

These relations can be expressed as

$$\begin{pmatrix} f_j(0) \\ f_j(\ell_j) \end{pmatrix} = \begin{pmatrix} 0 & 1 \\ \sin k\ell_j & \cos k\ell_j \end{pmatrix} \begin{pmatrix} a_j \\ b_j \end{pmatrix}, \quad (7.1)$$

$$\begin{pmatrix} f_j'(0) \\ -f_j'(\ell_j) \end{pmatrix} = k \begin{pmatrix} 1 & 0 \\ -\cos k\ell_j & \sin k\ell_j \end{pmatrix} \begin{pmatrix} a_j \\ b_j \end{pmatrix}. \quad (7.2)$$

On the half-lines we use external complex scaling $g_{j\theta}(x) = e^{\theta/2} g_j(xe^\theta)$ with an imaginary θ , we obtain

$$g_j(0) = e^{-\theta/2} g_{j\theta}, \quad g_j'(0) = ik e^{-\theta/2} g_{j\theta}. \quad (7.3)$$

We can now substitute equations (7.1), (7.2) and (7.3) into (2.2). We rearrange the equations so that we have in Ψ and Ψ' values corresponding to both ends of the first edge, then both ends of the second edge, etc. The matrix U is rearranged accordingly. After substituting we obtain

$$(U - I)C_1(k) \begin{pmatrix} a_1 \\ b_1 \\ a_2 \\ \vdots \\ b_N \\ e^{-\theta/2} g_{1\theta} \\ \vdots \\ e^{-\theta/2} g_{M\theta} \end{pmatrix} + ik(U + I)C_2(k) \begin{pmatrix} a_1 \\ b_1 \\ a_2 \\ \vdots \\ b_N \\ e^{-\theta/2} g_{1\theta} \\ \vdots \\ e^{-\theta/2} g_{M\theta} \end{pmatrix} = 0, \quad (7.4)$$

where the matrices $C_1(k)$, $C_2(k)$ consist of blocks

$$C_1(k) = \text{diag} (C_1^{(1)}(k), C_1^{(2)}(k), \dots, C_1^{(N)}(k), I_{M \times M})$$

and

$$C_2(k) = \text{diag} (C_2^{(1)}(k), C_2^{(2)}(k), \dots, C_2^{(N)}(k), iI_{M \times M}),$$

respectively, where

$$C_1^{(j)}(k) = \begin{pmatrix} 0 & 1 \\ \sin k\ell_j & \cos k\ell_j \end{pmatrix}, \quad C_2^{(j)}(k) = \begin{pmatrix} 1 & 0 \\ -\cos k\ell_j & \sin k\ell_j \end{pmatrix}$$

and $I_{M \times M}$ is a $M \times M$ identity matrix.

The equation of solvability of the system (7.4) is

$$\det [(U - I)C_1(k) + ik(U + I)C_2(k)] = 0.$$

This is our resonance condition.

8 The equivalence of resonances

In this section, we prove that for quantum graphs the two previous definitions of resonances are equivalent. To be precise, the set of resolvent resonances is equal to the set of scattering resonances unified with the set of eigenvalues with corresponding eigenfunctions supported on the internal part of the graph. This result was obtained first for a certain set of coupling conditions in [EL07], for all graphs and hedgehog manifolds it was proved in [EL13].

Theorem 8.1 *Let us consider the quantum graph with the Hamiltonian defined in section 2. Then there is a resolvent resonance at k_0^2 iff there is a scattering resonance at k_0^2 or there is an eigenvalue at k_0^2 with the eigenfunction supported on the internal part of the graph.*

Proof: We assume the coupling condition (2.2) with $\Psi = \begin{pmatrix} \Psi_{\text{int}} \\ \Psi_{\text{ext}} \end{pmatrix}$ and $\Psi' = \begin{pmatrix} \Psi'_{\text{int}} \\ \Psi'_{\text{ext}} \end{pmatrix}$. Since the solution on the j -th internal edge is a combination of two linearly independent solutions $a_j u_j(x) + b_j v_j(x)$, we have entries of the vector of functional values $a_j u_j(v) + b_j v_j(v)$ (v denotes the vertex), similarly for the vector of derivatives $a_j u'_j(v) + b_j v'_j(v)$. For an external edge we have solution as combination of incoming and outgoing wave $c_j e^{-ikx} + d_j e^{ikx}$, hence $\Psi_{\text{ext}} = \mathbf{c} + \mathbf{d}$, $\Psi'_{\text{ext}} = ik(\mathbf{d} - \mathbf{c})$.

Therefore, the coupling condition (2.2) can be rewritten as

$$A(k)\mathbf{a} + B(k)\mathbf{b} + C(k)\mathbf{c} + D(k)\mathbf{d} = 0,$$

where $A(k), B(k)$ are $(2N+M) \times N$ energy-dependent matrices, $C(k), D(k)$ are $(2N+M) \times M$ energy-dependent matrices and $\mathbf{a}, \mathbf{b}, \mathbf{c}, \mathbf{d}$ are vectors with entries a_j, b_j, c_j and d_j . We define a $(2N+M) \times 2N$ matrix $E(k) = (A(k), B(k))$ and the vector $\mathbf{e} = \begin{pmatrix} \mathbf{a} \\ \mathbf{b} \end{pmatrix}$ corresponding to the internal coefficients. The previous equation can be thus rewritten as

$$E(k)\mathbf{e} + C(k)\mathbf{c} + D(k)\mathbf{d} = 0. \tag{8.1}$$

If $E(k_0)$ has less than $2N$ linearly independent rows, it means that there exist a solution of (8.1) with $\mathbf{c} = \mathbf{d} = 0$, i.e. eigenvalue with eigenfunction supported only on the internal part of the graph. We know that $k_0^2 \in \mathbb{R}$. Clearly, this eigenvalue belongs also to the family of resolvent resonances (solutions with $\mathbf{c} = 0$).

Now we assume that $E(k_0)$ has exactly $2N$ linearly independent rows. We rearrange the equations (8.1) so that first $2N$ rows of $E(k_0)$ are linearly independent. From these first $2N$ equations we express \mathbf{e} and substitute it into the remaining M equations. We obtain

$$\tilde{C}(k)\mathbf{c} + \tilde{D}(k)\mathbf{d} = 0$$

with $M \times M$ matrices $\tilde{C}(k)$ and $\tilde{D}(k)$. The resolvent resonances are solutions with only outgoing waves, i.e. $\mathbf{c} = 0$; this means that the resonance condition is $\det \tilde{D}(k) = 0$. The scattering matrix is $S(k) = (\tilde{D}(k))^{-1} \tilde{C}(k)$, the condition for scattering resonances also is $\det \tilde{D}(k) = 0$. Therefore these families of resonances coincide. Q.E.D.

9 Effective coupling on a finite graph

The content of this section will be used later. We will introduce effective coupling equation in the case where all the half-lines of the graph are “cut off”.

Theorem 9.1 *Let H be a Schrödinger operator on a quantum graph Γ with $2N$ internal and M external edges and coupling given by $(2N + M) \times (2N + M)$ unitary matrix U consisting of blocks*

$$U = \begin{pmatrix} U_1 & U_2 \\ U_3 & U_4 \end{pmatrix},$$

where the $2N \times 2N$ matrix U_1 corresponds to the coupling between internal edges, $M \times M$ matrix U_4 corresponds to the coupling between the half-lines and $2N \times M$ matrix U_2 and $M \times 2N$ matrix U_3 correspond to the mixed coupling. Let $\{\lambda_i\}_{i=1}^M$ be eigenvalues of U_4 . Then all resolvent resonances of Γ with k on $\mathbb{C} \setminus \{\frac{\lambda_1-1}{\lambda_1+1}, \dots, \frac{\lambda_M-1}{\lambda_M+1}\}$ are given as eigenvalues of operator with the same action on the internal edges as H but satisfying energy-dependent coupling conditions

$$(\tilde{U}(k) - I_{2N})\mathbf{f} + i(\tilde{U}(k) + I_{2N})\mathbf{f}' = 0$$

with

$$\tilde{U}(k) = U_1 - (1 - k)U_2[(1 - k)U_4 - (k + 1)I_M]^{-1}U_3. \quad (9.1)$$

Proof: Let \mathbf{f} and \mathbf{g} denote the vector of amplitudes of functional values on the internal and external edges, respectively and let \mathbf{f}' and \mathbf{g}' be the vectors of amplitudes of outgoing derivatives. Then the coupling condition (2.2) can be rewritten as

$$\begin{pmatrix} U_1 - I_{2N} & U_2 \\ U_3 & U_4 - I_M \end{pmatrix} \begin{pmatrix} \mathbf{f} \\ \mathbf{g} \end{pmatrix} + i \begin{pmatrix} U_1 + I_{2N} & U_2 \\ U_3 & U_4 + I_M \end{pmatrix} \begin{pmatrix} \mathbf{f}' \\ \mathbf{g}' \end{pmatrix} = 0,$$

where I_N denotes the $N \times N$ identity matrix. Performing external complex scaling means replacing \mathbf{g} and \mathbf{g}' by $e^{-\theta/2}\mathbf{g}_\theta$ and $ike^{-\theta/2}\mathbf{g}'_\theta$, respectively.

$$\begin{pmatrix} U_1 - I_{2N} & U_2 \\ U_3 & U_4 - I_M \end{pmatrix} \begin{pmatrix} \mathbf{f} \\ e^{-\theta/2}\mathbf{g}_\theta \end{pmatrix} + \begin{pmatrix} i(U_1 + I_{2N}) & -kU_2 \\ iU_3 & -k(U_4 + I_M) \end{pmatrix} \begin{pmatrix} \mathbf{f}' \\ e^{-\theta/2}\mathbf{g}'_\theta \end{pmatrix} = 0.$$

Now eliminating \mathbf{g}_θ for $\det((1 - k)U_4 - (k + 1)I_M) \neq 0$ we get

$$\begin{aligned} & [U_1 - I_{2N} - (1 - k)U_2[(1 - k)U_4 - (k + 1)I_M]^{-1}U_3]\mathbf{f} + \\ & + [U_1 + I_{2N} - (1 - k)U_2[(1 - k)U_4 - (k + 1)I_M]^{-1}U_3]\mathbf{f}' = 0 \end{aligned}$$

which can be written as

$$(\tilde{U}(k) - I_{2N})\mathbf{f} + i(\tilde{U}(k) + I_{2N})\mathbf{f}' = 0 \quad (9.2)$$

with

$$\tilde{U}(k) = U_1 - (1 - k)U_2[(1 - k)U_4 - (k + 1)I_M]^{-1}U_3. \quad (9.3)$$

We can easily show that the condition $\det((1 - k)U_4 - (k + 1)I_M) = 0$ which for eigenvalues means $(1 - k)\lambda_j - (k + 1) = 0$ implies $k = \frac{\lambda_j - 1}{\lambda_j + 1}$. With exception of these points the construction works. Q.E.D.

10 Asymptotics of resonances for non-magnetic graphs

We start the main part of this text by a topic at the first sight different from quantum graphs and their resonance properties. The asymptotical behaviour of the number of eigenvalues of Laplace–Beltrami operator on a Riemannian manifold of the dimension d is given by Weyl’s law [Wey11]. We show the result of Ivrii from [Ivr80]. The number of eigenvalues which are in modulus smaller than λ is given by

$$N(\lambda) = \frac{\omega_d |\Omega|}{(2\pi)^d} \lambda^{d/2} \pm \frac{\omega_{d-1} |\partial\Omega|}{4(2\pi)^{d-1}} \lambda^{(d-1)/2} + o(\lambda^{(d-1)/2}),$$

where ω_d stands for the volume of a d -dimensional ball with radius 1 and $|\Omega|$ and $|\partial\Omega|$ denote the volume of the manifold and volume of its boundary, respectively. The plus sign corresponds to the Neumann condition on the boundary of the manifold, the minus sign to the Dirichlet condition.

The problem solved by Weyl was laid by Lorenz and is connected to Rayleigh-Jeans law. Let us consider a blackbody in the shape of a cube. If we want to find the energy radiated between frequencies ν and $\nu + d\nu$, we have to count the number of normal modes in this frequency interval and by an equipartition theorem multiply it by $k_B T$. The electric field of the n -th mode satisfies Maxwell’s equations; after separation of variables one obtains the equation for eigenvalues of the Laplacian. Since the blackbody is conducting, the electric field must vanish at the boundary. Hence we have the problem for the number of eigenvalues of the Dirichlet Laplacian in the cube. For $d = 3$ we obtain from the Weyl’s law

$$N(\lambda) \approx \frac{4\pi |\Omega|}{3(2\pi)^3} \lambda^{3/2} = \frac{1}{6\pi^2} |\Omega| \lambda^{3/2}.$$

Using the relation $\lambda = \frac{4\pi^2}{c^2} \nu^2$ we have

$$N(\nu) \approx \frac{1}{6\pi^2} \frac{8\pi^3}{c^3} |\Omega| \nu^3 = \frac{4\pi}{3c^3} |\Omega| \nu^3.$$

For the difference of the counting functions we have for small $d\nu$

$$N(\nu + d\nu) - N(\nu) \approx \frac{4\pi}{c^3} |\Omega| \nu^2 d\nu.$$

Using the equipartition theorem and the fact that taking both polarizations of light adds a factor of two, we obtain the Rayleigh-Jeans law. The energy density is

$$\rho = 8\pi k_B T \frac{\nu^2}{c^3} d\nu.$$

More details can be found in [Mus16].

Now we will get the expression for the asymptotics of the number of eigenvalues of a compact quantum graph. We will work in the k -plane, where k is the square root of energy. The formula for the number of eigenvalues in modulus smaller than R is

$$N(R) = \frac{2V}{\pi} R + \mathcal{O}(1), \tag{10.1}$$

where V is the sum of the lengths of the (internal) edges. This result follows from the previous equation taking $\lambda = R^2$ and adding an extra factor of 2, because we count every eigenvalue twice since $(-k)^2 = k^2$.

Our aim will be to find the asymptotical behaviour of the number of resolvent resonances for a non-compact quantum graph. To be precise, we want the number of resolvent resonances enclosed in the circle of radius R in the k -plane in the limit $R \rightarrow \infty$. We would expect that it behaves as the equation (10.1) with V being the sum of the lengths of the internal edges of the graph. It holds true for most of the graphs (we will call these graphs *Weyl*), but there is a class of graphs for which the constant in the asymptotics is smaller than expected (we denote these graphs as *non-Weyl*).

The behaviour of the counting function of resolvent resonances was studied first for quantum graphs with the standard condition by Davies and Pushnitski [DP11]. They found a nice geometric condition: the graph is non-Weyl iff it has a *balanced* vertex. By a balanced vertex, we mean the vertex which connects the same number of internal and external edges. Later this result was generalized to all possible couplings in [DEL10]. There was a condition found on the eigenvalues of the effective coupling matrix in the previous section which distinguishes the Weyl and non-Weyl graphs. In this text, both results will be stated in the opposite order. First, we prove the theorem on the general graphs and then we show the condition by Davies and Pushnitski as its corollary.

10.1 Main theorems

We state a lemma on the number of zeros of exponential polynomials. It was in this form stated in [DEL10], but it follows from the result from 1930's by Langer [Lan31] and previous results by Pólya. We present a sketch of the proof, more details can be found in [Lan31] for the first part and [DEL10] for the second part of the proof. See also the books [BC63, BG95].

Lemma 10.1 *Let $F(k) = \sum_{r=0}^n k^{\nu_r} a_r(k) e^{ik\sigma_r}$, where $\nu_r \in \mathbb{R}$, $a_r(k)$ are rational functions of the complex variable k with complex coefficients that do not vanish identically, and $\sigma_r \in \mathbb{R}$, $\sigma_0 < \sigma_1 < \dots < \sigma_n$. Suppose also that ν_r are chosen so that $\lim_{k \rightarrow \infty} a_r(k) = \alpha_r$ is finite and non-zero for all r . Then the counting function behaves in the limit $R \rightarrow \infty$ as*

$$N(R, F) = \frac{\sigma_n - \sigma_0}{\pi} R + \mathcal{O}(1).$$

Proof: Let us first assume function

$$\Phi(z) = \sum_{j=0}^n A_j(z) e^{c_j z}$$

of the complex variable $z = x + iy$. We are interested in zeros of this function. We will start from particular subcases and finally arrive to the general case.

1. $A_j = a_j$ constant, $c_j \in \mathbb{R}$ commensurable

We can take $c_j = \alpha p_j$, $j = 1, \dots, n$, $\alpha \in \mathbb{R}$, $p_j \in \mathbb{N}$ and without loss of generality also

$c_0 = p_0 = 0$. Since the exponents are commensurable, we have

$$\Phi(z) = \sum_{j=0}^n a_j (e^{\alpha z})^{p_j}, \quad p_0 = 0, \quad p_n \in \mathbb{N}.$$

This is a polynomial of degree p_n in $e^{\alpha z}$ and its roots are $e^{\alpha z} = \xi_j$, $j = 1, 2, \dots, p_n$. Therefore its zeros are in lines parallel to the y axis

$$z = \frac{1}{\alpha}(2\pi im + \ln \xi_j), \quad m \in \mathbb{Z}.$$

On the line $y = y_1$ we have

$$\operatorname{Im} \left[\frac{1}{a_0} \Phi(x + iy_1) \right] = \sum_{j=1}^n a_j \sin(\alpha y_1 p_j) (e^{\alpha x})^{p_j} = \sum_{j=1}^n b_j(y_1) (e^{\alpha x})^{p_j}, \quad (10.2)$$

where the coefficients b_j depend on y_1 and the sum is from 1 and not from 0 because from $p_0 = 0$ follows $\operatorname{Im}(e^{\alpha(x+iy)p_0}) = 0$. The expression (10.2) vanishes on $y = y_1$ at most $(n-1)$ -times. This follows from Descartes's rule of signs (number of roots of a polynomial is bounded from above by the number of sign changes).

Now we find the number of zeros in the rectangular region R' . We choose y_1 and y_2 so that there is no zero of $\Phi(z)$ on these lines. Then $\operatorname{Arg} \Phi(z)$ increases or decreases by at most $n\pi$, since (10.2) vanishes at most $(n-1)$ -times. Now we come to the lines $x = \pm K$. For sufficiently large K , $\Phi(z)$ goes to a_0 at $x = -K$ and hence $\operatorname{Arg} \Phi(z)$ is small. On $x = K$, $\Phi(z)$ goes to $a_n e^{c_n z}$ for sufficiently large K and hence $\operatorname{Arg} \Phi(z)$ increases its value arbitrarily near $c_n(y_2 - y_1)$.

Hence the number of zeros $n(R')$ in the region bounded by $|x| < K$ and lines $y = y_1$ and $y = y_2$ is bounded by

$$-n + \frac{c_n}{2\pi}(y_2 - y_1) \leq n(R') \leq n + \frac{c_n}{2\pi}(y_2 - y_1). \quad (10.3)$$

2. A_j constant, $c_j \in \mathbb{R}$ and general

Then we have

$$\Phi(z) = \sum_{j=0}^n a_j e^{c_j z}, \quad c_0 = 0. \quad (10.4)$$

Since the first term of the above function is dominant for $x = -K$ and the last term is dominant for $x = K$ with sufficiently large K , the zeros are again in a strip $|x| < K$. The change in $\operatorname{Arg} \Phi(z)$ at $x = \pm K$ can be computed similarly to the previous case. Establishing the relation (10.3) depends only on the relation (10.2) on a line with constant y . We cannot use the Descartes rule, but using the similar result by Pólya and Szegő [PS25] it can be proven that the expression (10.4) vanishes at most as many times that there are changes in sign in the sequence of a_j and hence we again have (10.3).

3. A_j asymptotically constant

We again study the number of resonances in the same rectangle R' bounded by curves $|x| < K$, $y = y_1$, $y = y_2$. We will assume that $a_0, a_n \neq 0$. Let

$$A_j(z) = a_j + \varepsilon(z) \quad \text{in} \quad |z| > M,$$

where $\varepsilon(z)$ denotes the set of functions analytic in every finite portion of R' , which approach to zero uniformly in R' as $|z| \rightarrow \infty$. Then we have

$$\Phi(z) = \sum_{j=0}^n (a_j + \varepsilon(z)) e^{c_j z}, \quad a_0, a_n \neq 0$$

and hence

$$\Phi(z) = \Phi_1(z) + \varepsilon(z), \quad \Phi_1(z) = \sum_{j=0}^n a_j e^{c_j z}, \quad |x| < K, \quad |z| > M.$$

By smartly choosing the contours enclosing the zeros of Φ_1 one has that zeros of $\Phi(z)$ lie within the distance δ from zeros of $\Phi_1(z)$ and for values not within this contours $|\Phi(z)|$ is bounded uniformly from zero and we have $\Phi(z) = \Phi_1(z)(1 + \varepsilon(z))$. The zeros of $\Phi(z)$ are asymptotically represented by zeros of $\Phi_1(z)$.

4. $A_j(z)$ asymptotically power functions $A_j(z) = z^{\nu_j}(a_j + \varepsilon(z))$, $a_0, a_n \neq 0$, and ν_j are proportional to c_j , i.e. $\nu_j = \beta c_j$

We have

$$\Phi(z) = \sum_{j=0}^n (a_j + \varepsilon(\zeta)) e^{c_j \zeta}$$

with $\zeta = z + \beta \ln z$, which is the previous case. If $\zeta = \xi + i\eta$, we have from the previous relation

$$\begin{aligned} \xi &= x + \beta \ln |z|, \\ \eta &= y + \beta \text{Arg } z. \end{aligned}$$

The condition $|\xi| < K$ now means that the resonances are in the region bounded by logarithmic curves

$$x + \beta \ln |z| = \pm K.$$

5. general values of ν_j

We have

$$\Phi(z) = \sum_{j=0}^n z^{\nu_j} (a_j + \varepsilon(z)) e^{c_j z}.$$

To each pair $P_j = (c_j, \nu_j)$ a point in the plane corresponds. We define a broken line L with the vertices in the subset of $\{P_j\}_{j=0}^n$ which is convex line and no points P_j lie above it. On its segment L_r there are points P_{rh} , $h = 1, \dots, n_r$.

Let us assume an intermediate segment of this line with the slope m_r , the slope of the previous segment is m_{r-1} . Then for parameter k ,

$$m_{r-1} - \delta \geq k > m_r - \delta,$$

with $\delta > 0$ but sufficiently small the curve

$$x = -k \ln |z| \tag{10.5}$$

is in the region bounded by curves

$$\begin{aligned} x &= -(m_{r-1} - \delta) \ln |z|, \\ x &= -(m_r - \delta) \ln |z|. \end{aligned}$$

On the curve (10.5) it holds

$$|z^{\nu_{ls}} e^{c_{ls} z}| = |z|^{\nu_{ls} - k c_{ls}}$$

and for $l \neq k$

$$\nu_{ls} - k c_{ls} < \nu_{r1} - k c_{r1}.$$

Therefore,

$$z^{\nu_{ls}} e^{c_{ls} z} = z^{\nu_{r1}} e^{c_{r1} z} \varepsilon(z), \quad l \neq r$$

for any curve (10.5) and hence we have

$$\Phi(z) = \sum_{h=1}^{\nu_r} z^{\nu_{rh}} (a_{rh} + \varepsilon(z)) e^{c_{rh} z},$$

which is the previous case.

6. Now we can realize that the function in our lemma belongs to the class in the previous point, only with $z = ik$. It remains to prove that there is asymptotically the same number of resonances in the rectangle as in the circle. This, a bit technical part, is shown in [DEL10].

First, we realize that the number of zeros in the circle with centre 0 and radius R can be estimated from above by the number of zeros satisfying $|\operatorname{Re} k| \leq R$. The bound from below satisfies

$$|\operatorname{Re} k| \geq \sqrt{R^2 - (K + m \ln R)^2}$$

with $K := \max_{1 \leq r \leq n} K_r$ and $m := \max_{1 \leq r \leq n} |m_r|$. Since

$$\lim_{R \rightarrow \infty} R - \sqrt{R^2 - (K + m \ln R)^2} = 0$$

both pairs of lines asymptotically approach each other. The only difference to [Lan31] is that the role of c_n is replaced by σ_j 's.

Q.E.D.

Theorem 10.2 *The asymptotics of the number of resolvent resonances in quantum graph is*

$$N(R) = \frac{2W}{\pi}R + \mathcal{O}(1), \quad (10.6)$$

where $0 \leq W \leq V$. We have strict inequality $W < V$ iff the matrix $\tilde{U}(k)$ has eigenvalue either $\frac{1+k}{1-k}$ or $\frac{1-k}{1+k}$; we call this graph non-Weyl.

Proof: We choose the ansatz on the j -th edge

$$f_j(x) = \alpha_j e^{ikx} + \beta_j e^{-ikx},$$

hence we have

$$f'_j(x) = ik(\alpha_j e^{ikx} - \beta_j e^{-ikx}).$$

This leads to

$$\begin{aligned} f_j(0) &= \alpha_j + \beta_j, & f_j(\ell_j) &= \alpha_j e^{ik\ell_j} + \beta_j e^{-ik\ell_j}, \\ f'_j(0) &= ik(\alpha_j - \beta_j), & -f'_j(\ell_j) &= ik(-\alpha_j e^{ik\ell_j} + \beta_j e^{-ik\ell_j}). \end{aligned}$$

From equation (9.2) we have

$$[(\tilde{U}(k) - I_{2N})E_1(k) + iik(\tilde{U}(k) + I_{2N})E_2(k)]\alpha = 0,$$

where $\alpha = (\alpha_1, \beta_1, \alpha_2, \beta_2, \dots, \alpha_N, \beta_N)^T$, E_1 and E_2 are $2N \times 2N$ block diagonal matrices with blocks

$$E_{j1} = \begin{pmatrix} 1 & 1 \\ e_{j+} & e_{j-} \end{pmatrix}, \quad E_{j2} = \begin{pmatrix} 1 & -1 \\ -e_{j+} & e_{j-} \end{pmatrix},$$

respectively, and $e_{j\pm} = e^{\pm ik\ell_j}$. Equation of solvability of the above system is

$$\begin{aligned} \det \left\{ [\tilde{U}(k)(1+k) - I_{2N}(1-k)]E_3(k) + [\tilde{U}(k)(1-k) - I_{2N}(1+k)]E_4(k) + \right. \\ \left. + (\tilde{U}(k) - I_{2N})E_5 - k(\tilde{U}(k) + I_{2N})E_6 \right\} = 0, \quad (10.7) \end{aligned}$$

where block diagonal matrices E_3, E_4, E_5 and E_6 consist of blocks

$$E_{j3} = \begin{pmatrix} 0 & 0 \\ e_{j+} & 0 \end{pmatrix}, \quad E_{j4} = \begin{pmatrix} 0 & 0 \\ 0 & e_{j-} \end{pmatrix}, \quad E_{j5} = \begin{pmatrix} 1 & 1 \\ 0 & 0 \end{pmatrix}, \quad E_{j6} = \begin{pmatrix} 1 & -1 \\ 0 & 0 \end{pmatrix}.$$

The coefficient by the exponential with the largest multiple of ik in the exponent is $\det [\tilde{U}(k)(1+k) - I_{2N}(1-k)]$, the coefficient by the exponential with the smallest multiple of ik in the exponent is $\det [\tilde{U}(k)(1-k) - I_{2N}(1+k)]$. From this fact and Lemma 10.1 the result follows. Q.E.D.

Now we will prove the result of Davies and Pushnitski [DP11] as a corollary of this theorem.

Corollary 10.3 *The graph with standard coupling is non-Weyl iff there is a balanced vertex, i.e. the vertex which connects the same number of internal and external edges.*

Proof: The coupling matrix for standard condition is $U_j = \frac{2}{d}J_d - I_d$, where d is the degree of the vertex, J_d is $d \times d$ matrix with all entries equal to one and I_d identity matrix. Clearly, the effective graph coupling matrix $\tilde{U}(k)$ has an eigenvalue $\frac{1+k}{1-k}$ or $\frac{1-k}{1+k}$ iff one of the vertex effective coupling matrices $\tilde{U}_j(k)$ has the same eigenvalue. The matrices $\tilde{U}_j(k)$ are constructed similarly to $\tilde{U}(k)$. If there is n internal and m external edges in the given vertex, one has

$$U_{1j} = \frac{2}{m+n}J_n - I_n, \quad U_{4j} = \frac{2}{m+n}J_m - I_m,$$

and the matrices U_{2j} and U_{3j} are $\frac{2}{m+n}$ -multiples of the matrices with all entries equal to one, which are $n \times m$ or $m \times n$, respectively. One can straightforwardly prove that

$$(aJ_m + bI_m)^{-1} = -\frac{1}{b} \left(\frac{a}{am+b} J_m - I_m \right). \quad (10.8)$$

Hence we have

$$[(1-k)U_4 - (1+k)I_m]^{-1} = [(1-k)\frac{2}{n+m}J_m - 2I_m]^{-1} = \frac{1}{2} \left(-\frac{1-k}{km+n} J_m - I_m \right).$$

This gives

$$\begin{aligned} \tilde{U}(k) &= \frac{2}{n+m}J_n - I_n - (1-k)\frac{4}{(m+n)^2} \left(-\frac{m^2}{2} \frac{1-k}{km+n} J_n - \frac{m}{2} J_n \right) = \\ &= \frac{2}{km+n} J_n - I_n. \end{aligned}$$

Since eigenvalues of J_n are n and 0 with multiplicity $n-1$, eigenvalues of $\tilde{U}(k)$ are $\frac{n-km}{n+km}$ and -1 with multiplicity $n-1$. Comparing it with $\frac{1 \mp k}{1 \pm k}$ gives

$$n - km \pm kn \mp k^2m = km + n \mp k^2m \mp kn \quad \Rightarrow \quad 2km = \pm 2kn$$

Hence the graph is non-Weyl iff $n = m$ for at least one vertex.

Q.E.D.

Finally, we illustrate the general theorems in a simple example.

Example 10.4 (two internal edges and two half-lines)

Let us consider the graph on figure 10.1 which consists of two internal edges of the same lengths ℓ and two half-lines attached at the central vertex (in the figure lines with arrows). There is standard coupling at the central vertex and Dirichlet coupling at the loose ends of the internal edges. We can see that the central vertex is balanced, hence the graph is non-Weyl. We will prove it by constructing explicitly the resonance condition. Let us denote the wavefunction components on the internal edges by $f_1(x)$, $f_2(x)$ with $x = 0$ at the loose end and $x = \ell$ at the central vertex. We denote the wavefunction components on the half-lines $g_1(x)$, $g_2(x)$ with $x = 0$ in the central vertex.

We have (using the Dirichlet condition)

$$f_1(x) = a_1 \sin kx, \quad f_2(x) = a_2 \sin kx, \quad g_1(x) = d_1 e^{ikx}, \quad g_2(x) = d_2 e^{ikx}.$$

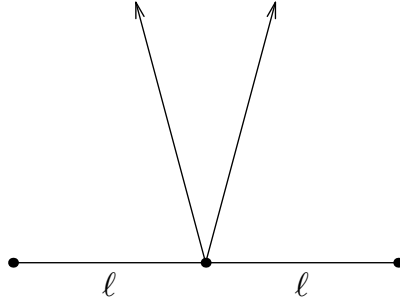


Fig. 10.1. Example: two internal edges and two half-lines.

Therefore we obtain

$$\begin{aligned} f_1(\ell) &= a_1 \sin k\ell, & f_2(\ell) &= a_2 \sin k\ell, \\ -f_1'(\ell) &= -a_1 k \cos k\ell, & -f_2'(\ell) &= -a_2 k \cos k\ell, \\ g_1(0) &= d_1, & g_2(0) &= d_2, & g_1'(0) &= ikd_1, & g_2'(0) &= ikd_2. \end{aligned}$$

This gives the following system of equations

$$\begin{pmatrix} 0 & 0 & 1 & -1 \\ \sin k\ell & 0 & -1 & 0 \\ 0 & \sin k\ell & -1 & 0 \\ -k \cos k\ell & -k \cos k\ell & ik & ik \end{pmatrix} \begin{pmatrix} a_1 \\ a_2 \\ d_1 \\ d_2 \end{pmatrix} = 0.$$

The determinant of the above matrix gives the condition of the solvability of the above equation, which is the resonance condition.

$$-2k \cos k\ell \sin k\ell + 2ik \sin^2 k\ell = 0,$$

which can be rewritten as

$$ik(1 - e^{-2ik\ell}) = 0.$$

We see that there is not the term with $e^{2ik\ell}$, so W in the asymptotics in the Theorem 10.2 is ℓ instead of 2ℓ .

10.2 Permutation symmetric coupling

Now we will show the result of [DEL10] which graphs with permutation symmetric coupling are non-Weyl. We can revise that graphs with permutation symmetric coupling have the coupling matrix $U_j = a_j J + b_j I$, where J is the matrix with all entries equal to one and I is the identity matrix and a_j, b_j are complex constants. These constants can be different for each vertex but for the sake of simplicity we will omit the index j .

Theorem 10.5 *Let us consider the graph with coupling matrices $U_j = a_j J + b_j I$ and with n_j internal edges and m_j half-lines in the j -th vertex. Then the graph is non-Weyl iff there exists a vertex for which $m_j = n_j$ and one of the following possibilities holds true*

a)

$$U_j = \frac{1}{m_j} J - I, \quad \text{i.e.} \quad f_i = f_j \quad \forall i, j \leq 2n, \quad \sum_{j=1}^{2n} f'_j = 0.$$

b)

$$U_j = -\frac{1}{m_j} J + I, \quad \text{i.e.} \quad f'_i = f'_j \quad \forall i, j \leq 2n, \quad \sum_{j=1}^{2n} f_j = 0.$$

Proof: In the proof we will omit the subscript j and we consider one particular vertex. The effective vertex coupling matrix is according to the equation (9.3)

$$\tilde{U}(k) = \frac{ab(1-k) - a(1+k)}{(am+b)(1-k) - (k+1)} J_{n \times n} + bI_{n \times n}.$$

We have used the inverse of the matrix (10.8).

Now we will use the fact that eigenvalues of the matrix $U = aJ_{n \times n} + bI_{n \times n}$ are b with multiplicity $n-1$ and $na+b$. We will compare these eigenvalues to $\frac{1 \pm k}{1 \mp k}$. Clearly, b cannot equal to neither of these values. For the second eigenvalue we have

$$an \frac{b(1-k) - (1+k)}{(am+b)(1-k) - (1+k)} + b = \frac{1 \pm k}{1 \mp k}.$$

We have for the case with the upper sign

$$[a(m+n) + b]b(1-k) - (an + am + 2b)(1+k) = -\frac{(1+k)^2}{1-k},$$

which cannot be satisfied for any value of the parameters a, b, n and m . The case with the lower sign gives

$$\{[a(n+m) + b]b + 1\}(1-k) - (1+k)(an+b) = (am+b) \frac{(1-k)^2}{1+k}.$$

This equation has to be fulfilled for all k and hence we obtain

$$\begin{aligned} an + b = 0, \quad am + b = 0 &\quad \Rightarrow \quad n = m, \\ [a(n+m) + b]b + 1 = 0 &\quad \Rightarrow \quad (an)^2 = 1, \end{aligned}$$

and hence the graph is non-Weyl iff $U = \pm \frac{1}{n} J_{n \times n} \mp I_{n \times n}$.

Q.E.D.

To conclude, this result shows that non-Weyl behaviour is quite exceptional. We have it either for standard (Kirchhoff) coupling or for its counterpart ‘‘anti-Kirchhoff’’ coupling. For both cases, there has to be the same number of internal and external edges in the vertex.

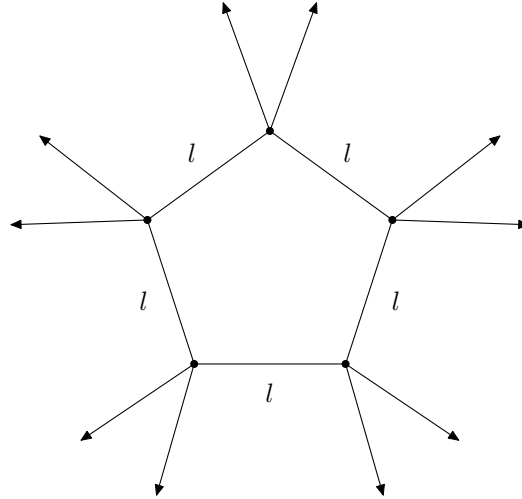


Fig. 10.2. A polygon considered in subsection 10.3. Reproduced from [DEL10].

10.3 Example with a regular polygon

We take the following example from [DEL10]. Let us consider a graph Γ_n which is a regular n -gon with all the internal edges of lengths ℓ (see figure 10.2). There are two half-lines attached at each vertex and we assume standard coupling at each vertex. Since the graph has two internal and two external edges attached to each vertex, it is by Corollary 10.3 non-Weyl. In this section, we will show that the “effective size” of the graph Γ_n , the coefficient W by the leading term of the asymptotics (10.6), depends on n . Unlike the criterion, whether the graph is non-Weyl, which was given by the (local) vertex properties of the graph, the effective size depends on global parameters of the graph.

Theorem 10.6 *The effective size of the graph Γ_n is given by*

$$W_n = \begin{cases} n\ell/2 & \text{if } n \not\equiv 0 \pmod{4}, \\ (n-2)\ell/2 & \text{if } n \equiv 0 \pmod{4}. \end{cases}$$

Proof: We will find the resonance condition by Bloch-Floquet decomposition of the Hamiltonian with respect to the cyclic rotational group \mathbb{Z}_n . We define by T the rotational operator in $L^2(\Gamma_n)$ which maps the vertex to the next one. The whole space $L^2(\Gamma_n)$ is an orthogonal direct sum of spaces

$$\mathcal{H}_\omega = \{f \in L^2(\Gamma_n) : Tf = \omega f\}.$$

ω with $\omega^n = 1$ are the eigenvalues of the operator T . Now we restrict our attention to the unit cell which consists of one internal edge and two half-lines (see figure 10.3). We also need to consider the neighbouring internal edge denoted by dashed line.

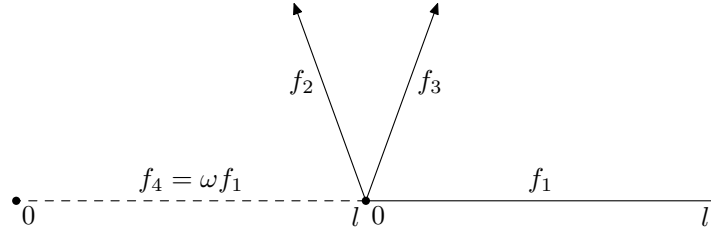


Fig. 10.3. The unit cell considered in subsection 10.3. Reproduced from [DEL10].

The resonance eigenfunction f on this cell has components (see figure 10.3)

$$\begin{aligned} f_1(x) &= ae^{ikx} + be^{-ikx}, & 0 \leq x \leq \ell, \\ f_2(x) &= (a+b)e^{ikx}, & 0 \leq x < \infty, \\ f_3(x) &= (a+b)e^{ikx}, & 0 \leq x < \infty, \\ f_4(x) &= \omega f_1(x), & 0 \leq x \leq \ell, \end{aligned}$$

The standard coupling condition gives

$$\begin{aligned} \omega a e^{ik\ell} + \omega b e^{-ik\ell} &= a + b, \\ \omega a e^{ik\ell} - \omega b e^{-ik\ell} &= 2(a + b) + a - b. \end{aligned}$$

The condition of solvability of the above system is given by determinant of certain 2×2 matrix is equal to zero. The direct computation of the determinant gives

$$-2(\omega^2 + 1) + 4\omega e^{-ik\ell} = 0. \quad (10.9)$$

From the condition we can see that the graph is non-Weyl for all n , because the term with $e^{ik\ell}$ is missing. If $\omega^2 + 1 \neq 0$ then the contribution of this cell to the effective size of the whole graph is $\ell/2$, if $\omega^2 + 1 = 0$ then it does not contribute to the effective size. We obtain the effective size of the whole graph as the sum of the contributions of particular cells. Clearly, there exists such ω for which $\omega^2 + 1 = 0$ iff $n = 0 \pmod{4}$. From this, the claim of the theorem follows. Q.E.D.

More complex study of the effective size can be found in [Lip16, Lip15]. In [Lip16] bounds on the effective size are found. The paper [Lip15] in examples shows how to obtain the effective size using the pseudo-orbits.

10.4 Size reduction

The simple example of a non-Weyl graph is a graph which has a vertex of degree two connecting one internal edge and one half-line with standard coupling. Since the coupling condition prescribes continuity of the functional value and the derivative, there is no physical interaction in this vertex at all. Therefore, this internal edge and the half-line can be replaced by one half-line, which reduces the size of the graph (sum of the lengths of the internal edges). For a general

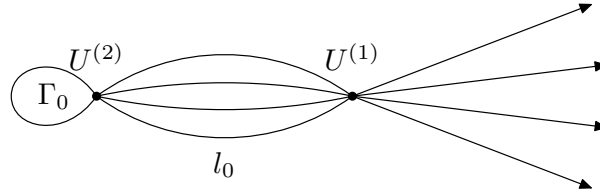


Fig. 10.4. Figure to size reduction in subsection 10.4. Reproduced from [DEL10].

coupling condition the size reduction is more complicated, one has to choose the proper subspace in which the quantum particle can propagate freely through the vertex. We show a result from [DEL10] which presents this size reduction for a large class of non-Weyl graphs.

We consider the flower-like graph in Figure 2.1. The coupling matrix in the only vertex of this graph is denoted by $U^{(1)}$. The internal edges can have different lengths. Let the smallest internal edge have length $2\ell_0$. Then we introduce another vertex in this graph in the distance ℓ_0 from the former vertex of this flower-like graph on all the internal edges and join these vertices to one (see Figure 10.4). The coupling matrix in this vertex is $U^{(2)}$. Let there be p half-lines, p internal edges between the vertices \mathcal{X}_1 and \mathcal{X}_2 with coupling matrices $U^{(1)}$ and $U^{(2)}$, respectively, and let $U^{(2)}$ be $q \times q$ matrix with $q \geq p$.

Theorem 10.7 *Let Γ be the graph described above with the coupling given by arbitrary $U^{(1)}$ and $U^{(2)}$. Let V be an arbitrary unitary $p \times p$ matrix, $V^{(1)} := \text{diag}(V, V)$ and $V^{(2)} := \text{diag}(I_{(q-p) \times (q-p)}, V)$ be $2p \times 2p$ and $q \times q$ block diagonal matrices, respectively. Then H on Γ is unitarily equivalent to the Hamiltonian H_V on topologically the same graph with the coupling given by the matrices $[V^{(1)}]^{-1}U^{(1)}V^{(1)}$ and $[V^{(2)}]^{-1}U^{(2)}V^{(2)}$.*

Proof: We define u an element of the domain of H , which consists of edge components u_1, \dots, u_p on the internal edges connected to \mathcal{X}_1 , f_1, \dots, f_p the components on the half-lines, and u_0 component on the rest of the graph Γ_0 . We define the following map

$$\begin{aligned} (u_1, \dots, u_p)^T &\mapsto (v_1, \dots, v_p)^T = V^{-1}(u_1, \dots, u_p)^T \\ (f_1, \dots, f_p)^T &\mapsto (g_1, \dots, g_p)^T = V^{-1}(f_1, \dots, f_p)^T \\ u_0(x) &\mapsto v_0(x) = u_0(x) \end{aligned}$$

which is a bijection of the domain H to H_V . One can check that the new Hamiltonian H_V satisfies the coupling conditions (2.1) with the matrices $[V^{(1)}]^{-1}U^{(1)}V^{(1)}$ and $[V^{(2)}]^{-1}U^{(2)}V^{(2)}$. Q.E.D.

Using this theorem we can transform the Hamiltonian on a non-Weyl graph with a given coupling matrix into the Hamiltonian with different coupling matrices which decouple into line standard condition. Therefore, one can “delete” some internal edges of the graph and hence reduce the size of the graph. For instance, one can choose a graph with standard coupling and a balanced vertex and by symmetrization of the components of the wavefunction on the internal edges and symmetrization of the components on the external edges obtain an equivalent Hamiltonian corresponding to this symmetrical subspace. This equivalent graph is a half-line and an internal edge connected by line standard condition.

11 Asymptotics of the resonances for magnetic graphs

The results from this section come from the letter [EL11]. We will consider slightly different setting than in the previous part of our review. We add magnetic potential to the graph. Again we consider a graph with N internal and M external edges. On this graph the Hamiltonian acts as $-d^2/dx^2$ on the infinite leads and as $-(d/dx + iA_j(x))^2$ on the internal edges. Here $A_j(x)$ is the tangent component of the vector magnetic potential. The reason why we choose magnetic potential as zero on the half-lines is that it can be transformed out by gauge transformation.

The domain of the Hamiltonian consists of functions in $W^{2,2}(\Gamma)$ which satisfy the coupling conditions

$$(U_j - I)\Psi_j + i(U_j + I)(\Psi'_j + i\mathcal{A}_j\Psi_j) = 0,$$

where Ψ_j and Ψ'_j are the corresponding vectors of functional values and derivatives, respectively, and \mathcal{A}_j is the matrix with limits of the magnetic potential A_j to the vertices on the diagonal and zeros outside diagonal.

Similarly to a non-magnetic graph, we can introduce a flower-like graph on Figure 2.1 and the coupling condition becomes

$$(U - I)\Psi + i(U + I)(\Psi' + i\mathcal{A}\Psi) = 0. \quad (11.1)$$

Here Ψ and Ψ' are the vectors of functional values and derivatives which have $2N + M$ entries and \mathcal{A} is the $(2N + M) \times (2N + M)$ diagonal matrix

$$\mathcal{A} = \text{diag}(A_1(0), -A_1(l_1), \dots, A_N(0), -A_N(l_N), 0, \dots, 0).$$

There is a trick how to obtain formally the same coupling condition as (2.1). We use local gauge transformation $\psi_j(x) \mapsto \psi_j(x)e^{-i\chi_j(x)}$ with $\chi_j(x)' = A_j(x)$ and we get rid of the term with \mathcal{A} . The new coupling condition is

$$(U_A - I)\Psi + i(U_A + I)\Psi' = 0, \quad U_A := \mathcal{F}U\mathcal{F}^{-1} \quad (11.2)$$

where

$$\mathcal{F} = \text{diag}(1, \exp(i\Phi_1), \dots, 1, \exp(i\Phi_N), 1, \dots, 1)$$

with magnetic fluxes $\Phi_j = \int_0^{l_j} A_j(x) dx$.

Similarly to the construction in Section 9 we can construct the effective coupling matrix $\tilde{U}(k)$ from the coupling matrix U_A .

Now we will prove a theorem on the resonance asymptotics of a graph with transformed coupling condition, which has a corollary about asymptotics of magnetic graphs.

Theorem 11.1 *Let us consider a graph Γ with N internal and M external edges and the coupling condition (11.2) with a $(2N + M) \times (2N + M)$ unitary matrix U . Let Γ_V be quantum graph with coupling (11.2) and the coupling matrix $V^{-1}UV$ where*

$$V = \begin{pmatrix} V_1 & 0 \\ 0 & V_2 \end{pmatrix}$$

is a unitary block-diagonal matrix consisting of a $2N \times 2N$ block V_1 and an $M \times M$ block V_2 . Then Γ is non-Weyl iff Γ_V is.

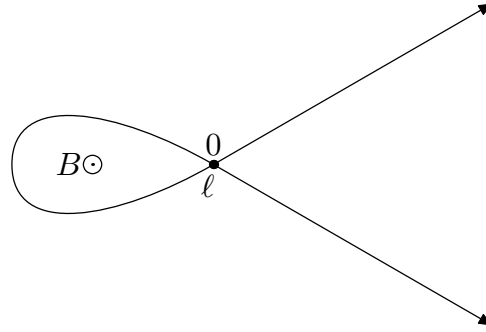


Fig. 11.1. Graph to example 11.3. Reproduced from [EL11].

Proof: Let the matrix U have the same block structure as in Section 9; U_1 , U_2 , U_3 and U_4 being the blocks corresponding to the coupling between internal edges (U_1), external edges (U_4) and mixed coupling (U_2 and U_3). The corresponding blocks of U_V are $V_1^{-1}U_1V_1$, $V_1^{-1}U_2V_2$, $V_2^{-1}U_3V_1$, and $V_2^{-1}U_4V_2$. From equation (9.3) we have

$$\begin{aligned} \tilde{U}_V(k) &= V_1^{-1}U_1V_1 - (1-k)V_1^{-1}U_2V_2[(1-k)V_2^{-1}U_4V_2 - (k+1)I]^{-1} \cdot \\ &\quad \cdot V_2^{-1}U_3V_1 = V_1^{-1}\tilde{U}(k)V_1, \end{aligned}$$

where $\tilde{U}_V(k)$ is the effective coupling matrix for U_V and $\tilde{U}(k)$ the effective coupling matrix for U . Similar matrices have the same eigenvalues and hence by Theorem 10.2 one graph is non-Weyl if and only if the second one is non-Weyl. Q.E.D.

Corollary 11.2 *Let Γ be a non-magnetic quantum graph with the coupling matrix U and the coupling condition (2.2). Let Γ_A be a magnetic graph with coupling matrix U and the coupling condition (11.1). Then the graph Γ_A has non-Weyl resonance asymptotics iff the graph Γ has non-Weyl resonance asymptotics. This holds true for any profile of the magnetic field.*

Proof: The coupling condition (11.1) is equivalent to (11.2) with transformed coupling matrix U_A . This transformation is of type used in Theorem 11.1, hence both effective coupling matrices have same eigenvalues. Q.E.D.

This corollary means that one cannot switch a non-Weyl graph to a Weyl one and vice versa using the magnetic field.

Now we will consider an example which shows that one can change the effective size of a non-Weyl graph. This example also appeared in [EL11].

Example 11.3 *Let us consider a graph which consists of one loop of length ℓ and two half-lines attached to this loop (see Figure 11.1). It is placed into the magnetic field with a constant value of the tangent component of the potential A . One can obtain the resonance condition by the method of complex scaling (see Section 5). We use the ansatz*

$$f(x) = e^{-iAx}(ae^{ikx} + be^{-ikx})$$

for the wavefunction component on the loop and $g_j(x) = c_j e^{ikx}$, $j = 1, 2$ for the wavefunction components on the half-lines. Substituting into the coupling conditions we obtain

$$\begin{aligned} ik[a - b - e^{-iA\ell}(ae^{ik\ell} - be^{-ik\ell}) + 2e^{-\theta/2}g_\theta(0)] &= 0, \\ a + b &= e^{-iA\ell}(ae^{ik\ell} + be^{-ik\ell}) = e^{-\theta/2}g_\theta(0), \end{aligned}$$

where g_θ denotes the scaled function on the half-line. The equation of solvability of the above system is the resonance condition

$$-2 \cos \Phi + e^{-ik\ell} = 0,$$

where we have denoted by $\Phi = A\ell$ the magnetic flux.

Clearly, the graph is non-Weyl, since there is not the term with $e^{ik\ell}$ in the resonance condition. One can have zero effective size (finite number of resonances) if $\Phi = \frac{\pi}{2} + n\pi$, $n \in \mathbb{Z}$, because the term with cosine disappears. The effective coupling matrix has the form

$$\tilde{U}_A(k) = \frac{1}{k+1} \begin{pmatrix} -k & e^{i\Phi} \\ e^{-i\Phi} & -k \end{pmatrix}. \quad (11.3)$$

Inspired by the previous example, we present a theorem from [EL11], which shows when the effective size of a one-loop graph is zero. One sees from equation (11.3) that the graph has zero effective size if the sum of the non-diagonal terms of \tilde{U}_A is zero.

Theorem 11.4 *The effective size of a graph with one loop is zero iff it is non-Weyl and its effective coupling matrix $\tilde{U}(k)$ satisfies $\tilde{u}_{12} + \tilde{u}_{21} = 0$.*

Proof: By a similar construction as in equation (10.7) only with the ansatz $f_j(x) = \alpha_j \sin kx + \beta_j \cos kx$ we obtain the resonance condition as $F(k) = 0$ with

$$\begin{aligned} F(k) := \det \left\{ \frac{1}{2} [(\tilde{U} - I) + k(\tilde{U} + I)] \begin{pmatrix} 0 & 0 \\ -i & 1 \end{pmatrix} e^{ik\ell} + \right. \\ \left. \frac{1}{2} [(\tilde{U} - I) - k(\tilde{U} + I)] \begin{pmatrix} 0 & 0 \\ i & 1 \end{pmatrix} e^{-ik\ell} + k(\tilde{U} + I) \begin{pmatrix} i & 0 \\ 0 & 0 \end{pmatrix} + (\tilde{U} - I) \begin{pmatrix} 0 & 1 \\ 0 & 0 \end{pmatrix} \right\}; \end{aligned}$$

The first term vanishes, because the graph is non-Weyl and the matrix $\tilde{U}(k)$ has eigenvalue $\frac{1-k}{1+k}$. To obtain zero effective size one needs to cancel the term without exponentials in the determinant. This can be obtained either from combination of the first two terms in equation for $F(k)$, which gives

$$-ik\tilde{u}_{12}(\tilde{u}_{22} - 1) + ik\tilde{u}_{12}(\tilde{u}_{22} + 1) = 2ik\tilde{u}_{12},$$

and the last two terms, which gives

$$ik[(\tilde{u}_{11} + 1)\tilde{u}_{21} - \tilde{u}_{21}(\tilde{u}_{11} - 1)] = 2ik\tilde{u}_{21}.$$

From this we obtain the condition $\tilde{u}_{12} + \tilde{u}_{21} = 0$.

Q.E.D.

12 Pseudo-orbit expansion for the eigenvalue condition in compact graphs

In this section, we turn to the graphs without half-lines and introduce the method of finding the secular equation via pseudo-orbits. In this construction, we will mostly follow [BHJ12].

Before we come to the pseudo-orbits, we start with defining notions which will be used in the formula for the secular determinant. Let us assume a graph Γ with N finite edges and no half-lines. We define a graph Γ_2 which is obtained from Γ by replacing each edge e_j by two directed edges b_j, \hat{b}_j (which we will call *bonds*) of the same length as e_j and with opposite directions. For each vertex of the graph Γ we define a *vertex-scattering matrix*.

Definition 12.1 *Let v be a vertex of the graph Γ connecting n finite edges. The wavefunction on each edge can be written as a combination of incoming and outgoing wave $f_j(x) = \alpha_j^{\text{in}} e^{-ikx} + \alpha_j^{\text{out}} e^{ikx}$, $j = 1, \dots, n$. Then the vertex-scattering matrix $\sigma^{(v)}(k)$ is the matrix which maps the vector of amplitudes of the incoming waves into the vector of amplitudes of the outgoing waves $\vec{\alpha}_v^{\text{out}} = \sigma^{(v)} \vec{\alpha}_v^{\text{in}}$, where $\vec{\alpha}_v^{\text{out}}$ is $n \times 1$ vector with entries α_j^{out} and, similarly, $\vec{\alpha}_v^{\text{in}}$ has entries α_j^{in} .*

The vertex-scattering matrix is in general energy-dependent, but for some special couplings it does not depend on energy. Now we present a result how this matrix is connected with the unitary coupling matrix.

Lemma 12.2 *Let us consider a graph Γ without half-lines and its vertex v connecting n (internal) edges. Let I_n denote $n \times n$ identity matrix. Let the coupling at the vertex v be described by condition (2.1) with the coupling matrix U_v . If we drop the sub- (super-)script v the connection between U and the vertex-scattering matrix σ is*

$$\sigma(k) = -[(1-k)U(k) - (1+k)I_n]^{-1}[(1+k)U(k) - (1-k)I_n].$$

Proof: We substitute to the equation (2.1) limits of functional values and derivatives at the vertex

$$\Psi_j = \alpha_j^{\text{in}} + \alpha_j^{\text{out}}, \quad \Psi'_j = ik(\alpha_j^{\text{out}} - \alpha_j^{\text{in}}).$$

We obtain

$$[(U - I_n) + k(U + I_n)]\alpha_j^{\text{in}} + [(U - I_n) - k(U + I_n)]\alpha_j^{\text{out}} = 0.$$

This leads to the above vertex-scattering matrix. Q.E.D.

Now we move to the oriented graph Γ_2 . On each bond b_j, \hat{b}_j we use the following ansatz which again corresponds to the combination of the incoming and outgoing edge.

$$\begin{aligned} f_{b_j}(x) &= \alpha_{b_j}^{\text{in}} e^{-ikx_{b_j}} + \alpha_{b_j}^{\text{out}} e^{ikx_{b_j}}, \\ f_{\hat{b}_j}(x) &= \alpha_{\hat{b}_j}^{\text{in}} e^{-ikx_{\hat{b}_j}} + \alpha_{\hat{b}_j}^{\text{out}} e^{ikx_{\hat{b}_j}}, \end{aligned}$$

Here x_{b_j} is the coordinate on the bond b_j and $x_{\hat{b}_j}$ is the coordinate on the bond \hat{b}_j . Since both bond correspond to the same edge e_j of the graph Γ , the functional values on both bonds must be the same. The points $x_{b_j} = 0$ and $x_{\hat{b}_j} = 0$ are at the opposite vertices of the edge, hence we have the relation $x_{b_j} + x_{\hat{b}_j} = \ell_{b_j}$ with the length of the bonds $\ell_{b_j} \equiv \ell_j$. For the correspondence of the

functional values we obtain $f_{b_j}(x_{b_j}) = f_{\hat{b}_j}(\ell_j - x_{\hat{b}_j})$ and this leads to the following relations between the incoming and outgoing coefficients.

$$\alpha_{b_j}^{\text{in}} = e^{ik\ell_j} \alpha_{\hat{b}_j}^{\text{out}}, \quad \alpha_{\hat{b}_j}^{\text{in}} = e^{ik\ell_j} \alpha_{b_j}^{\text{out}}. \quad (12.1)$$

Furthermore, we define several matrices, which will be used in the secular equation.

Definition 12.3 *The matrix $\Sigma(k)$ is an energy-dependent block-diagonalizable $2N \times 2N$ matrix with blocks $\sigma^v(k)$. The similarity transformation, under which the matrix is block-diagonal, is given as a transformation between the basis*

$$\vec{\alpha} = (\alpha_{b_1}^{\text{in}}, \dots, \alpha_{b_N}^{\text{in}}, \alpha_{\hat{b}_1}^{\text{in}}, \dots, \alpha_{\hat{b}_N}^{\text{in}})^{\text{T}}$$

and the basis

$$(\alpha_{b_{v_1 1}}^{\text{in}}, \dots, \alpha_{b_{v_1 d_1}}^{\text{in}}, \alpha_{b_{v_2 1}}^{\text{in}}, \dots, \alpha_{b_{v_2 d_2}}^{\text{in}}, \dots)^{\text{T}},$$

where $b_{v_1 j}$ is the j -th edge ending in the vertex v_1 .

Moreover, we define three $2N \times 2N$ matrices $Q = \begin{pmatrix} 0 & I_N \\ I_N & 0 \end{pmatrix}$, scattering matrix $S(k) = Q\Sigma(k)$ and

$$L = \text{diag}(\ell_1, \dots, \ell_N, \ell_1, \dots, \ell_N).$$

The defined matrices will be subject of the following theorem on the secular equation.

Theorem 12.4 *The secular condition is given by*

$$\det(e^{ikL}Q\Sigma(k) - I_{2N}) = 0.$$

Proof: If we introduce the vectors

$$\vec{\alpha}_b^{\text{in}} = (\alpha_{b_1}^{\text{in}}, \dots, \alpha_{b_N}^{\text{in}})^{\text{T}}$$

and

$$\vec{\alpha}_b^{\text{out}} = (\alpha_{b_1}^{\text{out}}, \dots, \alpha_{b_N}^{\text{out}})^{\text{T}},$$

we may subsequently write

$$\begin{pmatrix} \vec{\alpha}_b^{\text{in}} \\ \vec{\alpha}_b^{\text{in}} \end{pmatrix} = e^{ikL} \begin{pmatrix} \vec{\alpha}_b^{\text{out}} \\ \vec{\alpha}_b^{\text{out}} \end{pmatrix} = e^{ikL} Q \begin{pmatrix} \vec{\alpha}_b^{\text{out}} \\ \vec{\alpha}_b^{\text{out}} \end{pmatrix} = e^{ikL} Q\Sigma(k) \begin{pmatrix} \vec{\alpha}_b^{\text{in}} \\ \vec{\alpha}_b^{\text{in}} \end{pmatrix}.$$

In the first equation we used relations (12.1). The second one uses definition of the matrix Q . The last equation uses definition of the matrix $\Sigma(k)$, since the matrices $\sigma^{(v)}$ map the vector of amplitudes of the incoming waves into the vector of the amplitudes of the outgoing waves. Now we realize that the vector of the *lhs* is the same as the vector on the *rhs*. The equation can be rewritten as

$$(e^{ikL}Q\Sigma(k) - I_{2N}) \begin{pmatrix} \vec{\alpha}_b^{\text{in}} \\ \vec{\alpha}_b^{\text{in}} \end{pmatrix} = 0.$$

We obtain the secular equation as the condition of the solvability of this system of equations. Q.E.D.

In the previous theorem, we obtained the secular equation in the terms of certain matrices. In the following part of the section, we rewrite the determinant in the terms of pseudo-orbits. Following the notation of [BHJ12] we define periodic orbits, pseudo-orbits and irreducible pseudo-orbits.

Definition 12.5 *Let us describe the bond b by end vertices $b = (u, v)$; let the origin be $o(b) = u$ and terminus $t(b) = v$. A periodic orbit γ on the graph Γ_2 is a closed path that begins and ends in the same vertex. We can denote it by the bonds that it subsequently contains, e.g. $\gamma = (b_1, b_2, \dots, b_n)$; this means $t(b_i) = o(b_{i+1})$, $i = 1, \dots, n-1$ and $t(b_n) = o(b_1)$. Cyclic permutation of bonds does not change the periodic orbit. A pseudo-orbit is a collection of periodic orbits ($\tilde{\gamma} = \{\gamma_1, \gamma_2, \dots, \gamma_m\}$). An irreducible pseudo-orbit $\bar{\gamma}$ is a pseudo-orbit that does not contain any bond more than once. The metric length of a periodic orbit is defined as $\ell_\gamma = \sum_{b_j \in \gamma} \ell_{b_j}$; the length of a pseudo-orbit is the sum of the lengths of all periodic orbits the pseudo-orbit is composed of. We denote the product of scattering amplitudes along the periodic orbit $\gamma = (b_1, b_2, \dots, b_n)$ as $A_\gamma = S_{b_2 b_1} S_{b_3 b_2} \dots S_{b_1 b_n}$, where $S_{b_i b_j}$ denotes the entry of the matrix $S(k)$ in the row corresponding to the bond b_i and column corresponding to the bond b_j . For a pseudo-orbit we define $A_{\tilde{\gamma}} = \prod_{\gamma_j \in \tilde{\gamma}} A_{\gamma_j}$. By $m_{\bar{\gamma}}$ we denote the number of periodic orbits in the pseudo-orbit $\bar{\gamma}$. The set of irreducible pseudo-orbits also contains the null orbit, an irreducible pseudo-orbit on zero edges, with $m_{\bar{\gamma}} = 0$, $\ell_{\bar{\gamma}} = 0$ and $A_{\bar{\gamma}} = 1$.*

Now we rewrite the Theorem 12.4 in the terms of irreducible pseudo-orbits.

Theorem 12.6 *The condition for the eigenvalues of the graph is given by*

$$\sum_{\bar{\gamma}} (-1)^{m_{\bar{\gamma}}} A_{\bar{\gamma}}(k) e^{ik\ell_{\bar{\gamma}}} = 0,$$

where the sum goes over all irreducible pseudo-orbits $\bar{\gamma}$.

Proof: We rewrite the determinant in Theorem 12.4 using permutation

$$\det(I - U(k)) = \sum_{\rho \in S_{2N}} \text{sgn}(\rho) \prod_{b=1}^{2N} [I - U(k)]_{\rho(b), b}, \quad (12.2)$$

where S_{2N} is the set of permutation of $2N$ elements, $U(k) = e^{ikL} S(k)$, the indices of the matrix $\rho(b)$, b label the bonds. Each permutation can be uniquely determined by disjoint cycles.

$$\rho = (b_1, b_2, \dots, b_{n_1})(b_{n_1+1}, \dots, b_{n_1+n_2}) \dots (b_{(\sum_{j=1}^{m_\rho} n_j)+1}, \dots, b_{\sum_{j=1}^{m_\rho} n_j}), \quad (12.3)$$

where m_ρ denotes the number of cycles of the permutation, the parentheses in the above equation denote the cycle. The notation means $\rho(b_i) = b_{i+1}$, $i = 1, \dots, n_1 - 1$, $\rho(b_{n_1}) = b_1$ and similarly for the other cycles. This representation is unique up to permutation of each cycle and no bond is used more than once.

We have $[U(k)]_{\rho(b), b} \neq 0$ only if $o(\rho(b)) = t(b)$, which means that the bond $\rho(b)$ is connected to the bond b . Hence a non-identical permutation ρ can have a non-zero contribution only if $o(\rho(b)) = t(b)$. Therefore, we can interpret the permutation (12.3) as irreducible pseudo-orbit

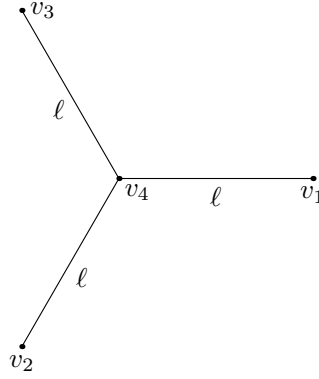


Fig. 12.1. Figure of a graph in Subsection 12.1: star graph with three edges.

(no directed bond is included more than once) and each disjoint cycle corresponds to periodic orbit in this irreducible pseudo-orbit.

We can rewrite (12.2) as

$$\sum_{\rho \in S_{2N}} \operatorname{sgn}(\rho) (-1)^{\sum_{j=1}^{m_\rho} n_j} (U_{b_2 b_1} U_{b_3 b_2} \cdots U_{b_1 b_{n_1}}) (U_{b_{n_1+2} b_{n_1+1}} U_{b_{n_1+3} b_{n_1+2}} \cdots U_{b_{n_1+1} b_{n_1+n_2}}) \cdots$$

Since now $U_{b_2 b_1} = e^{ik\ell_{b_2}} S_{b_2 b_1}$, we obtain the term $e^{ik\ell_{\bar{\gamma}}} A_{\bar{\gamma}}$. The sign is obtained by

$$\operatorname{sgn}(\rho) (-1)^{\sum_{j=1}^{m_\rho} n_j} = (-1)^{\sum_{j=1}^{m_\rho} (n_j+1)} (-1)^{\sum_{j=1}^{m_\rho} n_j} = (-1)^{m_\rho},$$

since the sign of one-cycle permutation is $(-1)^{n_j+1}$.

Q.E.D.

12.1 Example: star graph with three edges

We illustrate the method of finding the secular equation using pseudo-orbits in a simple example. Consider a star graph Γ consisting of three edges of the same length ℓ with δ -condition of strength α in the middle vertex (v_4 in Figure 12.1) and Dirichlet conditions at the loose ends of the edges (v_1, v_2 and v_3 in Figure 12.1).

First, we compute the vertex-scattering matrix for the middle vertex σ_4 . We use both approaches: we compute it using Lemma 12.2 and directly. Using expression for the unitary coupling matrix in Section 3 we have $U = \frac{2}{3+i\alpha} J_3 - I_3$. We recall that by J_3 we denote the 3×3 matrix with all entries equal to 1 and by I_3 the 3×3 identity matrix. From Lemma 12.2 using (10.8) and $J_3^2 = 3J_3$

$$\begin{aligned} \sigma_4 &= -[(1-k)U - (1+k)I_3]^{-1} [(1+k)U - (1-k)I_3] = \\ &= - \left[\frac{2(1-k)}{3+i\alpha} J_3 - 2I_3 \right]^{-1} \left[\frac{2(1+k)}{3+i\alpha} J_3 - 2I_3 \right] = \end{aligned}$$

$$\begin{aligned}
&= - \left(\frac{(1-k)(1+k)}{(-3k-i\alpha)(3+i\alpha)} 3 - \frac{1-k}{-3k-i\alpha} - \frac{1+k}{3+i\alpha} \right) J_3 - I_3 = \\
&= \frac{3(1-k^2) - (1-k)(3+i\alpha) + (3k+i\alpha)(1+k)}{(3k+i\alpha)(3+i\alpha)} J_3 - I_3 = \frac{2k}{3k+i\alpha} J_3 - I_3.
\end{aligned}$$

Now we compute the vertex scattering matrix directly. We use the ansatz on the edges $f_j(x) = \alpha_j^{\text{in}} e^{-ikx} + \alpha_j^{\text{out}} e^{ikx}$ and the coupling conditions become

$$\begin{aligned}
\alpha_j^{\text{in}} + \alpha_j^{\text{out}} &= \alpha_i^{\text{in}} + \alpha_i^{\text{out}}, \quad i, j \in 1, 2, 3, \\
ik \sum_{j=1}^3 (\alpha_j^{\text{out}} - \alpha_j^{\text{in}}) &= \alpha(\alpha_i^{\text{in}} + \alpha_i^{\text{out}}).
\end{aligned}$$

From the first of the above equations we have

$$\alpha_j^{\text{out}} = \alpha_i^{\text{in}} + \alpha_i^{\text{out}} - \alpha_j^{\text{in}}$$

and substituting it into the second one

$$3ik(\alpha_i^{\text{in}} + \alpha_i^{\text{out}}) - 2ik \sum_{j=1}^3 \alpha_j^{\text{in}} = \alpha(\alpha_i^{\text{in}} + \alpha_i^{\text{out}}).$$

Hence

$$\alpha_i^{\text{out}} = -\frac{2ik}{\alpha - 3ik} \sum_{j=1}^3 \alpha_j^{\text{in}} - \alpha_i^{\text{in}},$$

from which we have

$$\sigma_4(k) = -\frac{2ik}{\alpha - 3ik} J_3 - I_3 = \frac{2k}{3k+i\alpha} J_3 - I_3. \quad (12.4)$$

The vertex scattering matrices for other vertices can be constructed easily; one substitutes to the expression in Lemma 12.2 $U = -1$ and finds $\sigma_1 = \sigma_2 = \sigma_3 = -1$.

The graph Γ_2 is in Figure 12.2. It consists of six bonds the ones without a hat have direction into the central vertex and those with a hat out from the central vertex.

The matrix Σ is

$$\Sigma = \begin{pmatrix} -\frac{k+i\alpha}{3k+i\alpha} & \frac{2k}{3k+i\alpha} & \frac{2k}{3k+i\alpha} & 0 & 0 & 0 \\ \frac{3k+i\alpha}{2k} & -\frac{k+i\alpha}{3k+i\alpha} & \frac{3k+i\alpha}{2k} & 0 & 0 & 0 \\ \frac{2k}{3k+i\alpha} & \frac{2k}{3k+i\alpha} & -\frac{k+i\alpha}{3k+i\alpha} & 0 & 0 & 0 \\ 0 & 0 & 0 & -1 & 0 & 0 \\ 0 & 0 & 0 & 0 & -1 & 0 \\ 0 & 0 & 0 & 0 & 0 & -1 \end{pmatrix}$$

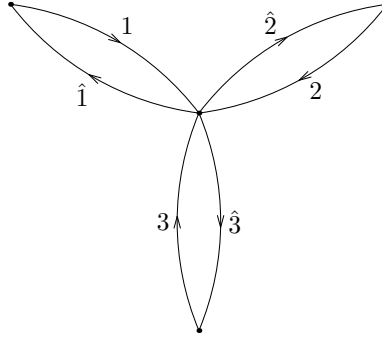


Fig. 12.2. Graph Γ_2 for example in Subsection 12.1: star graph with three edges. Reproduced from [Lip16].

The matrix $S = Q\Sigma$ is (rows and columns are denoted by the corresponding bonds)

$$S = \begin{array}{c|ccc|ccc} & 1 & 2 & 3 & \hat{1} & \hat{2} & \hat{3} \\ \hline 1 & 0 & 0 & 0 & -1 & 0 & 0 \\ 2 & 0 & 0 & 0 & 0 & -1 & 0 \\ 3 & 0 & 0 & 0 & 0 & 0 & -1 \\ \hat{1} & -\frac{k+i\alpha}{3k+i\alpha} & \frac{2k}{3k+i\alpha} & \frac{2k}{3k+i\alpha} & 0 & 0 & 0 \\ \hat{2} & \frac{2k}{3k+i\alpha} & -\frac{k+i\alpha}{3k+i\alpha} & \frac{2k}{3k+i\alpha} & 0 & 0 & 0 \\ \hat{3} & \frac{2k}{3k+i\alpha} & \frac{2k}{3k+i\alpha} & -\frac{k+i\alpha}{3k+i\alpha} & 0 & 0 & 0 \end{array}$$

The matrix S is constructed in the following way: the entry of the vertex scattering matrix corresponding to the way from bond b to the bond b' (which follows in the irreducible pseudo-orbit) is written into the column corresponding to b and row corresponding to b' . If these bonds correspond to the same edge of the graph Γ , we write the diagonal term of the vertex-scattering matrix, otherwise the non-diagonal term. If b is not followed by b' in any irreducible pseudo-orbit, then the entry in the b -th column and b' -th row is 0.

The secular condition is

$$\begin{aligned} 0 &= \det(e^{ikL}S - I_6) = \det \left[\begin{pmatrix} 0 & -I_3 \\ \sigma_4 & 0 \end{pmatrix} e^{ik\ell} - \begin{pmatrix} I_3 & 0 \\ 0 & I_3 \end{pmatrix} \right] = \\ &= \det \begin{pmatrix} -I_3 & -I_3 e^{ik\ell} \\ \sigma_4 e^{ik\ell} & -I_3 \end{pmatrix} = \det(I_3 + \sigma_4 e^{2ik\ell}) = \\ &= \det \begin{pmatrix} 1 + \frac{3k-i\alpha}{3k+i\alpha} e^{2ik\ell} & 0 & 0 \\ 0 & 1 - e^{2ik\ell} & 0 \\ 0 & 0 & 1 - e^{2ik\ell} \end{pmatrix}. \end{aligned}$$

In the rearrangements we used Laplace's formula to obtain a determinant 3×3 from a determinant 6×6 , the fact that eigenvalues of the matrix σ_4 are $\frac{3k-i\alpha}{3k+i\alpha}$ and -1 with multiplicity two (the eigenvalues of σ_4 can be simply obtained using the fact that eigenvalues of J_n are n and 0 of multiplicity $n-1$) and the fact that determinant of a matrix is not changed by similarity transformation. Determinant of the last matrix is obtained as multiplication of its diagonal entries. The

secular equation becomes

$$0 = (1 - e^{2ik\ell})^2(3k + i\alpha + (3k - i\alpha)e^{2ik\ell}) = -8e^{3ik\ell} \sin^2 k\ell (3k \cos k\ell + \alpha \sin k\ell)$$

We will rewrite the secular equation to a different form, which we will use later.

$$\begin{aligned} 0 &= \left(1 + \frac{3k - i\alpha}{3k + i\alpha} e^{2ik\ell}\right) (1 - e^{2ik\ell})^2 = 1 + \left(\frac{3k - i\alpha}{3k + i\alpha} - 2\right) e^{2ik\ell} + \\ &\quad + \left(1 - 2\frac{3k - i\alpha}{3k + i\alpha}\right) e^{4ik\ell} + \frac{3k - i\alpha}{3k + i\alpha} e^{6ik\ell} = \\ &= 1 - 3\frac{k + i\alpha}{3k + i\alpha} e^{2ik\ell} - 3\frac{k - i\alpha}{3k + i\alpha} e^{4ik\ell} + \frac{3k - i\alpha}{3k + i\alpha} e^{6ik\ell}. \end{aligned} \quad (12.5)$$

Now we come to the construction of the secular equation using pseudo-orbits. Let us consider the graph Γ_2 in Figure 12.2. Let us find the irreducible pseudo-orbits. One can simply realize that there are no irreducible pseudo-orbits on a odd number of bonds. This is because the graph is *bipartite*. Bipartite graph has two sets of vertices (in this example one set consists of the middle vertex and the second one from three other vertices) for which there are no edges between the vertices of one set, there are only edges between the vertex from the first set and the vertex from the second set. Another possible definition is that the graph can be colored with only two colors.

We have trivial irreducible pseudo-orbit on zero edges. We have the following irreducible pseudo-orbits on two bonds (the irreducible pseudo-orbits are divided by semicolons, one periodic orbit is in the parenthesis): $(1\hat{1})$; $(2\hat{2})$ and $(3, \hat{3})$. We have the following irreducible pseudo-orbits on four bonds: $(1\hat{1})(2\hat{2})$; $(1\hat{1})(3\hat{3})$; $(2\hat{2})(3\hat{3})$; $(1\hat{2}\hat{2}\hat{1})$; $(1\hat{3}\hat{3}\hat{1})$; $(2\hat{3}\hat{3}\hat{2})$. The first three consist of two periodic orbits and the last three of one periodic orbit. And finally, the irreducible pseudo-orbits on six bonds are $(1\hat{1})(2\hat{2})(3\hat{3})$; $(1\hat{2}\hat{2}\hat{1})(3\hat{3})$; $(1\hat{3}\hat{3}\hat{1})(2\hat{2})$; $(2\hat{3}\hat{3}\hat{2})(1\hat{1})$; $(1\hat{2}\hat{2}\hat{3}\hat{3}\hat{1})$ and $(1\hat{3}\hat{3}\hat{2}\hat{2}\hat{1})$. The first consists of three periodic orbits, next three of two periodic orbits and the last two of one periodic orbit.

Now we write the contributions of these irreducible pseudo-orbits to the secular condition. We compute the constant by each $e^{nik\ell}$ by Theorem 12.6.

$$\begin{aligned} e^{0ik\ell} &: 1, \\ e^{2ik\ell} &: 3(-1) \left(-\frac{k + i\alpha}{3k + i\alpha}\right) (-1)^1 = -3\frac{k + i\alpha}{3k + i\alpha}, \\ e^{4ik\ell} &: 3(-1)^2 \left(-\frac{k + i\alpha}{3k + i\alpha}\right)^2 (-1)^2 + 3(-1)^2 \left(\frac{2k}{3k + i\alpha}\right)^2 (-1)^1 = \\ &\quad \frac{3(k + i\alpha - 2k)(k + i\alpha + 2k)}{(3k + i\alpha)^2} = 3\frac{-k + i\alpha}{3k + i\alpha}, \\ e^{6ik\ell} &: (-1)^3 \left(-\frac{k + i\alpha}{3k + i\alpha}\right)^3 (-1)^3 + 3(-1)^3 \left(-\frac{k + i\alpha}{3k + i\alpha}\right) \left(\frac{2k}{3k + i\alpha}\right)^2 (-1)^2 + \\ &\quad + 2(-1)^3 \left(\frac{2k}{3k + i\alpha}\right)^3 (-1)^1 = \frac{-(k + i\alpha)^3 + 3(k + i\alpha)(2k)^2 + 2(2k)^3}{(3k + i\alpha)^3} = \\ &= \frac{(3k - i\alpha)(3k + i\alpha)^2}{(3k + i\alpha)^3} = \frac{3k - i\alpha}{3k + i\alpha}. \end{aligned}$$

This gives again condition (12.5).

13 Pseudo-orbit expansion for the resonance condition

The method of pseudo-orbit expansion can be adapted for finding the resonance condition for graphs with attached half-lines. The method is similar to the one in Section 12, only the vertex-scattering matrix is replaced by the effective vertex-scattering matrix. The method was developed in [Lip16] and it was illustrated in many examples in [Lip15].

We first define the effective vertex scattering matrix.

Definition 13.1 *Let us assume a graph Γ and its vertex v . Let there be n internal and m external edges emanating from v . The internal edges are parametrized by $(0, \ell_j)$ with $x = 0$ corresponding to v and the half-lines by $(0, \infty)$ with 0 corresponding to v . Let us assume solutions as combination of incoming and outgoing waves on the internal edges $f_j(x) = \alpha_j^{\text{in}} e^{-ikx} + \alpha_j^{\text{out}} e^{ikx}$, $j = 1, \dots, n$ and only outgoing waves on the external edges $g_s(x) = \beta_s e^{ikx}$, $s = 1, \dots, m$. Then the effective vertex-scattering matrix $\tilde{\sigma}^{(v)}$ is $n \times n$ matrix which on the internal edges maps the vectors of incoming waves into the vector of outgoing waves $\vec{\alpha}_v^{\text{out}} = \tilde{\sigma}^{(v)} \vec{\alpha}_v^{\text{in}}$, where $\vec{\alpha}_v^{\text{in}}$ and $\vec{\alpha}_v^{\text{out}}$ are vectors with entries α_j^{in} and α_j^{out} , respectively. At the same time, the coupling conditions (2.1) at the vertex v must be satisfied.*

Now we, similarly to the compact case, state its correspondence to the coupling matrix or, in fact, the effective coupling matrix which can be made from the unitary coupling matrix. For simplicity, we drop the sub- (super-) script v .

Theorem 13.2 *(general form of the effective vertex-scattering matrix)*

Let us consider a graph Γ with the vertex v , the unitary matrix U describing the coupling (2.1) in v and effective vertex-scattering matrix $\tilde{\sigma}(k)$ at v . Let there be n internal edges and m half-lines in v . Let $\tilde{U}(k)$ be the effective coupling matrix at v defined by (9.1). Then the effective vertex-scattering matrix is given by

$$\tilde{\sigma}(k) = -[(1-k)\tilde{U}(k) - (1+k)I_n]^{-1}[(1+k)\tilde{U}(k) - (1-k)I_n].$$

The inverse relation is

$$\tilde{U}(k) = [(1+k)\tilde{\sigma}(k) + (1-k)I_n][(1-k)\tilde{\sigma}(k) + (1+k)I_n]^{-1}.$$

Proof: We use the ansatz on the internal edges emanating from v as $f_j(x) = \alpha_j^{\text{in}} e^{-ikx} + \alpha_j^{\text{out}} e^{ikx}$ and on the external edges emanating from v as $g_j(x) = \beta_j e^{ikx}$. We express the vectors of functional values and outgoing derivatives

$$\Psi = \begin{pmatrix} \vec{\alpha}^{\text{in}} + \vec{\alpha}^{\text{out}} \\ \vec{\beta} \end{pmatrix} \quad \text{and} \quad \Psi' = ik \begin{pmatrix} -\vec{\alpha}^{\text{in}} + \vec{\alpha}^{\text{out}} \\ \vec{\beta} \end{pmatrix}.$$

From the coupling condition (2.1) we have

$$(U - I) \begin{pmatrix} \vec{\alpha}^{\text{in}} + \vec{\alpha}^{\text{out}} \\ \vec{\beta} \end{pmatrix} + ik(U + I) \begin{pmatrix} -\vec{\alpha}^{\text{in}} + \vec{\alpha}^{\text{out}} \\ \vec{\beta} \end{pmatrix} = 0.$$

This yields the set of equations

$$\begin{aligned} [U_1 - I_n - k(U_1 + I_n)]\bar{\alpha}^{\text{out}} + [(U_1 - I_n) + k(U_1 + I_n)]\bar{\alpha}^{\text{in}} + (1 - k)U_2\bar{\beta} &= 0, \\ (1 - k)U_3\bar{\alpha}^{\text{out}} + (1 + k)U_3\bar{\alpha}^{\text{in}} + [(U_4 - I_m) - k(U_4 + I_m)]\bar{\beta} &= 0. \end{aligned}$$

From the second equation we can express $\bar{\beta}$ and substitute it in the first one.

$$\begin{aligned} \{(1 - k)U_1 - (1 + k)I_n - (1 - k)U_2[(1 - k)U_4 - (1 + k)I_m]^{-1}(1 - k)U_3\}\bar{\alpha}^{\text{out}} + \\ + \{(1 + k)U_1 - (1 - k)I_n - (1 - k)U_2[(1 - k)U_4 - (1 + k)I_m](1 + k)U_3\}\bar{\alpha}^{\text{in}} &= 0, \end{aligned}$$

and using equation (9.1) we obtain the claim.

The inverse relation can be straightforwardly obtained multiplying the equation

$$\tilde{\sigma}(k) = -[(1 - k)\tilde{U}(k) - (1 + k)I_n]^{-1}[(1 + k)\tilde{U}(k) - (1 - k)I_n]$$

from the left by $[(1 - k)\tilde{U}(k) - (1 + k)I_n]$ and expressing $\tilde{U}(k)$.

Q.E.D.

Now we state a corollary that shows the form of the effective vertex-scattering matrix for standard coupling.

Corollary 13.3 *Let us assume a vertex v of the graph Γ which connects n internal edges and m half-lines. Let us assume standard coupling at v (i.e. $U = \frac{2}{n+m}J_{n+m} - I_{n+m}$). Then the effective vertex scattering matrix is $\tilde{\sigma}(k) = \frac{2}{n+m}J_n - I_n$, in particular, for a balanced vertex we obtain $\tilde{\sigma}(k) = \frac{1}{n}J_n - I_n$.*

Proof: There are two main ways how to prove the corollary. First uses Theorem 13.2; the second possibility is to directly compute the effective vertex-scattering matrix. Let us start with the first way.

Since we have $U = \frac{2}{n+m}J_{n+m} - I_{n+m}$, we can express the matrices $U_1 = \frac{2}{n+m}J_n - I_n$, $U_2 = \frac{2}{n+m}J_{n \times m}$, $U_3 = \frac{2}{n+m}J_{m \times n}$, $U_4 = \frac{2}{n+m}J_m - I_m$ as in Section 9. Here matrices $J_{n \times m}$ and $J_{m \times n}$ are $n \times m$ and $m \times n$ matrices, respectively, with all entries equal to 1. We can compute the effective coupling matrix by (9.1).

$$\begin{aligned} \tilde{U}(k) &= \frac{2}{n+m}J_n - I_n - \frac{2}{n+m}J_{n \times m} \left(\frac{2}{n+m}J_m - I_m - \frac{1+k}{1-k}I_m \right)^{-1} \\ &\quad \cdot \frac{2}{n+m}J_{m \times n} = \frac{2}{n+m}J_n - I_n - \left(\frac{2}{n+m} \right)^2 J_{n \times m} \cdot \\ &\quad \left(\frac{2}{n+m}J_m - \frac{2}{1-k}I_m \right)^{-1} J_{m \times n} = \frac{2}{n+m}J_n - I_n - \left(\frac{2}{n+m} \right)^2 J_{n \times m} \cdot \\ &\quad \cdot \left(-\frac{1-k}{2} \right) \left(-\frac{\frac{2}{n+m}}{\frac{2}{n+m}m - \frac{2}{1-k}}J_m + I_m \right) J_{m \times n} = \\ &= \frac{2}{n+m}J_n - I_n + \frac{2(1-k)}{(n+m)^2}J_{n \times m} \left(\frac{1-k}{mk+n}J_m + I_m \right) J_{m \times n} = \\ &= \frac{2}{n+m}J_n - I_n + \frac{2(1-k)}{(n+m)^2} \left(\frac{1-k}{mk+n}m^2 + m \right) J_n = \\ &= \frac{2[mk+n+(1-k)m]}{(n+m)(mk+n)}J_n - I_n = \frac{2}{km+n}J_n - I_n. \end{aligned}$$

We have used equation (10.8) and rules for multiplying matrices J .

Using this result we can find the effective vertex-scattering matrix.

$$\begin{aligned}
\tilde{\sigma}(k) &= - \left[\frac{2(1-k)}{km+n} J_n - (1-k)I_n - (1+k)I_n \right]^{-1} \cdot \\
&\quad \cdot \left[\frac{2(1+k)}{km+n} J_n - (1+k)I_n - (1-k)I_n \right] = \\
&= - \left[\frac{1-k}{km+n} J_n - I_n \right]^{-1} \left[\frac{1+k}{km+n} J_n - I_n \right] = \\
&= \left[-\frac{\frac{1-k}{km+n}}{\frac{(1-k)n}{km+n} - 1} J_n + I_n \right] \left[\frac{1+k}{km+n} J_n - I_n \right] = \\
&= \left[-\frac{1-k}{n-nk-km-n} J_n + I_n \right] \left[\frac{1+k}{km+n} J_n - I_n \right] = \\
&= \left[\frac{1-k}{k(n+m)} \frac{1+k}{km+n} n - \frac{1-k}{k(n+m)} + \frac{1+k}{km+n} \right] J_n - I_n = \\
&= \frac{n-k^2n-km-n+k^2m+kn+kn+km+k^2n+k^2m}{k(n+m)(km+n)} J_n - I_n = \\
&= \frac{2k^2m+2kn}{k(n+m)(km+n)} J_n - I_n = \frac{2}{n+m} J_n - I_n.
\end{aligned}$$

The form of the effective vertex-scattering matrix for a balanced vertex can be obtained easily.

Let us now prove the Theorem directly. We will proceed in the lines of the proof of Theorem 3.2 in [Lip15].

We use the ansatz as in Definition 13.1. From the coupling condition we obtain

$$\begin{aligned}
\alpha_j^{\text{out}} + \alpha_j^{\text{in}} &= \alpha_i^{\text{out}} + \alpha_i^{\text{in}} = \beta_s \quad \forall i, j = 1, \dots, n, \quad \forall s = 1, \dots, m, \\
ik \sum_{j=1}^n (\alpha_j^{\text{out}} - \alpha_j^{\text{in}}) &+ ik \sum_{s=1}^m \beta_s = 0.
\end{aligned}$$

For a fixed i we substitute for $\beta_s = \alpha_i^{\text{out}} + \alpha_i^{\text{in}}$ and $\alpha_j^{\text{out}} = \alpha_i^{\text{out}} + \alpha_i^{\text{in}} - \alpha_j^{\text{in}}$. We have

$$\sum_{j=1}^n (\alpha_i^{\text{out}} + \alpha_i^{\text{in}} - 2\alpha_j^{\text{in}}) + m(\alpha_i^{\text{out}} + \alpha_i^{\text{in}}) = 0.$$

We can express α_i^{out} to find the effective vertex-scattering matrix.

$$\alpha_i^{\text{out}} = \frac{2}{n+m} \left(\sum_{j=1}^n \alpha_j^{\text{in}} \right) - \alpha_i^{\text{in}},$$

from which the form of $\tilde{\sigma}(k)$ follows.

Q.E.D.

We define the oriented graph Γ_2 similarly to Section 12. Each edge of the compact part of the graph Γ is replaced by two bonds of the same length and opposite direction. The rest of the

construction is also similar to Section 12, only the vertex-scattering matrix is replaced by the effective vertex-scattering matrix.

We define matrices $\tilde{\Sigma}(k)$ and $\tilde{S}(k)$.

Definition 13.4 *The matrix $\tilde{\Sigma}(k)$ is an energy-dependent block-diagonalizable $2N \times 2N$ matrix with blocks $\tilde{\sigma}^v(k)$. The similarity transformation, under which the matrix is block-diagonal, is given as a transformation between the basis*

$$\vec{\alpha} = (\alpha_{b_1}^{\text{in}}, \dots, \alpha_{b_N}^{\text{in}}, \alpha_{\tilde{b}_1}^{\text{in}}, \dots, \alpha_{\tilde{b}_N}^{\text{in}})^{\text{T}}$$

and the basis

$$(\alpha_{b_{v_1 1}}^{\text{in}}, \dots, \alpha_{b_{v_1 d_1}}^{\text{in}}, \alpha_{b_{v_2 1}}^{\text{in}}, \dots, \alpha_{b_{v_2 d_2}}^{\text{in}}, \dots)^{\text{T}},$$

where $b_{v_1 j}$ is the j -th edge ending in the vertex v_1 .

The scattering matrix is $\tilde{S}(k) = Q\tilde{\Sigma}(k)$.

Other matrices were defined in Section 12. Now we can state the theorem on the resonance condition.

Theorem 13.5 *The resonance condition is given by*

$$\det(e^{ikL}Q\tilde{\Sigma}(k) - I_{2N}) = 0.$$

Proof: The proof is exactly the same as the proof of Theorem 12.4, only Σ is replaced by $\tilde{\Sigma}$. Q.E.D.

Also definitions of periodic orbits, pseudo-orbits and irreducible pseudo-orbits from Definition 12.5 can be used unchanged. The only difference is that the scattering amplitude is defined by the matrix $\tilde{S}(k)$, i.e. $A_{\bar{\gamma}} = \tilde{S}_{b_2 b_1} \tilde{S}_{b_3 b_2} \dots \tilde{S}_{b_1 b_n}$, where $\tilde{S}_{b_i b_j}$ denotes the entry of the matrix $\tilde{S}(k)$.

After these changes Theorem 12.6 can be used to obtain the resonance condition.

Theorem 13.6 *The condition for the resolvent resonances of the graph is given by*

$$\sum_{\bar{\gamma}} (-1)^{m_{\bar{\gamma}}} A_{\bar{\gamma}}(k) e^{ik\ell_{\bar{\gamma}}} = 0,$$

where the sum goes over all irreducible pseudo-orbits $\bar{\gamma}$.

Proof: The proof is exactly the same as the proof of Theorem 12.6, only definition of the scattering amplitudes is different. Q.E.D.

13.1 Example: triangle with attached leads – pseudo-orbit expansion

Let us return once again to the example in Figure 5.3 studied in Subsections 5.2 and 6.2. We will show how the resonance condition can be obtained by the method of pseudo-orbit expansion.

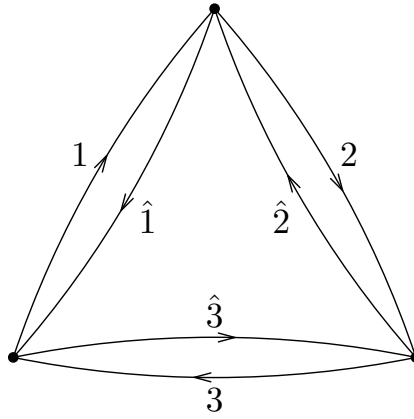


Fig. 13.1. Figure to the example in Subsection 13.1 – graph Γ_2 . Reproduced from [Lip15].

Let us first construct the effective vertex-scattering matrix. From Corollary 13.3 (we can use it since there is standard coupling at the vertices) we have

$$\tilde{\sigma}(k) = \frac{2}{2+1} J_2 - I_2 = \begin{pmatrix} -\frac{1}{3} & \frac{2}{3} \\ \frac{2}{3} & -\frac{1}{3} \end{pmatrix}.$$

Notice that for the case of standard coupling the effective vertex-scattering matrix is not energy dependent.

Graph Γ_2 is shown in Figure 13.1. Each internal edge of the graph Γ was replaced by two bonds. The matrix $\tilde{S} = Q\tilde{\Sigma}$ is

$$\tilde{S} = \begin{array}{c|cccccc} & 1 & 2 & 3 & \hat{1} & \hat{2} & \hat{3} \\ \hline 1 & 0 & 0 & 2/3 & -1/3 & 0 & 0 \\ 2 & 2/3 & 0 & 0 & 0 & -1/3 & 0 \\ 3 & 0 & 2/3 & 0 & 0 & 0 & -1/3 \\ \hat{1} & -1/3 & 0 & 0 & 0 & 2/3 & 0 \\ \hat{2} & 0 & -1/3 & 0 & 0 & 0 & 2/3 \\ \hat{3} & 0 & 0 & -1/3 & 2/3 & 0 & 0 \end{array}$$

Here we have denoted the columns and rows of this matrix by bonds to which they correspond. The matrix $L = \ell I_6$, hence $e^{ikL} = e^{ik\ell} I_6$. The resonance condition can be obtained by Theorem 13.5.

Now we use the pseudo-orbits to obtain this condition. There is a trivial irreducible pseudo-orbit on zero bonds. There are three irreducible pseudo-orbits on two bonds: $(1\hat{1})$; $(2, \hat{2})$ and $(3\hat{3})$. For these pseudo-orbits, the scattering amplitudes in both vertices are $-1/3$ for both vertices (we take the diagonal terms of the effective vertex-scattering matrix), $m_{\tilde{\gamma}} = 1$ and the contribution to the resonance condition for all three irreducible pseudo-orbits is the same. Hence the coefficient by $e^{2ik\ell}$ is $(-1/3)^2(-1)^3$. Similarly, we find contributions for other irreducible

pseudo-orbits. There are two irreducible pseudo-orbits on three bonds (123) and $(\hat{1}\hat{3}\hat{2})$. We have the following six irreducible pseudo-orbits on four bonds: $(\hat{1}\hat{1})(\hat{2}\hat{2})$; $(\hat{1}\hat{1})(\hat{3}\hat{3})$; $(\hat{2}\hat{2})(\hat{3}\hat{3})$; $(12\hat{2}\hat{1})$; $(23\hat{3}\hat{2})$ and $(31\hat{1}\hat{3})$. And finally, there are the following eight irreducible pseudo-orbits on all six bonds: $(\hat{1}\hat{1})(\hat{2}\hat{2})(\hat{3}\hat{3})$; $(12\hat{2}\hat{1})(\hat{3}\hat{3})$; $(23\hat{3}\hat{2})(\hat{1}\hat{1})$; $(31\hat{1}\hat{3})(\hat{2}\hat{2})$; $(123)(\hat{1}\hat{3}\hat{2})$; $(123\hat{3}\hat{2}\hat{1})$; $(231\hat{1}\hat{3}\hat{2})$ and $(312\hat{2}\hat{1}\hat{3})$. Now we use the pseudo-orbits to obtain this condition. There is a trivial irreducible pseudo-orbit on zero bonds. There are three irreducible pseudo-orbits on two bonds: $(\hat{1}\hat{1})$; $(2, \hat{2})$ and $(\hat{3}\hat{3})$. For these pseudo-orbits, the scattering amplitudes in both vertices are $-1/3$ for both vertices (we take the diagonal terms of the effective vertex-scattering matrix), $m_{\bar{\gamma}} = 1$ and the contribution to the resonance condition for all three irreducible pseudo-orbits is the same. Hence the coefficient by $e^{2ik\ell}$ is $(-1/3)^2(-1)^1 3$. Similarly, we find contributions for other irreducible pseudo-orbits. There are two irreducible pseudo-orbits on three bonds (123) and $(\hat{1}\hat{3}\hat{2})$. We have the following six irreducible pseudo-orbits on four bonds: $(\hat{1}\hat{1})(\hat{2}\hat{2})$; $(\hat{1}\hat{1})(\hat{3}\hat{3})$; $(\hat{2}\hat{2})(\hat{3}\hat{3})$; $(12\hat{2}\hat{1})$; $(23\hat{3}\hat{2})$ and $(31\hat{1}\hat{3})$. And finally, there are the following eight irreducible pseudo-orbits on all six bonds: $(\hat{1}\hat{1})(\hat{2}\hat{2})(\hat{3}\hat{3})$; $(12\hat{2}\hat{1})(\hat{3}\hat{3})$; $(23\hat{3}\hat{2})(\hat{1}\hat{1})$; $(31\hat{1}\hat{3})(\hat{2}\hat{2})$; $(123)(\hat{1}\hat{3}\hat{2})$; $(123\hat{3}\hat{2}\hat{1})$; $(231\hat{1}\hat{3}\hat{2})$ and $(312\hat{2}\hat{1}\hat{3})$.

The coefficients by $e^{nik\ell}$ are the following.

$$\begin{aligned}
e^0 & : & 1, \\
e^{2ik\ell} & : & \left(-\frac{1}{3}\right)^2 (-1)^1 \cdot 3 = -\frac{1}{3}, \\
e^{3ik\ell} & : & \left(\frac{2}{3}\right)^3 (-1)^1 \cdot 2 = -\frac{16}{27}, \\
e^{4ik\ell} & : & \left(-\frac{1}{3}\right)^4 (-1)^2 \cdot 3 + \left(-\frac{1}{3}\right)^2 \left(\frac{2}{3}\right)^2 (-1)^1 \cdot 3 = -\frac{1}{9}, \\
e^{6ik\ell} & : & \left(-\frac{1}{3}\right)^6 (-1)^3 \cdot 1 + \left(-\frac{1}{3}\right)^4 \left(\frac{2}{3}\right)^2 (-1)^2 \cdot 3 + \\
& & + \left(\frac{2}{3}\right)^6 (-1)^2 \cdot 1 + \left(-\frac{1}{3}\right)^2 \left(\frac{2}{3}\right)^4 (-1)^1 \cdot 3 = \frac{1}{27}.
\end{aligned}$$

Hence the resonance condition is

$$0 = 1 - \frac{1}{3}e^{2ik\ell} - \frac{16}{27}e^{3ik\ell} - \frac{1}{9}e^{4ik\ell} + \frac{1}{27}e^{6ik\ell}.$$

One can compare the resonance condition to the resonance condition obtained in Subsection 5.2 and find

$$\begin{aligned}
& \sin \frac{k\ell}{2} (3 - e^{ik\ell}) (3 + 2e^{ik\ell} + e^{2ik\ell})^2 = -\frac{i}{2}e^{-\frac{ik\ell}{2}} (e^{ik\ell} - 1) (3 - e^{ik\ell}) \cdot \\
& \cdot (3 + 2e^{ik\ell} + e^{2ik\ell})^2 = -\frac{i}{2}e^{-\frac{ik\ell}{2}} (-27 + 9e^{2ik\ell} + 16e^{3ik\ell} + 3e^{4ik\ell} - e^{6ik\ell}) = \\
& = \frac{27i}{2}e^{-\frac{ik\ell}{2}} \left(1 - \frac{1}{3}e^{2ik\ell} - \frac{16}{27}e^{3ik\ell} - \frac{1}{9}e^{4ik\ell} + \frac{1}{27}e^{6ik\ell}\right).
\end{aligned}$$

14 Method of simplifying the resonance condition by deleting the bonds of the directed graph

In this section we present a method from [Lip16] which simplifies the graph Γ_2 . It can be used for graphs with standard coupling and at least one balanced vertex. One directed bond which ends in the balanced vertex is deleted and instead of it, there are one or more “ghost edges” introduced. These “ghost edges” allow for hopping the pseudo-orbit to another directed bond, but they do not contribute to the scattering amplitude.

Theorem 14.1 *Let us assume an equilateral graph (all the internal edges have lengths ℓ) Γ with standard coupling. Let us assume that no edge starts and ends in one vertex and no two vertices are connected by more than one edge. Let there be a balanced vertex v_2 of the graph Γ and let the bonds b_1, b_2, \dots, b_d in the corresponding graph Γ_2 end in the vertex v_2 . (Part of the corresponding graph Γ_2 is shown in Figure 14.1.) Then the following construction does not change the resonance condition.*

- We delete the bond $b_1 = (v_1, v_2)$ of the graph Γ_2 .
- We introduce “ghost edges” $\hat{b}'_1, \hat{b}'_1, \dots, \hat{b}'_1^{(d-1)}$ that start in v_1 and are connected to the bonds b_2, b_3, \dots, b_d , respectively (see Figure 14.2).
- The resonance condition is given by Theorem 13.6, while the irreducible pseudo-orbits are defined by Definition 12.5 with the following rules.

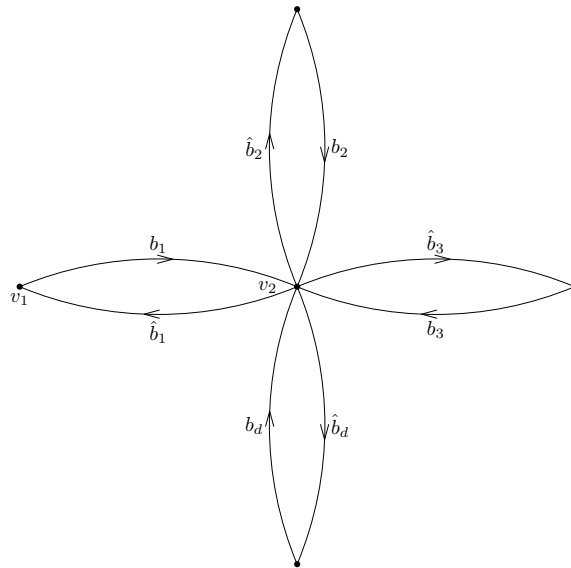


Fig. 14.1. Figure to Theorem 14.1. Part of the graph Γ_2 before deleting the bond b_1 . Reproduced from [Lip16].

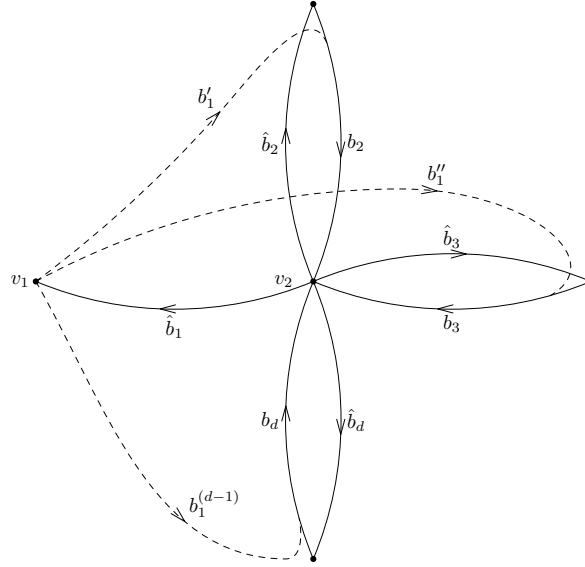


Fig. 14.2. Figure to Theorem 14.1. Part of the graph Γ_2 after deleting the bond b_1 and introducing “ghost edges” $b'_1, b''_1, \dots, b_1^{(d-1)}$. Reproduced from [Lip16].

- If a ghost edge is contained in the irreducible pseudo-orbit $\tilde{\gamma}$, its length does not contribute to the length of the irreducible pseudo-orbit $\ell_{\tilde{\gamma}}$.
- Let e.g. the “ghost edge” b'_1 be included in the irreducible pseudo-orbit $\tilde{\gamma}$. The scattering amplitude from the bond b ending in v_1 and the bond b_2 is the scattering amplitude on the previous graph Γ_2 from the bond b to b_1 taken with the opposite sign.
- Each “ghost edge” can be in the given irreducible pseudo-orbit used at most once.
- The procedure can be repeated; for each balanced vertex one bond can be deleted.

Proof: We will show how the matrix $\tilde{S} = Q\tilde{\Sigma}$ is changed by deleting the bond b_1 and introducing the “ghost edges”. Let us first show that the unitary transformation of \tilde{S} does not change the resonance condition. Since the graph is equilateral, the matrix e^{ikL} is multiple of the identity matrix $e^{ikL}I_{2N}$. Since the determinant is not changed by the unitary transformation, we have

$$\begin{aligned} \det(e^{ikL}V_1^{-1}Q\tilde{\Sigma}V_1 - I_{2N}) &= \det(e^{ikL}V_1^{-1}Q\tilde{\Sigma}V_1 - I_{2N}) = \\ &= \det[V_1^{-1}(e^{ikL}Q\tilde{\Sigma} - I_{2N})V_1] = \det(e^{ikL}Q\tilde{\Sigma} - I_{2N}). \end{aligned}$$

Our task is only to choose the matrix V_1 appropriately. Let us assume that we want to delete the bond b_1 ending in the balanced vertex v_2 and that bonds b_2, b_3, \dots, b_d also end in v_2 . We choose V_1 as $2n \times 2N$ matrix with entries

$$(V_1)_{ii} = 1 \quad \text{for } i = 1, \dots, 2N; \quad (V_1)_{b_i b_1} = 1 \quad \text{for } i = 2, \dots, d; \quad (V_1)_{ij} = 0 \quad \text{otherwise,}$$

where $(V_1)_{b_i b_1}$ is the entry with the row corresponding to the bond b_i and column corresponding to b_1 . It is not difficult to find that the inverse of this matrix has entries

$$(V_1^{-1})_{ii} = 1 \quad \text{for } i = 1, \dots, 2N; \quad (V_1^{-1})_{b_i b_1} = -1 \quad \text{for } i = 2, \dots, d; \\ (V_1^{-1})_{ij} = 0 \quad \text{otherwise.}$$

The eigenvalues of the matrix J_d are d with multiplicity 1 (the corresponding eigenvector has all entries equal to 1) and 0 with multiplicity $d - 1$. Hence the effective vertex-scattering matrix $\tilde{\sigma}_{v_2} = \frac{1}{d}J_d - I_d$ has one of its eigenvalues equal to 0 and it therefore has linearly dependent columns. Hence, if one multiplies it from the right by a matrix with all 1s on the diagonal and all entries in one of its column equal to 1, one gets a matrix which has one column with all 0s and other columns same as $\tilde{\sigma}_{v_2}$. The matrix \tilde{S} has entries of $\tilde{\sigma}_{v_2}$ in the columns corresponding to bonds ending at v_2 and rows corresponding to bonds starting from v_2 . By a similar argument, we obtain that $\tilde{S}V_1$ has 0s in the column corresponding to b_1 and other columns are the same as in \tilde{S} .

Now we find how the matrix is changed by multiplying from the left by V_1^{-1} . The matrix V_1^{-1} has non-diagonal entries only in the rows corresponding to the bonds b_2, b_3, \dots, b_d . Therefore, only these rows are changed in $V_1^{-1}\tilde{S}V_1$. Moreover, the non-diagonal entries of V_1^{-1} are only in the column corresponding to b_1 and hence only columns of $\tilde{S}V_1$ that have nontrivial entry in the row corresponding to b_1 can be changed. These columns correspond to bonds which end in v_1 (and can be followed by b_1 in an irreducible pseudo-orbit) and are multiplied by rows of V_1^{-1} which have -1 at the b_j -th position, $j = 2, 3, \dots, d$ and 1 at the b_1 -th position. Since no two vertices are connected by two or more edges, the only bond starting at v_1 and ending at v_2 is b_1 . Hence the entries of $\tilde{S}V_1$ in the column corresponding to the edges ending at v_1 and in the row corresponding to the edges b_2, b_3, \dots, b_d are 0. Therefore, 1 in the b_j -th position in the b_j -th row of V_1^{-1} is multiplied by 0 and -1 is multiplied by the scattering amplitude between the bonds ending in v_1 and b_1 . Multiplying from the left by V_1^{-1} introduces in $\tilde{S}V_1$ new entries: in the columns corresponding to the bonds that end in v_1 and the rows corresponding to b_2, b_3, \dots, b_d the scattering amplitude between v_1 and b_1 taken with the opposite sign appears. These entries are represented by the “ghost edges”.

One has to take the entry of I_{2N} in the determinant in Theorem 13.5 in the column corresponding to b_1 (since the matrix $V_1^{-1}\tilde{S}\Sigma V_1$ has all zeros in this column), hence this bond effectively does not exist. The new entries are represented by the “ghost edges”, which do not contribute to the length of the irreducible pseudo-orbit. One can repeat this construction for other balanced vertices by a different unitary transformation of the matrix under the determinant. One cannot delete bonds to which “ghost edge” leads because these edges end in the balanced vertex from which one bond was already deleted. Q.E.D.

14.1 Example: two abscissas and two half-lines

Now we will show an example from Section 5 of [Lip15] illustrating the pseudo-orbit expansion for the resonance condition and the method of deleting edges. The graph consists of two internal edges of lengths ℓ and two half-lines connected at one central vertex (see Figure 14.3). We consider standard coupling at the central vertex v_2 and Dirichlet coupling at the loose ends of the abscissas (vertices v_1 and v_3).

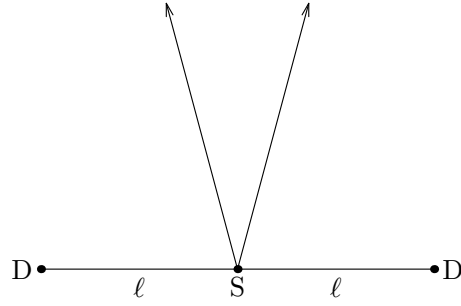


Fig. 14.3. Figure to Subsection 14.1 – graph Γ : two abscissas and two half-lines.

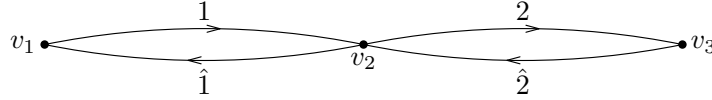


Fig. 14.4. Figure to Subsection 14.1 – graph Γ_2 . Reproduced from [Lip15].

The effective vertex-scattering matrix at the central vertex is by Corollary 13.3

$$\tilde{\sigma}^{(v_2)} = \frac{1}{2} \begin{pmatrix} -1 & 1 \\ 1 & -1 \end{pmatrix},$$

the effective vertex-scattering matrices for Dirichlet condition ($U = -1$) are $\tilde{\sigma}^{(v_1)} = \tilde{\sigma}^{(v_3)} = -1$.

The oriented graph Γ_2 is shown in Figure 14.4.

The matrix $\tilde{S} = Q\tilde{\Sigma}$ is

	1	2	$\hat{1}$	$\hat{2}$
1	0	0	-1	0
2	1/2	0	0	-1/2
$\hat{1}$	-1/2	0	0	1/2
$\hat{2}$	0	-1	0	0

The matrix \tilde{S} is built by the following rule: if a bond b' follows a bond b , then in the column corresponding to b and the row corresponding to b' is the entry of the effective vertex-scattering matrix between these two bonds.

Let us now find the resonance condition using the pseudo-orbits. The contribution of the trivial irreducible pseudo-orbit on zero bonds is 1. We have two irreducible pseudo-orbits on two bonds: $(\hat{1}\hat{1})$ and $(\hat{2}\hat{2})$. The scattering amplitude between $\hat{1}$ and 1 is -1 , the scattering amplitude between 1 and $\hat{1}$ is the diagonal entry of the effective vertex-scattering matrix, i.e. $-1/2$. Since there is one periodic orbit in the irreducible pseudo-orbit $(\hat{1}\hat{1})$, we have $m_{\tilde{\gamma}} = 1$ and hence the term $(-1)^1$. The contribution of the irreducible pseudo-orbit $(\hat{2}\hat{2})$ is the same. We have two irreducible pseudo-orbits on four bonds: $(\hat{1}\hat{1})(\hat{2}\hat{2})$ and $(1\hat{2}\hat{2}\hat{1})$. For both of them, the scattering amplitude between $\hat{1}$ and 1 is equal to (-1) (and similarly for the scattering amplitude between 2 and $\hat{2}$). For the former irreducible pseudo-orbit, we have the scattering amplitudes between 1

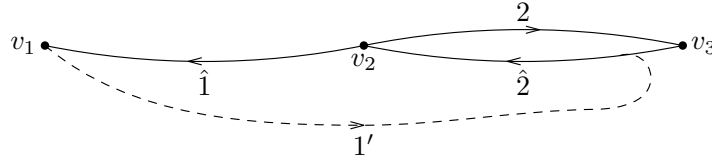


Fig. 14.5. Figure to Subsection 14.1 – graph Γ_2 after deleting the bond 1 and introducing the “ghost edge” $1'$. Reproduced from [Lip15].

and $\hat{1}$ and between $\hat{2}$ and 2 equal to $-1/2$ and since there are two periodic orbits $m_{\bar{\gamma}} = 2$. For the irreducible pseudo-orbit $(12\hat{2}\hat{1})$ we have the scattering amplitude between 1 and 2 (and similarly between $\hat{2}$ and $\hat{1}$) equal to $1/2$ and since there is one periodic orbit $m_{\bar{\gamma}} = 1$. Trivially, there are no irreducible pseudo-orbits on one or three bonds.

To summarize, we have the following contributions to the resonance condition.

$$\begin{aligned} \exp(0) &: 1, \\ \exp(2ik\ell) &: (-1) \left(-\frac{1}{2}\right) (-1)^1 \cdot 2 = -1, \\ \exp(4ik\ell) &: (-1)^2 \left(-\frac{1}{2}\right)^2 (-1)^2 + (-1)^2 \left(\frac{1}{2}\right)^2 (-1)^1 = 0. \end{aligned}$$

Hence the resonance condition is

$$1 - e^{2ik\ell} = 0. \quad (14.1)$$

Now we show how the method of deleting the edges simplifies finding the resonance condition. We delete one bond ending in the central (balanced) vertex v_2 , e.g. the bond 1. We obtain the changed graph Γ_2 (see Figure 14.5) with one new “ghost edge” $1'$ starting from v_1 and continuing to the bond $\hat{2}$ (because $\hat{2}$ is the other bond ending in v_2).

We again find irreducible pseudo-orbits on this graph. The contribution of the irreducible pseudo-orbit on zero bonds is 1. We have two irreducible pseudo-orbits on two “non-ghost” bonds: $(2\hat{2})$ and $(\hat{1}1'\hat{2})$. The contribution of the former one was already computed. The scattering amplitude from $\hat{1}$ to $\hat{2}$ via $1'$ is the scattering amplitude from $\hat{1}$ to 1 in the former graph Γ_2 taken with the opposite sign, i.e. 1. The scattering amplitude between $\hat{2}$ and $\hat{1}$ is $1/2$. There is one periodic orbit in the irreducible pseudo-orbit $(\hat{1}1'\hat{2})$, hence $m_{\bar{\gamma}} = 1$. One can easily see that there are no irreducible pseudo-orbits on three “non-ghost” bonds and clearly also on four bonds. We have the following contributions.

$$\begin{aligned} \exp(0) &: 1, \\ \exp(2ik\ell) &: 1 \left(\frac{1}{2}\right) (-1)^1 + (-1) \left(-\frac{1}{2}\right) (-1)^1 = -1. \end{aligned}$$

We obtain again the resonance condition (14.1). The advantage of this method is that we do not need to compute the contribution of the irreducible pseudo-orbits on four bonds.

15 Asymptotics of the resonances – the effective size of a non-Weyl graph

Let us now return to the asymptotics of the number of resolvent resonances in quantum graphs. We present results from [Lip16]. We study the value of the coefficient by the leading term of the asymptotics (which is connected to the effective size of the graph) for non-Weyl graphs using the machinery developed in previous sections. We focus on equilateral graphs (graphs which have all internal edges of lengths ℓ). First, we find the effective size using the properties of the matrix $\tilde{S}(k)$ and then we find bounds on the effective size for equilateral graphs. As we stated in Subsection 10.3, unlike the criterion if the graph is non-Weyl (which depends on the vertex properties of the graph) finding the effective size is more difficult and depends on the structure of the whole graph.

Let us first state a theorem on the criterion whether the graph is Weyl or non-Weyl.

Theorem 15.1 *Let us consider a graph Γ with internal edges of lengths ℓ_j . Graph Γ is non-Weyl iff $\det \tilde{\Sigma}(k) = 0$ for all $k \in \mathbb{C}$. Equivalently, the graph is non-Weyl iff there exists a vertex for which $\det \tilde{\sigma}^{(v)}(k) = 0$ for all $k \in \mathbb{C}$.*

Proof: According to the Theorem 13.5 the leading term of the asymptotics (the highest multiple of ik in the exponential) is $\det [Q\tilde{\Sigma}(k)] e^{2ik \sum_{j=1}^N \ell_j}$; the term with the lowest multiple of ik in the exponential is 1. By Lemma 10.1 the graph is non-Weyl (the effective size is strictly smaller than $\sum_{j=1}^N \ell_j$) iff $\det [Q\tilde{\Sigma}(k)] = 0$. Since the matrix Q only rearranges the rows of the matrix $\tilde{\Sigma}(k)$, this condition is equivalent to $\det \tilde{\Sigma}(k) = 0$. Since $\tilde{\Sigma}(k)$ is similar to a block-diagonal matrix with blocks $\tilde{\sigma}^{(v)}(k)$, we have that the graph is non-Weyl iff there exists a vertex with $\det \tilde{\sigma}^{(v)}(k) = 0$. Q.E.D.

The Corollary 10.3 follows from this theorem and Corollary 13.3. Determinant of $\tilde{\sigma}^{(v)}(k)$ is zero for a standard condition iff $n = m$ and hence we obtain the corollary by Davies and Pushnitski.

The following theorem gives the effective size of a non-Weyl graph.

Theorem 15.2 *Let us assume an equilateral graph Γ (all internal edges of lengths ℓ). Then its effective size is $\frac{\ell}{2} n_{\text{nonzero}}$, where n_{nonzero} is the number of nonzero eigenvalues of the matrix $\tilde{S}(k) = Q\tilde{\Sigma}(k)$.*

Proof: We will use Theorem 13.5. The matrix L is for an equilateral graph multiple of identity matrix, hence $e^{ikL} = e^{ik\ell} I$. The unitary transformation of the matrix under the determinant does not change the determinant, hence the resonance condition is

$$\det (e^{ik\ell} D(k) - I_{2N}) = 0$$

with $D(k)$ being the Jordan form of the matrix $\tilde{S}(k) = Q\tilde{\Sigma}$. The matrix under the determinant is upper triangular, therefore the determinant is given by multiplication of its diagonal entries. In the term with the highest multiple of ik in the exponential there will be n_{nonzero} terms $e^{ik\ell}$. Hence the effective size is by Lemma 10.1 $\frac{\ell}{2} n_{\text{nonzero}}$. Q.E.D.

Now we prove bounds on the effective size W of a non-Weyl graph using the method of deleting the edges.

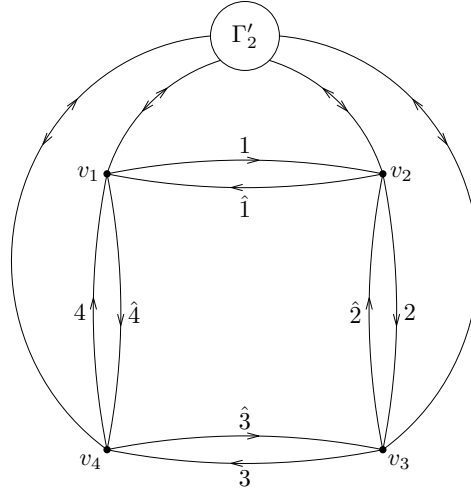


Fig. 15.1. Figure to Theorem 15.4. The graph Γ_2 : the bonds between Γ'_2 and the vertices v_1, v_2, v_3 and v_4 with arrows in both directions represent possible bonds in both direction. Reproduced from [Lip16].

Theorem 15.3 *Let us assume an equilateral graph Γ (N internal edges of lengths ℓ) with standard coupling, n_{bal} balanced vertices, and n_{nonneig} balanced vertices that do not neighbor any other balanced vertex. Then the effective size is bounded by $W \leq N\ell - \frac{\ell}{2}n_{\text{bal}} - \frac{\ell}{2}n_{\text{nonneig}}$.*

Proof: The sum of the lengths of the internal edges is $N\ell$. Let us assume a balanced vertex of the graph Γ with n internal and n external edges. Then in the graph Γ_2 there are n incoming and n outgoing bonds for this vertex. Since the vertex is balanced, we can delete one incoming bond. Since n_{bal} bonds are deleted, the size of the graph decreases by $\frac{\ell}{2}n_{\text{bal}}$. Let us assume that our vertex does not neighbor any other balanced vertex. Then any irreducible pseudo-orbit does not use one of the bonds going out of this vertex (there are $n - 1$ incoming bonds and n outgoing bonds after deletion) since it cannot get to the vertex for n -th time. This decreases the size of the graph by $\frac{\ell}{2}n_{\text{nonneig}}$. Q.E.D.

Theorem 15.4 *Let us assume an equilateral graph Γ (with N internal edges of the lengths ℓ) with standard coupling containing a square of balanced vertices v_1, v_2, v_3 and v_4 without diagonals. This means that v_1 neighbors v_2, v_2 neighbors v_3, v_3 neighbors v_4, v_4 neighbors v_1, v_1 does not neighbor v_3 and v_2 does not neighbor v_4 . Then the effective size of Γ is bounded by $W \leq (N - 3)\ell$.*

Proof: The graph Γ_2 is shown in Figure 15.1. We denote the bond between v_1 and v_2 by 1, the bond between v_2 and v_3 by 2, the bond between v_3 and v_4 by 3, and the bond between v_4 and v_1 by 4, the bonds in the opposite direction by $\hat{1}, \hat{2}, \hat{3}$, and $\hat{4}$. The rest of the graph is denoted by Γ'_2 ; there might be bonds between the subgraph Γ'_2 and the vertices v_1, v_2, v_3 and v_4 that are in this figure represented by bonds with arrows in both directions.

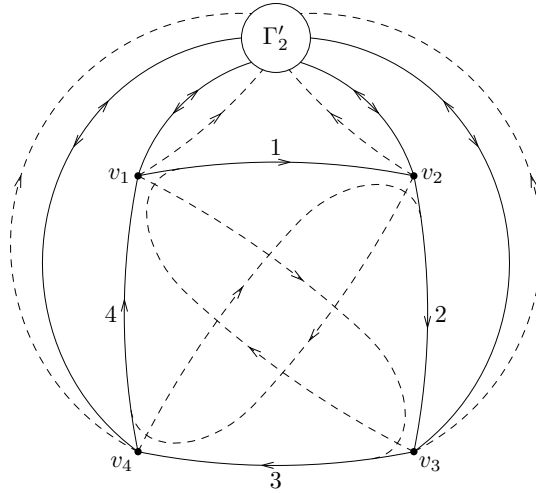


Fig. 15.2. Figure to Theorem 15.4. The graph Γ_2 after deletion of the bonds $\hat{1}$, $\hat{2}$, $\hat{3}$ and $\hat{4}$: the bonds between Γ'_2 and the vertices v_1 , v_2 , v_3 and v_4 with arrows in both directions represent possible bonds in both direction. The dashed lines from the vertices v_1 , v_2 , v_3 and v_4 to Γ'_2 represent possible “ghost edges”. Reproduced from [Lip16].

Now we, following Theorem 14.1, delete bonds $\hat{1}$, $\hat{2}$, $\hat{3}$ and $\hat{4}$. We obtain graph in Figure 15.2. Here again bonds between Γ'_2 and the vertices v_1 , v_2 , v_3 and v_4 are denoted by solid lines with arrows in both directions and possible “ghost edges” are represented by dashed lines. In the square, there appear four “ghost edges”. The irreducible pseudo-orbit can continue from the bond 4 to the bond 3 via the ghost edge (with the scattering amplitude equal to the scattering amplitude from 4 to $\hat{4}$ with the opposite sign) a similarly for the other bonds. Hence the graph Γ_2 can be represented by the one in Figure 15.3.

Now we find the effective size of the graph. The size of the graph $N\ell$ is reduced by 2ℓ since we have deleted four bonds (for each bond the effective size is reduced by $\ell/2$). The contribution of the irreducible pseudo-orbits (1234) and (12)(34) cancels out since both irreducible pseudo-orbits have same scattering amplitudes and differ only in the number of periodic orbits (the minus sign). A similar argument holds for all irreducible pseudo-orbits which contain these pseudo-orbits. One can argue similarly also for irreducible pseudo-orbits containing the pseudo-orbits (1432) and (14)(32). Therefore, contributions of the irreducible pseudo-orbits on all bonds of the graph in Figure 15.3 cancels out.

Now we prove that also all irreducible pseudo-orbits on all but one bonds of the graph in Figure 15.3 cancel. If the bond that is missing is not 1, 2, 3 or 4, we can use the same cancellation argument as in the previous paragraph. Let us suppose that one of the bonds 1, 2, 3 or 4 is not included, without loss of generality the bond 4. Because we use bonds 1, 2, 3, the irreducible pseudo-orbit must include the path from the right-bottom vertex in Figure 15.3 to the left-bottom vertex through Γ'_2 . At the same time, the irreducible pseudo-orbit must contain all the bonds but 4. Since with each bond, the bond with the opposite orientation is contained and since no “ghost

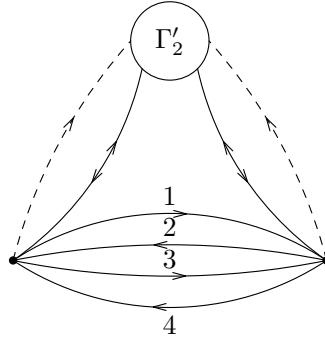


Fig. 15.3. Figure to Theorem 15.4. The effective form of the graph Γ_2 after deletion of the edges. Reproduced from [Lip16].

edge” ends in 1, 2, 3 or 4, it is not possible to obtain such irreducible pseudo-orbit.

Hence the longest irreducible pseudo-orbit that is not canceled has the length smaller or equal to $(2N - 6)\ell$. By Lemma 10.1 we obtain the claim. Q.E.D.

In the next theorem, we find positions of the resonances.

Theorem 15.5 *Let us assume an equilateral graph (N edges of lengths ℓ) with standard coupling. Let the eigenvalues of $\tilde{S} = Q\tilde{\Sigma}$ be $c_j = r_j e^{i\varphi_j}$. The positions of resolvent resonances are such $\lambda = k^2$ with*

$$k = \frac{1}{\ell}(-\varphi_j + 2n\pi + i \ln r_j), \quad n \in \mathbb{Z}.$$

Moreover, $|c_j| \leq 1$ and for a graph with no edge starting and ending in one vertex also $\sum_{j=1}^{2N} c_j = 0$ holds.

Proof: From the resonance condition in Theorem 13.5, the fact that the matrix $L = \ell I$ is multiple of an identity matrix and that a similarity transformation does not change the determinant we have

$$\prod_{j=1}^{2N} (e^{ik\ell} c_j - 1) = 0.$$

From this equation one finds for $k = k_R + ik_I$

$$r_j e^{-k_I \ell} e^{ik_R \ell} e^{i\varphi_j} = 1.$$

and therefore

$$k_I \ell = \ln r_j, \quad k_R \ell = -\varphi_j + 2n\pi.$$

If $|c_j| > 1$ (i.e. $r > 1$), we obtain $k_I > 0$. This for nontrivial real part of k contradicts Theorem 5.2.

If no edge starts and ends in one vertex, there are zeros on the diagonal of \tilde{S} . Hence its trace (the sum of the eigenvalues) is zero. Q.E.D.

16 Numerically finding the resonances

In this section, we show in an example one way how to numerically find the positions of resonances from the resonance condition.

Example 16.1 (a line with an appendix: positions of the resonances)

We again consider a simple graph consisting of a half-line and an abscissa connected with δ -coupling with Dirichlet coupling at the other end of an abscissa (see Example 5.1 and Figure 5.2). The condition to find the resolvent resonances is

$$(\alpha - ik) \sin k\ell + k \cos k\ell = 0.$$

We find the real and imaginary part of this equation to use it in the future.

$$\begin{aligned} (\alpha + k_I) \sin k_R \ell \cosh k_I \ell + k_R \cos k_R \ell \sinh k_I \ell + k_R \cos k_R \ell \cosh k_I \ell + \\ + k_I \sin k_R \ell \sinh k_I \ell = 0, \\ (\alpha + k_I) \cos k_R \ell \sinh k_I \ell - k_R \sin k_R \ell \cosh k_I \ell - k_R \sin k_R \ell \sinh k_I \ell + \\ + k_I \cos k_R \ell \cosh k_I \ell = 0, \end{aligned}$$

where k_R is the real part of k and k_I is the imaginary part. The first equation corresponds to the real part of the resonance condition and the second one to the imaginary part.

We present a code in a Python-based program SageMath [SAGE16] using SageMath Cloud [SMC16].

The positions of resonances for $\ell = 1$ and $\alpha = 1$ and $\alpha = 10$ are shown in Figures 16.1 and 16.2, respectively.

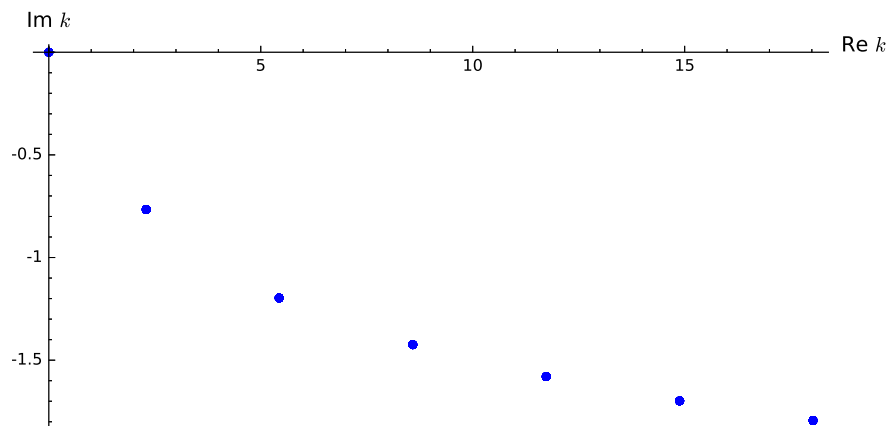


Fig. 16.1. Positions of the resonances for Example 16.1 with $\ell = 1$, $\alpha = 1$.

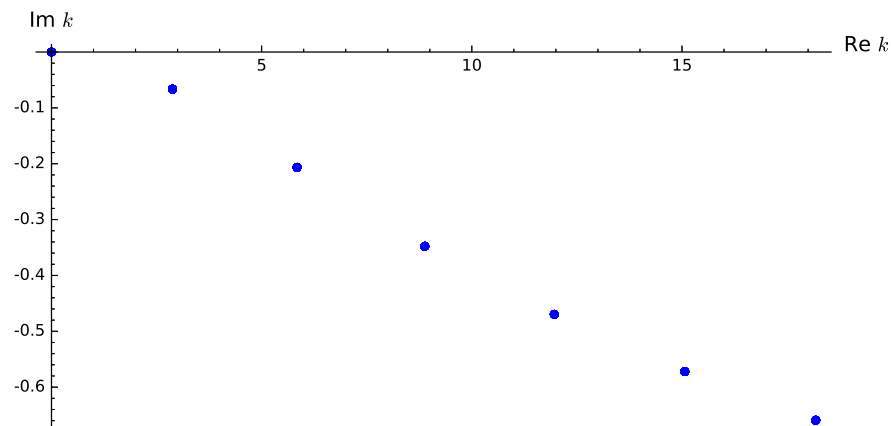


Fig. 16.2. Positions of the resonances for Example 16.1 with $\ell = 1$, $\alpha = 10$.

```

## first we import scipy optimize, a tool which allows us
## to find roots of the equation
import scipy
from scipy import optimize
## we define variables
var('l,alpha,j,jj')
## we set values of constants
alpha = 1;
l = 1;
## we define a function fun which returns the vector
## with entries equal to real part of the resonance condition
## and imaginary part of the resonance condition
def fun(x):
    return [(alpha+x[1])*sin(x[0]*l)*cosh(x[1]*l)+x[0]
*cos(x[0]*l)*sinh(x[1]*l)+x[0]*cos(x[0]*l)*cosh(x[1]*l)
+x[1]*sin(x[0]*l)*sinh(x[1]*l),
            (alpha+x[1])*cos(x[0]*l)*sinh(x[1]*l)-x[0]
*sin(x[0]*l)*cosh(x[1]*l)-x[0]*sin(x[0]*l)*sinh(x[1]*l)
+x[1]*cos(x[0]*l)*cosh(x[1]*l)]
## we define a list of positions of the resonances
list1 = [];
## we use a grid of starting values, j corresponds to
## the real part of k, jj corresponds to the imaginary part of k
for j in xrange(0,20,1):
    for jj in xrange(-5,0,0.3):
        ## we find the solution using the function optimize
        ## with starting point [j,jj]
        sol = optimize.root(fun, [j, jj])
        ## if the program converges to a solution, we add it to list1
        if sol.success: list1 = list1+[[sol.x[0],sol.x[1]]]
list1
## we define a figure p which plots points for entries of list1
p = point(list1,size=30,axes_labels=['Re $k$', 'Im $k$'],
axes_labels_size=1.3);
## this figure can be either shown on the screen or
## saved into a file
p.show()
p.save('obr5_alpha1_l1.pdf')

```

17 Trajectories of resonances

An interesting problem is to study trajectories of the resonances in the complex plane if the parameter of the interaction or the lengths of the edges are changed. It has been addressed in several papers, e.g. [EŠ94, Exn97, EL10, LZ16]. For some setting, one has an eigenvalue, but if one changes the parameters, the eigenvalue becomes resonance and “travels” in the complex plane.

Eigenvalues, which appear for the rational ratio of the lengths of the edges were studied in [EL10]. Let us assume that all the lengths of the edges in some cycle of edges are multiples of ℓ_0 . For a certain class of coupling conditions (e.g. δ -conditions) and for the length of the cycle being even multiple of ℓ_0 there is an eigenvalue for $k = \frac{n\pi}{\ell_0}$, $n \in \mathbb{Z}$ with the eigenfunction, which behaves as $\sin k_0 x$ on the cycle, has zeros in the vertices of the cycle and is zero outside the cycle. If we change the lengths of the edges of the cycle, the former eigenvalue becomes pure resonance. When the lengths of the edges are multiples of ℓ_0 again, it may return to the point k_0 . It has been found in [EL10] that resonances may “hop” between different eigenvalues. Resonances which arise from the eigenvalues for the rational ratio of the lengths of the edges are sometimes called *topological resonances* (see [GSS13, CdVT]) and will be also studied in Section 19.

As the resonance moves away from the real axis, its “life time” in the inner part of the graph decreases. When the lengths are again rationally related, an eigenvalue with eigenfunction supported on the inner part of the graph can again appear; i.e. we obtain a state with infinite “life time”.

Examples of such trajectories can be found in the mentioned papers. In this paper, we present a new example, which is slightly different than the cross-shaped resonator in subsection 4.2 of [EL10].

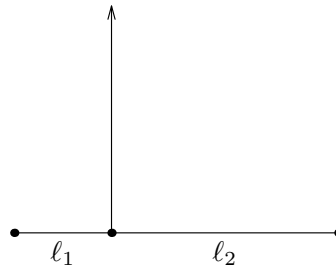


Fig. 17.1. Graph to example 17.1

Example 17.1 *Let us consider a graph (see Figure 17.1) which consists of two internal edges of lengths ℓ_1 and ℓ_2 , and two of their end vertices are connected in one vertex with one half-line. We assume δ -coupling of strength α at the central vertex and Dirichlet coupling at the loose ends. We will change the lengths of the edges as $\ell_1 = 1 - t$, $\ell_2 = 1 + t$ and hence the half-line moves from the center of the internal edge to the vertex with Dirichlet coupling.*

We can use the ansatz

$$f_j(x) = a_j \sin kx, \quad j = 1, 2$$

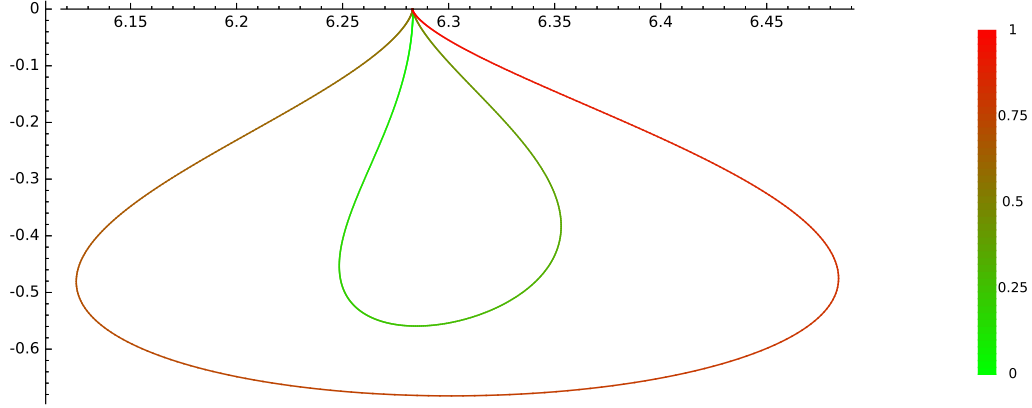


Fig. 17.2. Trajectory of the resonance for the graph with two internal edges and one half-line. The lengths of the edges are $\ell_1 = 1 - t$, $\ell_2 = 1 + t$, $t \in [0, 1]$, values of parameter t are denoted by the colour of the trajectory. Starting eigenvalue $k_0 = 2\pi$, strength of the δ -interaction $\alpha = 0$. The trajectory returns to the point k_0 two times. There is $\operatorname{Re} k$ on the x -axis and $\operatorname{Im} k$ on the y -axis.

on the internal edges with $x = 0$ corresponding to the vertex with Dirichlet boundary and $x = \ell_j$ corresponding to the central vertex. On the half-line we use the ansatz

$$g_j(x) = ce^{ikx}.$$

The coupling conditions lead to

$$\begin{aligned} a_1 \sin k\ell_1 &= a_2 \sin k\ell_2 = c, \\ -a_1 \cos k\ell_1 - a_2 \cos k\ell_2 + ikc &= \alpha c. \end{aligned}$$

The above set of equations can be written as

$$\begin{pmatrix} \sin k\ell_1 & 0 & -1 \\ 0 & \sin k\ell_2 & -1 \\ k \cos k\ell_1 & k \cos k\ell_2 & \alpha - ik \end{pmatrix} \begin{pmatrix} a_1 \\ a_2 \\ c \end{pmatrix} = 0.$$

Condition of solvability of the system is therefore determinant of the above matrix equals zero.

$$(\alpha - ik) \sin k\ell_1 \sin k\ell_2 + k \sin k(\ell_1 + \ell_2) = 0. \quad (17.1)$$

By differentiating the equation (17.1) with respect to t ($k = k(t)$, $\ell_1 = 1 - t$, $\ell_2 = 1 + t$) we obtain

$$\begin{aligned} [-i \sin k\ell_1 \sin k\ell_2 + (\alpha - ik)(\ell_1 \cos k\ell_1 \sin k\ell_2 + \ell_2 \cos k\ell_2 \sin k\ell_1) + \\ + \sin k(\ell_1 + \ell_2) + k \cos k(\ell_1 + \ell_2)(\ell_1 + \ell_2)] \dot{k} + \\ + k(\alpha - ik)(-\cos k\ell_1 \sin k\ell_2 + \sin k\ell_1 \cos k\ell_2) = 0, \end{aligned}$$

where \dot{k} is derivative of k with respect to t . We use this equation to obtain the trajectories in Figures 17.2, 17.3, 17.4, and 17.5.

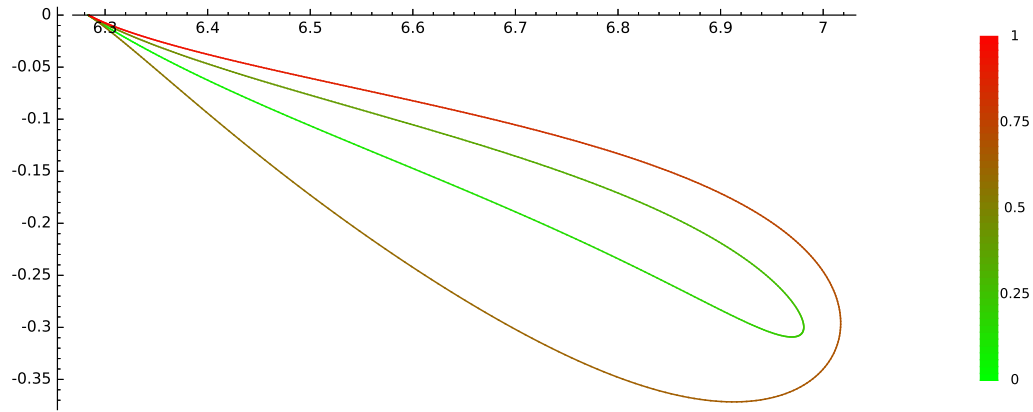


Fig. 17.3. Trajectory of the resonance for the graph with two internal edges and one half-line. The lengths of the edges are $\ell_1 = 1 - t$, $\ell_2 = 1 + t$, $t \in [0, 1]$, values of parameter t are denoted by the colour of the trajectory. Starting eigenvalue $k_0 = 2\pi$, strength of the δ -interaction $\alpha = 10$. The trajectory returns to the point k_0 two times. There is $\operatorname{Re} k$ on the x -axis and $\operatorname{Im} k$ on the y -axis.

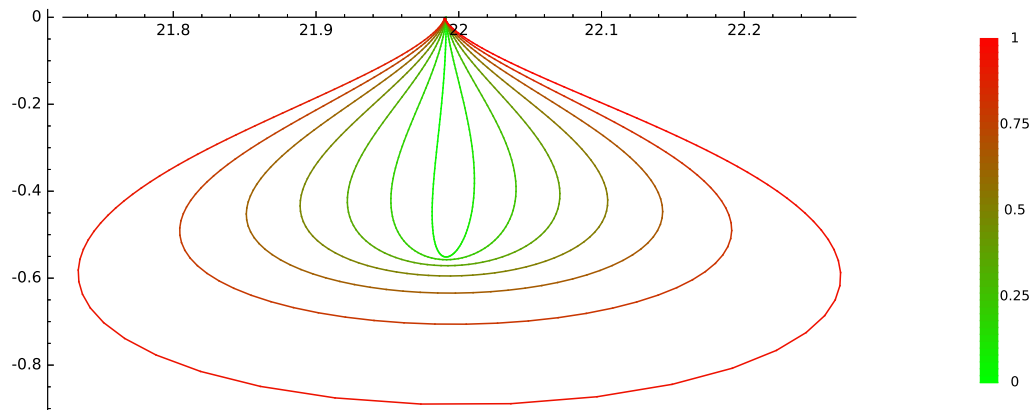


Fig. 17.4. Trajectory of the resonance for the graph with two internal edges and one half-line. The lengths of the edges are $\ell_1 = 1 - t$, $\ell_2 = 1 + t$, $t \in [0, 1]$, values of parameter t are denoted by the colour of the trajectory. Starting eigenvalue $k_0 = 7\pi$, strength of the δ -interaction $\alpha = 0$. The trajectory returns to the point k_0 seven times. There is $\operatorname{Re} k$ on the x -axis and $\operatorname{Im} k$ on the y -axis.

The trajectories of the resonances were found by SageMath [SAGE16, SMC16]. The code for obtaining the trajectory for Figure 17.5 can be found below.

```
## define all variables
var('l1,l2,alpha,k,t,dk,st,p,j')
## set values of the constants
alpha = 10;
k = 7*pi; #starting value for k
```

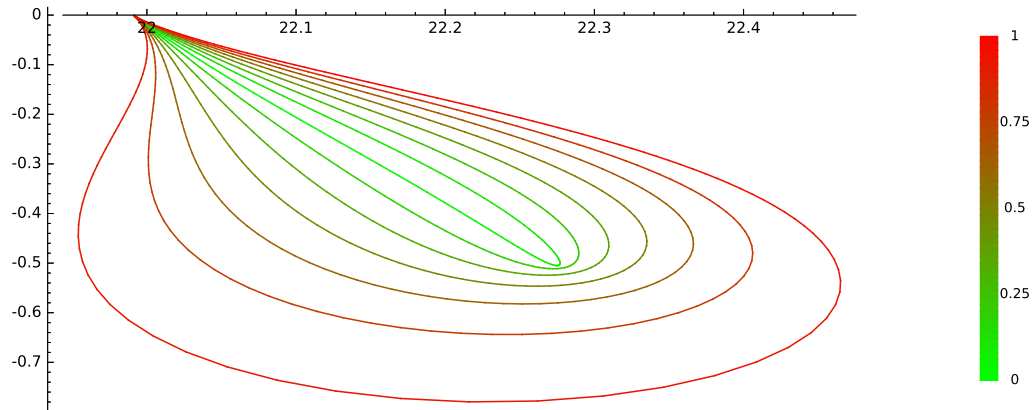


Fig. 17.5. Trajectory of the resonance for the graph with two internal edges and one half-line. The lengths of the edges are $\ell_1 = 1 - t$, $\ell_2 = 1 + t$, $t \in [0, 1]$, values of parameter t are denoted by the colour of the trajectory. Starting eigenvalue $k_0 = 7\pi$, strength of the δ -interaction $\alpha = 10$. The trajectory returns to the point k_0 seven times. There is $\text{Re } k$ on the x -axis and $\text{Im } k$ on the y -axis.

```

st = 0.001; #step
## defining list with points of the trajectory
list1 = [[(7*pi).n(), 0]];
## using a parameter t we change lengths of the edges l1 and l2
## the parameter t goes from 0 to 1 using steps st
for t in srange(0,1,st):
    l1 = 1-t; l2 = 1+t;
## differential of k: here we compute how k changes in the
## given step; dk is computed as derivative of k with respect
## to t multiplied by step st
## .n() is there to give a numerical result
    dk = (-k*(alpha-i*k)*(-cos(k*l1)*sin(k*l2)+sin(k*l1)*cos(k*l2))
    /(-i*sin(k*l1)*sin(k*l2)+(alpha-i*k)*(l1*cos(k*l1)*sin(k*l2)+
    l2*cos(k*l2)*sin(k*l1))+sin(k*(l1+l2))+k*cos(k*(l1+l2))*(l1+l2))*st).n();
## updating k and list1
    k = k+dk;
    list1 = list1 + [[k.real(),k.imag()]];
## plotting the line: first step
p=line([list1[0],list1[1]],color=Color(0,1,0))
## plotting the line: other pieces of the line with color changing
## from green to red
for j in srange(0,len(list1)-2):
    p=p+line([list1[j],list1[j+1]],color=Color(j/(len(list1)-2),
    1-j/(len(list1)-2),0))
## showing the result on the screen
p.show()
## saving the figure to a file
p.save('obr5_alpha10_7pi.pdf')

```

18 Fermi's golden rule

Fermi's golden rule is usually in quantum physics understood as a formula giving the transition rate from one eigenstate to the other embedded in the continuous spectrum. There is an alternative reformulation of this rule (Theorem XII.24 in [RS78]) dealing with the imaginary part of the resonance position. It relates the imaginary part of the coefficient by t^2 of the position of the resonance arising from the small perturbation of the eigenvalue in the parameter t with the energy derivative of a certain scalar product.

In this section, we will review the Fermi's golden rule for quantum graphs with standard coupling introduced in the paper [LZ16]. This rule allows approximating the trajectories of the resonances near the eigenvalue.

Let us assume the quantum graph Γ with N internal edges e_j of lengths ℓ_j , $1 \leq j \leq N$ and M external edges e_j , $N+1 \leq j \leq N+M$ and with standard coupling at all the vertices. Let us consider eigenvalue k_0^2 embedded into the continuous spectrum and corresponding eigenfunction u with the components u_j . For $k^2 \notin \sigma_{\text{pp}}(H)$ we define generalized eigenfunctions $e^s(k)$, $N+1 \leq s \leq N+M$ as

$$e^s(k) \in \mathcal{D}_{\text{loc}}(H), \quad (H - k^2)e^s(k) = 0, \quad (18.1)$$

$$e_j^s(k, x) = \delta_{js} e^{-ikx} + s_{js}(k) e^{ikx}, \quad N+1 \leq j \leq N+M, \quad (18.2)$$

where e_j^s are the half-line components of e^s . This family can be holomorphically extended to the points of the spectrum of H and therefore it is defined for all k .

Let there be a family of quantum graphs with a one-parameter transformation of the lengths of the internal edges. For $1 \leq j \leq N$ we have

$$\ell_j(t) = e^{-a_j(t)} \ell_j, \quad a_j(0) = 0,$$

where a_j are constant on the edges. The Hamiltonian for the graph Γ_t with the edges of lengths $\ell_j(t)$ will be denoted $H(t)$ and its eigenvalues $k^2(t)$. Moreover, we denote

$$\dot{a} \equiv \frac{\partial a}{\partial t}(0), \quad (\dot{a}u)_j \equiv \dot{a}_j u_j(x).$$

We state the Fermi's golden rule from [LZ16].

Theorem 18.1 *Consider a simple eigenvalue $k_0^2 > 0$ of the Hamiltonian $H \equiv H(0)$ and let u be the corresponding eigenfunction. Then for $|k| \leq k_{\text{max}}$ there exists a smooth function $t \mapsto k(t)$ such that $k^2(t)$ is the resolvent resonance of $H(t)$. Moreover, we have*

$$\begin{aligned} \text{Im } \ddot{k}(0) &= - \sum_{s=N+1}^{N+M} |F_s|^2, \\ F_s &= k_0 \langle \dot{a}u, e^s(k_0) \rangle + \frac{1}{k_0} \sum_{v \in \Gamma} \sum_{e_j \ni v} \frac{1}{4} \dot{a}_j (3\partial_\nu u_j(v) \overline{e_j^s(k, v)} - u(v) \partial_\nu \overline{e_j^s(k, v)}), \end{aligned}$$

where double dot denotes the second derivative with respect to t , $\langle \bullet, \bullet \rangle$ is the inner product in $\oplus_{j=1}^N L^2([0, \ell_j]) \oplus \oplus_{s=N+1}^{N+M} L^2([0, \infty))$, the sum $\sum_{v \in \Gamma}$ goes through all the vertices of the graph Γ , $\partial_\nu u_j(0) = -u_j'(0)$ and $\partial_\nu u_j(\ell_j) = u_j'(\ell_j)$.

Remark 18.2 We will show how this formulation of the Fermi's rule is related to the formulation from Section XII.6 and Notes to Chapter XII in [RS78]. We will study the problem in the energy plane. Let us consider a simple eigenvalue $E_0 \equiv E(0)$ for the Hamiltonian H_0 and resonance $E(t) = \sum_{n=0}^{\infty} a_n t^n$ for its perturbation $H_0 + tV$ depending on the parameter t , where the case $t = 0$ corresponds to the mentioned eigenvalue. Clearly, $a_0 \in \mathbb{R}$ (the eigenvalue is real) and also $a_1 \in \mathbb{R}$ (the resonances lie in the lower half-plane, compare with Theorem 5.2). Therefore, for small t we have $E(t) \approx a_2 t^2$. If we denote the imaginary part of $E(t)$ by $\Gamma(t)/2$, we have

$$\partial_t^2 \Gamma(t) = 2\text{Im} \partial_t^2 E(t) = 4\text{Im} a_2 = 4\pi \left. \frac{d}{dE} \langle u, V \tilde{P}(E) V \rangle \right|_{E=E_0}, \quad (18.3)$$

where in the last equality we used Theorem XII.24 in [RS78], u is the eigenfunction corresponding to the eigenvalue $E(0)$ and $\tilde{P}(E) = P_{(-\infty, E) \setminus \{E_0\}}$ is the modified spectral projection. If the continuous spectrum has a nice parametrization by the generalized eigenfunctions $e(E, a)$, one can write

$$\partial_E \tilde{P}(E) = \int_{\mathcal{A}} e(E, a) \otimes e(E, a)^* d\mu(a), \quad a \in \mathcal{A}.$$

The equation (18.3) becomes

$$\partial_t^2 \Gamma(t) = 4\pi \int_{\mathcal{A}} |\langle V u, e(E, a) \rangle|^2 d\mu(a), \quad (18.4)$$

Since for quantum graphs the set \mathcal{A} is discrete, the integral becomes the sum. Therefore this formula resembles the formula in Theorem 18.1.

Another formulation mentioned in [RS78] is

$$\Gamma = 2t^2 \text{Im} a_2 = 2\pi t^2 \left. \frac{d}{dE} \langle u, V \tilde{P}(E) V \rangle \right|_{E=E_0}$$

and since Γ can be related to the transition probability between two states and the *rhs* by equation (18.4) to the matrix elements of the perturbation between initial and final state, more usual formulation of the Fermi's golden rule also follows. (More details in Notes to Chapter XII of [RS78]).

Proof of Theorem 18.1: Let $\partial_x f = \frac{\partial f}{\partial x}$ and $\partial_x^2 f = \frac{\partial^2 f}{\partial x^2}$. Then by twice integrating by parts we get for $f, g \in W^{2,2}(\Gamma)$

$$\begin{aligned} -\langle \partial_x^2 f, g \rangle_{L^2} &= -\sum_{j=1}^{N+M} \int_{e_j} (\partial_x^2 f_j(x) \bar{g}_j(x)) dx = \sum_{j=1}^{N+M} \int_{e_j} \partial_x f_j(x) \partial_x \bar{g}_j(x) dx - \\ &- \sum_{v \in \Gamma} \sum_{e_j \ni v} \partial_\nu f_j(v) \bar{g}_j(v) = -\sum_{j=1}^{N+M} \int_{e_j} f_j(x) \partial_x^2 \bar{g}_j(x) dx + \\ &+ \sum_{v \in \Gamma} \sum_{e_j \ni v} [f_j(v) \partial_\nu \bar{g}_j(v) - \partial_\nu f_j(v) \bar{g}_j(v)] = \\ &= -\langle f, \partial_x^2 g \rangle_{L^2} + \sum_{j=1}^{N+M} \sum_{v \in \partial e_j} [f_j(v) \partial_\nu \bar{g}_j(v) - \partial_\nu f_j(v) \bar{g}_j(v)]. \quad (18.5) \end{aligned}$$

Here ∂e_j is the set of the vertices of the edge e_j . In the last equality we rearranged the sum over all vertices.

Now we define operator $\tilde{P}(t) \equiv H(t)$ and unitarily equivalent operator $P(t)$.

$$L_t^2 := \bigoplus_{j=1}^N L^2([0, e^{-a_j(t)} \ell_j]) \oplus \bigoplus_{s=N+1}^{N+M} L^2([0, \infty)), \quad U(t) : L_t^2 \rightarrow L_0^2,$$

$$(U(t)u)_j(y) := e^{-a_j(t)/2} u_j(e^{-a_j(t)} y), \quad U(t)^{-1} = U(t)^*.$$

Let the operator $\tilde{P}(t) \equiv H(t)$ be defined in L_t^2 by

$$(\tilde{P}(t)u)_j = -\partial_x^2 u_j,$$

$$\mathcal{D}(\tilde{P}(t)) = \{u : u_j \in W^{2,2}([0, e^{-a_j(t)} \ell_j]), u_j(v) = u_i(v), v \in e_j \cap e_i, \sum_{e_j \ni v} \partial_\nu u_j(v) = 0\}.$$

This is just the Laplacian on the graph Γ_t with standard coupling, i.e. $H(t)$.

We define a family of operators $P(t)$ on L_0^2 as $P(t) := U(t)\tilde{P}(t)U(t)^{-1}$. One can compute the action of this operator explicitly

$$(P(t)u)_j = \left[U(t) \left(-\frac{\partial^2}{\partial x^2} \right) U^{-1}(t)u(x) \right]_j = U(t) \left(-\frac{\partial^2}{\partial x^2} \right) e^{a_j(t)/2} u_j(e^{a_j(t)} x) =$$

$$= -U(t) e^{2a_j(t)} e^{a_j(t)/2} u_j''(e^{a_j(t)} x) = -e^{-a_j(t)/2} e^{2a_j(t)} e^{a_j(t)/2} u_j''(e^{-a_j(t)} e^{a_j(t)} x) =$$

$$= -e^{2a_j(t)} u_j''(x) = -e^{2a_j(t)} \partial_x^2 u_j(x).$$

The domain of this operator is

$$\mathcal{D}(P(t)) = \left\{ u \in W^{2,2}(\Gamma) : e^{a_j(t)/2} u_j(v) = e^{a_i(t)/2} u_i(v), v \in e_j \cap e_i, \right.$$

$$\left. 0 = \sum_{e_j \ni v} e^{3a_j(t)/2} \partial_\nu u_j(v) \right\}. \quad (18.6)$$

From Proposition 4.3 in [LZ16] it follows that for small t there exists a smooth family $t \mapsto u(t) \in W_{\text{loc}}^{2,2}(\Gamma_t)$ such that

$$(P(t) - z(t))u(t) = 0, \quad u_s(t, x) = a(t) e^{ik(t)x}, \quad N+1 \leq s \leq N+M,$$

$$\text{Im } k(t) \leq 0, \quad k(0)^2 = z, \quad k(0) > 0.$$

To simplify the notation we will use following [LZ16] $P \equiv P(t)$ and $z \equiv z(t)$. First, we define the following space and orthogonal projection.

$$\mathcal{H}_R := \bigoplus_{j=1}^N L^2([0, \ell_j]) \oplus \bigoplus_{s=N+1}^{N+M} L^2([0, R]).$$

Then by $\mathbb{1}_{x \geq R} : L_0^2 \rightarrow \mathcal{H}_R$ we mean the projection on \mathcal{H}_R . We obtain

$$\langle Pu, \mathbb{1}_{x \geq R} u \rangle = - \sum_{j=1}^N \int_{e_j} (\partial_x^2 u_j(x)) \bar{u}_j(x) dx - \sum_{s=N+1}^{N+M} \int_0^R (\partial_x^2 u_s(x)) \bar{u}_s(x) dx =$$

$$\begin{aligned}
&= \sum_{j=1}^N \int_{e_j} |\partial_x u_j(x)|^2 dx + \sum_{s=N+1}^{N+M} \int_0^R |\partial_x u_s(x)|^2 dx - \\
&\quad - \sum_{v \in \Gamma} \sum_{e_j \ni v} (\partial_\nu u_j(v)) \bar{u}_j(v) - \sum_{s=N+1}^{N+M} \partial_x u_s(R) \bar{u}_s(R).
\end{aligned}$$

From equation (18.5) and the fact that P is symmetric we have

$$0 = \sum_{v \in \Gamma} \sum_{e_j \ni v} [(\partial_\nu u_j(v)) \bar{u}_j(v) - u_j(v) \partial_\nu \bar{u}_j(v)] = 2 \operatorname{Im} \sum_{v \in \Gamma} \sum_{e_j \ni v} (\partial_\nu u_j(v)) \bar{u}_j(v).$$

Hence we obtain

$$0 = \operatorname{Im} \langle (P - z)u, \mathbb{1}_{x \geq R} u \rangle = -\operatorname{Im} \sum_{s=N+1}^{N+M} \partial_x u_s(R) \bar{u}_s(R) - \operatorname{Im} z \|u\|_{\mathcal{H}_R}^2. \quad (18.7)$$

Differentiating equation (18.7) twice with respect to t we obtain

$$\begin{aligned}
&(\partial_t^2 \|u\|_{\mathcal{H}_R}^2) \operatorname{Im} z + 2 (\partial_t \|u\|_{\mathcal{H}_R}^2) \operatorname{Im} \dot{z} + \|u\|_{\mathcal{H}_R}^2 \operatorname{Im} \ddot{z} = \\
&= -2 \operatorname{Im} \sum_{s=N+1}^{N+M} \partial_x \dot{u}_s(R) \bar{\dot{u}}_s(R) - \operatorname{Im} \sum_{s=N+1}^{N+M} (\partial_x \ddot{u}_s(R) \bar{u}_s(R) + \partial_x u_s(R) \ddot{\bar{u}}_s(R)).
\end{aligned}$$

Using $\operatorname{Im} z(0) = 0$, $\operatorname{Im} \dot{z}(0) = 0$, $u(t=0)|_{L_0^2 \setminus \mathcal{H}_R} = 0$ and $\|u\|_{\mathcal{H}_R}^2|_{t=0} = 1$ we get at $t = 0$

$$\operatorname{Im} \ddot{z} = -2 \operatorname{Im} \sum_{s=N+1}^{N+M} \partial_x \dot{u}_s(R) \bar{\dot{u}}_s(R). \quad (18.8)$$

Moreover, we have using equation (18.5)

$$\begin{aligned}
2 \operatorname{Im} \langle (P - z)\dot{u}, \mathbb{1}_{x \geq R} \dot{u} \rangle &= -2 \operatorname{Im} z \|\dot{u}\|_{\mathcal{H}_R}^2 + 2 \operatorname{Im} \|\partial_x \dot{u}\|_{\mathcal{H}_R}^2 - \\
&- 2 \operatorname{Im} \sum_{v \in \Gamma} \sum_{e_j \ni v} \partial_\nu \dot{u}_j(v) \bar{\dot{u}}_j(v) - 2 \operatorname{Im} \sum_{s=N+1}^{N+M} \partial_x \dot{u}_s(R) \dot{u}_s(R)
\end{aligned}$$

Now we obtain at $t = 0$ using $\operatorname{Im} z(0) = 0$, $\|\partial_x \dot{u}\|_{\mathcal{H}_R}^2 \in \mathbb{R}$ and equation (18.8)

$$\operatorname{Im} \ddot{z} = 2 \operatorname{Im} \langle (P - z)\dot{u}, \mathbb{1}_{x \geq R} \dot{u} \rangle + 2 \operatorname{Im} \sum_{v \in \Gamma} \sum_{e_j \ni v} \partial_\nu \dot{u}_j(v) \bar{\dot{u}}_j(v). \quad (18.9)$$

We can write

$$\begin{aligned}
0 &= \partial_t [(P(t) - z(t))u(t)]_j|_{t=0} = \partial_t \left[- \left(e^{2a_j(t)} \partial_x^2 + z(t) \right) u_j(t) \right] \Big|_{t=0} = \\
&= 2\dot{a}_j(0)(-\partial_x^2 u_j) - \dot{z}(0)u_j + [(P(0) - z(0))\dot{u}]_j = [(2\dot{a}_j z - \dot{z})u + (P - z)\dot{u}]_j, \quad (18.10)
\end{aligned}$$

where we have used $(P(t) - z(t))u = 0$. Using this relation again for the *lhs* of the previous displayed equation we have

$$(-\partial_x^2 - z)\dot{u}_j = (\dot{z} - 2z\dot{a}_j)u_j. \quad (18.11)$$

Differentiating the last equation in the definition of the domain of $P(t)$ (18.6) with respect to t at $t = 0$ we have

$$0 = \partial_t \left(\sum_{e_j \ni v} e^{3a_j(t)/2} \partial_\nu u_j(v) \right) \Big|_{t=0} = \frac{3}{2} \sum_{e_j \ni v} \dot{a}_j(0) \partial_\nu u_j(v) + \sum_{e_j \ni v} \partial_\nu \dot{u}_j(v).$$

Hence

$$\sum_{e_j \ni v} \partial_\nu \dot{u}_j(v) = -\frac{3}{2} \sum_{e_j \ni v} \dot{a}_j \partial_\nu u_j(v). \quad (18.12)$$

Differentiating equation $e^{a_j(t)/2} u_j(v) = e^{a_i(t)/2} u_i(v)$ (see eq. (18.6)) with respect to t at $t = 0$ we obtain

$$\frac{1}{2} \dot{a}_j(0) u_j(v) + \dot{u}_j(v) = \frac{1}{2} \dot{a}_i(0) u_i(v) + \dot{u}_i(v) \quad (18.13)$$

Defining $u(v) := u_j(v)$ which by (18.6) does not depend on j and $w := \partial_t(e^{a(t)/2} u(t))|_{t=0}$ we have from the previous displayed equation

$$\dot{u}_j(v) = w(v) - \frac{1}{2} \dot{a}_j(v) u(v). \quad (18.14)$$

To obtain the expression for \dot{u} we first define the function g

$$g \in \bigoplus_{j=1}^N C^\infty([0, \ell_j]) \oplus \bigoplus_{s=N+1}^{N+M} C_c^\infty([0, \infty))$$

such that

$$\sum_{e_j \ni v} \partial_\nu g_j(v) = -\frac{3}{2} \sum_{e_j \ni v} \dot{a}_j \partial_\nu u_j(v), \quad (18.15)$$

$$g_j(v) - g_i(v) = \frac{1}{2} (\dot{a}_i - \dot{a}_j) u(v). \quad (18.16)$$

We assume without loss of generality that both g and u are real.

We can write first using equation (18.11) and then equation (18.5)

$$\begin{aligned} & \langle (\dot{z} - 2\dot{a}z)u - (P - z)g, u \rangle = \langle (P - z)(\dot{u} - g), u \rangle = \\ & = \langle \dot{u} - g, (P - \bar{z})u \rangle + \sum_{v \in \Gamma} \sum_{e_j \ni v} [(\dot{u}_j - g_j)(v) \partial_\nu \bar{u}_j(v) - \partial_\nu (\dot{u}_j - g_j)(v) \bar{u}_j(v)]. \end{aligned}$$

Now using $z(0) \in \mathbb{R}$ and $(P - z)u = 0$ the first term disappears. With the use of equations (18.13) and (18.16) we find that $(\dot{u} - g)(v) := (\dot{u}_j - g_j)(v)$ does not depend on j . Using this fact, the coupling conditions (18.6) for u at $t = 0$ and the previous displayed equation we have

$$\begin{aligned} & \langle (\dot{z} - 2\dot{a}z)u - (P - z)g, u \rangle = \\ & = \sum_{v \in \Gamma} (\dot{u} - g)(v) \sum_{e_j \ni v} \partial_\nu \bar{u}_j(v) - \sum_{v \in \Gamma} \bar{u}(v) \sum_{e_j \ni v} \partial_\nu (\dot{u}_j - g_j)(v) = 0. \end{aligned}$$

We have used $\sum_{e_j \ni v} \partial_\nu \bar{u}_j(v) = 0$ (this follows from the coupling conditions (18.6) at $t = 0$) and $\sum_{e_j \ni v} \partial_\nu (\dot{u}_j - g_j)(v) = 0$ (which follows from equations (18.15) and (18.12)).

We subsequently obtain

$$\begin{aligned}
0 &= - \frac{d}{dt} \langle (P(t) - z(t))u(t), \mathbb{1}_{x \leq R} u(t) \rangle \Big|_{t=0} = \langle \dot{z}u - 2\dot{a}zu - (P - z)\dot{u}, u \rangle = \\
&= \dot{z} - 2z \langle \dot{a}u, u \rangle + \sum_{v \in \Gamma} \sum_{e_j \ni v} [\partial_\nu \dot{u}_j(v)u(v) - \dot{u}_j(v)\partial_\nu u_j(v)] = \\
&= \dot{z} - 2z \langle \dot{a}u, u \rangle + \sum_{v \in \Gamma} \sum_{e_j \ni v} \left[-\frac{3}{2} \dot{a}_j \partial_\nu u_j(v)u(v) - \left(w(v) - \frac{1}{2} \dot{a}_j u(v) \right) \partial_\nu u_j(v) \right] = \\
&= \dot{z} - 2z \langle \dot{a}u, u \rangle - \sum_{v \in \Gamma} \sum_{e_j \ni v} \dot{a}_j \partial_\nu u_j(v)u(v).
\end{aligned} \tag{18.17}$$

In the first equality we used $(P(t) - z(t))u(t) = 0$. In the second equality we differentiated the inner product with respect to t using (18.10); the term where $\mathbb{1}_{x \leq R} u(t)$ is differentiated disappears because in that case the first entry of the inner product is zero due to $(P(t) - z(t))u(t) = 0$. The third equality follows from the fact that u is normalized, equation (18.5), the fact that $z(0) \in \mathbb{R}$ and $(P - z)u = 0$. The fourth equality uses equations (18.12) and (18.14). The fifth equality follows from the coupling conditions $\sum_{e_j \ni v} \partial_\nu u_j(v) = 0$.

We define

$$\tilde{v} := g + R(k)(\dot{z}u - 2z\dot{a}u - (P - z)g), \quad z = k^2, \quad k > 0,$$

where $R(k)$ is the resolvent $(P - k^2)^{-1}$. Function \tilde{v} is well defined, outgoing and solves the problem (18.11), (18.12) and (18.13) satisfied by \dot{u} . Since z is a simple eigenvalue, we have by Theorem 4.18 in [DZ] that $\dot{u} - \tilde{v}$ is a multiple of u . Hence we can write

$$\dot{u} = \alpha u + g + R(k)(\dot{z}u - 2z\dot{a}u - (P - z)g) \tag{18.18}$$

with complex α .

Now we return to the equation (18.9) again and try to rewrite first term on the *rhs*.

$$\begin{aligned}
&2 \operatorname{Im} \langle (P - z)\dot{u}, \mathbb{1}_{x \leq R} \dot{u} \rangle = 2 \operatorname{Im} \langle \dot{z}u - 2z\dot{a}u, \dot{u} \rangle = \\
&= 2 \operatorname{Im} \langle \dot{z}u - 2z\dot{a}u, \alpha u + g + R(k)(\dot{z}u - 2z\dot{a}u - (P - z)g) \rangle = \\
&2 (\operatorname{Im} \bar{\alpha})(\dot{z} - 2z \langle \dot{a}u, u \rangle) - 4z \operatorname{Im} \langle \dot{a}u, R(k)(\dot{z}u - 2z\dot{a}u - (P - z)g) \rangle.
\end{aligned} \tag{18.19}$$

In the first equality we used equation (18.11); the term $\mathbb{1}_{x \leq R}$ is no longer needed because u has support only on the internal part of the graph. In the second equality we substituted (18.18). The third equality uses the fact that $\dot{z} \langle u, g \rangle \in \mathbb{R}$ and $\langle 2z\dot{a}u, g \rangle \in \mathbb{R}$, because all \dot{z} , u , g , z and \dot{a} are (assumed) to be real. Moreover, we use $\|u\|^2 = 1$

We recall a property of the resolvent

$$R(k)(x, y) = \overline{R(-\bar{k})(x, y)},$$

which follows from considering $\text{Im } k \gg 1$, $z = k^2$ and noting $((P-z)^{-1})^* = (P-\bar{z})^{-1}$. From this we have for real k

$$2i\text{Im } R(k) = R(k) - \overline{R(k)} = R(k) - R(-\bar{k}) = R(k) - R(-k) \quad (18.20)$$

and subsequently

$$2i\text{Im } R(k)u(k) = [R(k) - R(-k)]u(k) = 0, \quad (18.21)$$

which follows from $u(-k) = u(k)$ and

$$(P - k^2)f(k) = u(k) \quad \Rightarrow \quad (P - (-k)^2)f(k) = u(-k)$$

and hence

$$R(k)u(k) - R(-k)u(-k) = 0.$$

The identity $\text{Im } \langle u, R(k)(z\dot{u} - 2z\dot{a}u - (P-z)g) \rangle = 0$, which is used in the third equality in (18.19), follows from (18.21).

Using (18.20) we can rearrange the last term in (18.19).

$$\begin{aligned} 4z \text{Im } \langle \dot{a}u, R(k)(-z\dot{u} + 2z\dot{a}u + (P-z)g) \rangle &= \\ = \frac{2z}{i} \langle \dot{a}u, (R(k) - R(-k))(2z\dot{a}u + (P-z)g) \rangle. \end{aligned} \quad (18.22)$$

We have used equation (18.20). The term $\text{Im } \langle \dot{a}u, R(k)(z\dot{u}) \rangle$ vanishes because of equation (18.21).

Theorem 4.20 in [DZ] gives

$$(R(k) - R(-k))f = \frac{i}{2k} \sum_{s=N+1}^{N+M} e^s(k, x) \langle f, e^s(k, \bullet) \rangle, \quad k \in \mathbb{R}, \quad f \in \mathcal{H}_R. \quad (18.23)$$

Using it one finds

$$\begin{aligned} \frac{2z}{i} \langle \dot{a}u, (R(k) - R(-k))(2z\dot{a}u + (P-z)g) \rangle &= \\ = -k \sum_{s=N+1}^{N+M} \langle \dot{a}u, e^s \rangle \overline{\langle 2k^2\dot{a}u + (P-z)g, e^s \rangle} &= \\ = -2k^3 \sum_{s=N+1}^{N+M} |\langle \dot{a}u, e^s \rangle|^2 - k \sum_{s=N+1}^{N+M} \langle \dot{a}u, e^s \rangle \langle e^s, (P-z)g \rangle. \end{aligned} \quad (18.24)$$

For the inner product in the last term of the previous equation, we can write

$$\begin{aligned} \langle e^s, (P-z)g \rangle &= \langle (P-z)e^s, g \rangle - \sum_{v \in \Gamma} \sum_{e_j \ni v} (e^s(v) \partial_\nu g_j(v) - \partial_\nu e_j^s(v) g_j(v)) = \\ &= \sum_{v \in \Gamma} \sum_{e_j \ni v} \frac{1}{2} \dot{a}_j (3\partial_\nu u_j(v) e^s(v) - u(v) \partial_\nu e_j^s(v)) + \\ &\quad + \sum_{v \in \Gamma} \left(g_i(v) + \frac{1}{2} \dot{a}_i(v) u(v) \right) \sum_{e_j \ni v} \partial_\nu e_j^s(v) = \\ &= \sum_{v \in \Gamma} \sum_{e_j \ni v} \frac{1}{2} \dot{a}_j (3\partial_\nu u_j(v) e^s(v) - u(v) \partial_\nu e_j^s(v)). \end{aligned} \quad (18.25)$$

In the first equality we used $z \in \mathbb{R}$, equation (18.5) and the fact that g is real. The second equality uses $(P - z)e^s = 0$ and the equations (18.15) and (18.16). In the third equality we use the fact that e^s fulfills the standard coupling conditions at the vertices.

To summarize, using (18.19), (18.22), (18.24) and (18.25) we get

$$\begin{aligned} 2 \operatorname{Im} \langle (P - z)\dot{u}, \mathbb{1}_{x \leq R}\dot{u} \rangle &= 2 (\operatorname{Im} \bar{\alpha})(\dot{z} - 2z \langle \dot{u}, u \rangle) - 2k^3 \sum_{s=N+1}^{N+M} |\langle \dot{u}, e^s \rangle|^2 - \\ &- 2k \sum_{s=N+1}^{N+M} \langle \dot{u}, e^s \rangle \sum_{v \in \Gamma} \sum_{e_j \ni v} \frac{1}{4} \dot{a}_j (3\partial_\nu u_j(v)e^s(v) - u(v)\partial_\nu e_j^s(v)). \end{aligned} \quad (18.26)$$

Now we turn to the second term on the *rhs* of the equation (18.9)

$$\begin{aligned} &2 \operatorname{Im} \sum_{v \in \Gamma} \sum_{e_j \ni v} \partial_\nu \dot{u}_j(v) \bar{u}_j(v) = \\ &= 2 \operatorname{Im} \sum_{v \in \Gamma} \sum_{e_j \ni v} \partial_\nu \dot{u}_j(v) (\bar{\alpha} u_j + g_j + \overline{R(k)}(\dot{z}u - 2z\dot{a}u - (P - z)g))_j(v) = \\ &= 2 (\operatorname{Im} \bar{\alpha}) \sum_{v \in \Gamma} \sum_{e_j \ni v} \left(-\frac{3}{2} \right) \dot{a}_j \partial_\nu u_j(v) u(v) + \\ &+ 2 \operatorname{Im} \sum_{v \in \Gamma} \sum_{e_j \ni v} \partial_\nu \dot{u}_j(v) \left(-\frac{1}{2} \dot{a}_j u(v) + \frac{1}{2} \dot{a}_i u(v) + g_i(v) \right) - \\ &- 2 \operatorname{Im} \sum_{v \in \Gamma} \sum_{e_j \ni v} \partial_\nu \dot{u}_j(v) \overline{R(k)}(2z\dot{a}u + (P - z)g)(v). \end{aligned} \quad (18.27)$$

In the first equality we used equation (18.18). In the second equality we used equations (18.12), (18.16) and (18.21). The term

$$\begin{aligned} \operatorname{Im} \sum_{v \in \Gamma} \sum_{e_j \ni v} \partial_\nu \dot{u}_j(v) \left(\frac{1}{2} \dot{a}_i u(v) + g_i(v) \right) &= \operatorname{Im} \sum_{v \in \Gamma} \left(\frac{1}{2} \dot{a}_i u(v) + g_i(v) \right) \sum_{e_j \ni v} \partial_\nu \dot{u}_j(v) = \\ &= \operatorname{Im} \sum_{v \in \Gamma} \left(\frac{1}{2} \dot{a}_i u(v) + g_i(v) \right) \sum_{e_j \ni v} \left(-\frac{3}{2} \dot{a}_j \partial_\nu u_j(v) \right) = 0 \end{aligned}$$

vanishes, because u , g and \dot{a} are real functions.

Now we will study the second term in (18.27).

$$\begin{aligned} &2 \operatorname{Im} \sum_{v \in \Gamma} \sum_{e_j \ni v} \partial_\nu \dot{u}_j(v) \left(-\frac{1}{2} \right) \dot{a}_j u(v) = \\ &- (\operatorname{Im} \alpha) \sum_{v \in \Gamma} \sum_{e_j \ni v} \partial_\nu u_j(v) \dot{a}_j u(v) - \operatorname{Im} \sum_{v \in \Gamma} \sum_{e_j \ni v} \partial_\nu g(v) \dot{a}_j u(v) + \\ &+ \operatorname{Im} \sum_{v \in \Gamma} \sum_{e_j \ni v} \partial_\nu \overline{R(k)}(2z\dot{a}u + (P - z)g)_j \dot{a}_j u(v) = (\operatorname{Im} \bar{\alpha}) \sum_{v \in \Gamma} \sum_{e_j \ni v} \partial_\nu u_j(v) \dot{a}_j u(v) + \end{aligned}$$

$$\begin{aligned}
& + \sum_{v \in \Gamma} \sum_{e_j \ni v} u(v) \dot{a}_j \frac{1}{4k} \sum_{s=N+1}^{N+M} \partial_\nu e_j^s(v) \langle 2z \dot{a}u + (P-z)g, e^s \rangle = \\
& = (\text{Im } \bar{\alpha}) \sum_{v \in \Gamma} \sum_{e_j \ni v} \partial_\nu u_j(v) \dot{a}_j u(v) + \sum_{v \in \Gamma} \sum_{e_j \ni v} \sum_{s=N+1}^{N+M} u(v) \dot{a}_j \partial_\nu e_j^s(v) \cdot \\
& \cdot \left[\frac{k}{2} \langle \dot{a}u, e^s \rangle + \frac{1}{4k} \langle (P-z)g, e^s \rangle \right] = (\text{Im } \bar{\alpha}) \sum_{v \in \Gamma} \sum_{e_j \ni v} \partial_\nu u_j(v) \dot{a}_j u(v) + \\
& \quad + \sum_{v \in \Gamma} \sum_{e_j \ni v} \sum_{s=N+1}^{N+M} u(v) \dot{a}_j \partial_\nu e_j^s(v) \cdot \\
& \quad \cdot \left[\frac{k}{2} \langle \dot{a}u, e^s \rangle + \frac{1}{8k} \sum_{v' \in \Gamma} \sum_{e_i \ni v'} \dot{a}_i \left(3\partial_\nu u_i(v) \overline{e^s(v)} - u(v) \partial_\nu \overline{e_i^s(v)} \right) \right]
\end{aligned} \tag{18.28}$$

In the first equality we used equations (18.18) and (18.21). In the second equality we used the fact that u , g and \dot{a} are real functions and equation (18.23). In the last equality we used equation (18.25).

Now we rearrange the third term in (18.27).

$$\begin{aligned}
& -2 \text{Im} \sum_{v \in \Gamma} \sum_{e_j \ni v} \partial_\nu \dot{u}_j(v) \overline{R(k)} (2z \dot{a}u + (P-z)g)(v) = \\
& = 2 \sum_{v \in \Gamma} \sum_{e_j \ni v} \left(-\frac{3}{2} \right) \dot{a}_j \partial_\nu u_j(v) \frac{1}{4k} \sum_{s=N+1}^{N+M} e^s(v) \langle 2z \dot{a}u + (P-z)g, e^s \rangle = \\
& = -\frac{3}{4} \sum_{v \in \Gamma} \sum_{e_j \ni v} \sum_{s=N+1}^{N+M} \dot{a}_j \partial_\nu u_j(v) e^s(v) \left[2k \langle \dot{a}u, e^s \rangle + \frac{1}{k} \overline{\langle e^s, (P-z)g \rangle} \right] = \\
& \quad = -\frac{3}{4} \sum_{v \in \Gamma} \sum_{e_j \ni v} \sum_{s=N+1}^{N+M} \dot{a}_j \partial_\nu u_j(v) e^s(v) \cdot \\
& \quad \cdot \left[2k \langle \dot{a}u, e^s \rangle + \frac{1}{2k} \sum_{v' \in \Gamma} \sum_{e_i \ni v'} \dot{a}_i \left(3\partial_\nu u_i(v) \overline{e^s(v)} - u(v) \partial_\nu \overline{e_i^s(v)} \right) \right].
\end{aligned} \tag{18.29}$$

In the first equality we used equations (18.12), (18.20) and (18.23). The last equality follows from equation (18.25).

To summarize, we have from substituting (18.28) and (18.29) to (18.27)

$$\begin{aligned}
& 2 \text{Im} \sum_{v \in \Gamma} \sum_{e_j \ni v} \partial_\nu \dot{u}_j(v) \bar{u}_j(v) = \\
& = -2(\text{Im } \bar{\alpha}) \sum_{v \in \Gamma} \sum_{e_j \ni v} \dot{a}_j \partial_\nu u_j(v) u(v) +
\end{aligned}$$

$$\begin{aligned}
& +2k \sum_{v \in \Gamma} \sum_{e_j \ni v} \sum_{s=N+1}^{N+M} \frac{1}{4} \dot{a}_j \langle \dot{a}u, e^s \rangle [\partial_\nu e_j^s(v)u(v) - 3\partial_\nu u_j(v)e_j(v)] + \\
& - \frac{2}{k} \sum_{s=N+1}^{N+M} \left| \sum_{v \in \Gamma} \sum_{e_j \ni v} \frac{1}{4} \dot{a}_j [u(v)\partial_\nu e_j^s(v) - 3\partial_\nu u_j(v)e^s(v)] \right|^2
\end{aligned} \tag{18.30}$$

Using equation (18.23) we can prove that

$$\begin{aligned}
& -\frac{i}{2k} \sum_{s=N+1}^{N+M} \overline{e^s(k, x) \langle f, e^s(k, x) \rangle} = \overline{R(k, x)} - \overline{R(-k, x)} = \\
& = R(-k, x) - R(k, x) = -\frac{i}{2k} \sum_{s=N+1}^{N+M} e^s(k, x) \langle f, e^s(k, x) \rangle
\end{aligned}$$

from which

$$\sum_{s=N+1}^{N+M} \overline{e^s(k, x) \langle f, e^s(k, x) \rangle} = \sum_{s=N+1}^{N+M} e^s(k, x) \langle f, e^s(k, x) \rangle$$

follows. Minding this and substituting equations (18.26) and (18.30) into (18.9) with the use of $\text{Im } \ddot{k} = 2k \text{Im } \dot{k}$ we finally obtain the claim of the theorem. The term multiplied by $\text{Im } \bar{\alpha}$ vanishes due to equation (18.17). Q.E.D.

Now we give a theorem presented as Example 1 in [LZ16] which states how the formula in the Theorem 18.1 is simplified for certain eigenvalues.

Theorem 18.3 *Let us assume a graph Γ with N internal and M external edges. Let there be a simple eigenvalue k^2 of the Hamiltonian H on Γ for which the following relation holds*

$$\ell_j = n_j \ell_0, \quad k \ell_0 = \pi, \quad n_j \in \mathbb{N}, \quad 1 \leq j \leq N.$$

Then

$$\text{Im } \ddot{k} = - \sum_{s=N+1}^{N+M} |k \langle \dot{a}u, e^s(k) \rangle|^2.$$

Proof: If a half-line is attached to some vertex, functional value of the eigenfunction must be zero there and we have $u_j(x) = C_j \sin kx$. Because the graph is connected and $k\ell_j$ is a multiple of π , this relation holds for all edges of the graph. For $e_j^s(k, x)$ we use the ansatz

$$e_j^s(k, x) = A_{j_s} \sin kx + B_{j_s} \cos kx.$$

There are zeros of the eigenfunction at all the vertices of the graph: $u_j(0) = u_j(\ell_j) = 0$. Moreover, we have

$$\begin{aligned}
\partial_\nu u_j(0) &= -C_j k \cos k0 = -C_j k, \\
\partial_\nu u_j(\ell_j) &= C_j k \cos k\ell_j = C_j k (-1)^{n_j}, \\
e_j^s(k, 0) &= A_{j_s} \sin k0 + B_{j_s} \cos k0 = B_{j_s}, \\
e_j^s(k, \ell_j) &= A_{j_s} \sin k\ell_j + B_{j_s} \cos k\ell_j = B_{j_s} (-1)^{n_j}.
\end{aligned}$$

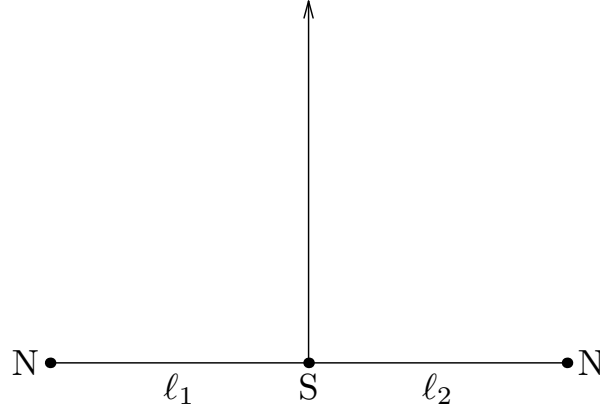


Fig. 18.1. Figure to Subsection 18.1 – graph Γ : two segments and a half-line.

Hence

$$\partial_\nu u_j(0) = \partial_\nu u_j(\ell_j)(-1)^{n_j+1}, \tag{18.31}$$

$$e_j^s(k, 0) = e_j^s(k, \ell_j)(-1)^{n_j}. \tag{18.32}$$

We can rewrite the second part of F_s in the following way

$$\begin{aligned} & \sum_{v \in \Gamma} \sum_{e_j \ni v} \frac{1}{4} \dot{a}_j \left[3\partial_\nu u_j(v) \overline{e^s(k, v)} - u(v) \partial_\nu \overline{e_j^s(k, v)} \right] = \\ &= \sum_{j=1}^{N+M} \sum_{v \in \partial e_j} \frac{3}{4} \dot{a}_j \partial_\nu u_j(v) \overline{e^s(k, v)} = \sum_{j=1}^{N+M} \frac{3}{4} \dot{a}_j \left[\partial_\nu u_j(0) \overline{e^s(k, 0)} - \partial_\nu u_j(\ell_j) \overline{e^s(k, \ell_j)} \right] = \\ &= \sum_{j=1}^{N+M} \frac{3}{4} \dot{a}_j \partial_\nu u_j(\ell_j) \overline{e^s(k, \ell_j)} [(-1)^{n_j+1} (-1)^{n_j} + 1] = 0. \end{aligned}$$

In the first equality we have used the fact that $u(v) = 0$ for all v and changed the sums as in equation (18.5). The last equality follows from equations (18.31) and (18.32). The claim of the theorem follows now from Theorem 18.1. Q.E.D.

We illustrate the usage of Theorem 18.1 in two simple examples.

18.1 Example: two segments and a half-line

We consider a graph consisting of two segments (abscissas) of length $\ell_j(t) = e^{-a_j(t)} \ell$, $a_j(0) = 0$. Both abscissas are in the central vertex connected with one half-line (see Figure 18.1). We assume standard coupling at the central vertex and Neumann coupling at the loose ends of the segments. We parametrize the segments by intervals $(0, \ell_j(t))$ with $x = 0$ at the loose ends and we parametrize the half-line by the interval $(0, \infty)$ with $x = 0$ at the central vertex.

Let us first find the eigenfunction for $t = 0$ and for $k = \pi/2$ and $\ell = 1$. Since there is the Neumann condition at the loose ends of the segments, we use the ansatz

$$u_1(k, x) = \alpha \cos kx, \quad u_2(k, x) = -\alpha \cos kx, \quad u_3(k, x) \equiv 0,$$

where $j = 1, 2$ corresponds to the segment-components of the wavefunction and $j = 3$ to the half-line component. We find the constant α which normalizes u

$$1 = 2 \int_0^\ell |u_1(k, x)|^2 dx = 2|\alpha|^2 \int_0^\ell \cos^2 kx dx = |\alpha|^2 \ell.$$

We have used the fact that integral of $\cos^2 kx$ over half of its period is equal to the length of the interval divided by two. Therefore, we choose $\alpha = 1/\sqrt{\ell}$ and have

$$u_1(k, x) = \frac{1}{\sqrt{\ell}} \cos kx, \quad u_2(k, x) = -\frac{1}{\sqrt{\ell}} \cos kx, \quad u_3(k, x) \equiv 0.$$

Now we find the generalized eigenfunction $e^1(k, x)$. Following definition in equations (18.1) and (18.2) we choose the ansatz

$$e_1^1(k, x) = \beta_1 \cos kx, \quad e_2^1(k, x) = \beta_2 \cos kx, \quad e_3^1(k, x) = e^{-ikx} + s_{11}e^{ikx}.$$

From the coupling conditions at the central vertex we have for k^2 not in the spectrum

$$\begin{aligned} \beta_1 \cos k\ell_1(t) &= \beta_2 \cos k\ell_2(t) = 1 + s_{11}, \\ \beta_1 \sin k\ell_1(t) + \beta_1 \sin k\ell_1(t) + i(-1 + s_{11}) &= 0. \end{aligned}$$

From the limit to $t = 0$ we have

$$s_{11} = -1, \quad \beta_1 = \beta_2, \quad \beta_1 + \beta_2 - 2i = 0,$$

from which we obtain $\beta_1 = \beta_2 = i$ and hence we have

$$e_1^1(k, x) = i \cos kx, \quad e_2^1(k, x) = i \cos kx, \quad e_3^1(k, x) = e^{-ikx} + e^{ikx}.$$

Let the loose ends of the segments be vertices v_1 and v_3 and the central vertex be v_2 . We find

$$\begin{aligned} \partial_\nu u_1(v_1) &= 0, \quad \partial_\nu u_2(v_3) = 0, \\ \partial_\nu e_1^1(v_1) &= 0, \quad \partial_\nu e_2^1(v_3) = 0, \\ u_1(v_2) &= 0, \quad u_2(v_2) = 0, \\ e_1^1(v_2) &= 0, \quad e_2^1(v_2) = 0. \end{aligned}$$

Hence the second term in F_s vanishes similarly to Theorem 18.3. From Theorem 18.1 we have

$$\begin{aligned} \operatorname{Im} \ddot{k} &= -|k \langle \dot{a}u, e^1 \rangle|^2 = -k^2 \left| \sum_{j=1}^2 \int_0^\ell \dot{a}_j u_j(x) \overline{e_j^1(k, x)} dx \right|^2 = \\ &= -k^2 \left| -\dot{a}_1 \frac{i}{\sqrt{\ell}} \int_0^\ell \cos^2 kx dx + \dot{a}_2 \frac{i}{\sqrt{\ell}} \int_0^\ell \cos^2 kx dx \right|^2 = \\ &= -k^2 \frac{1}{\ell} \left(\frac{\ell}{2} \right)^2 (\dot{a}_1 - \dot{a}_2)^2 = -\frac{k^2 \ell}{4} (\dot{a}_1 - \dot{a}_2)^2. \end{aligned}$$

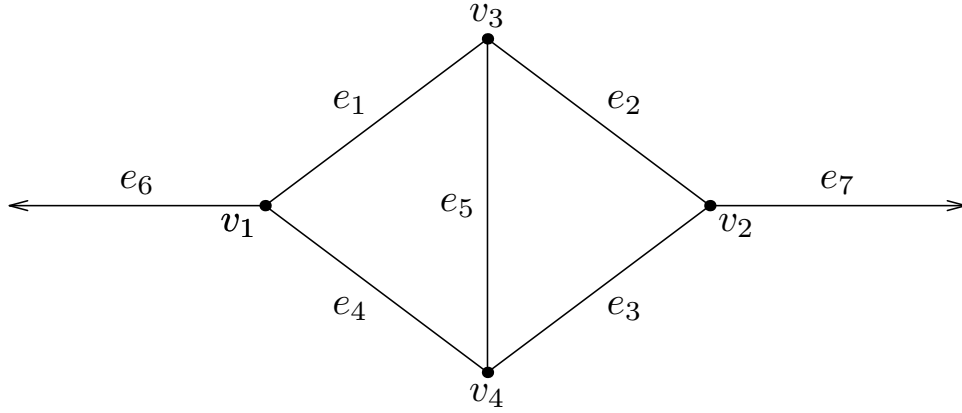


Fig. 18.2. Figure to Subsection 18.2 – graph Γ : five internal edges and two half-lines.

18.2 Example: five internal edges and two half-lines

Let us consider the graph in Figure 18.2 previously studied in [LZ16] as Example 2. For this graph, the second part of the expression for F_s will be nontrivial. We will study the Fermi's rule in more detail than in [LZ16].

The graph has five internal edges $e_j, j = 1, \dots, 5$ denoted in Figure 18.2 and two half-lines e_6 and e_7 . There are four vertices v_1, v_2, v_3 and v_4 . Let the lengths of the internal edges be $\ell_j(t)$ with $\ell_j(0) = 1$, for all $j = 1, \dots, 5$. We will represent these internal edges by intervals $(0, \ell_j(t))$ with $x = 0$ at v_1 for e_1 and e_4 , $x = 0$ at v_2 for e_2 and e_3 and $x = 0$ at v_3 for e_5 . The half-lines have $x = 0$ at the vertices v_1 or v_2 , respectively.

First, we will find the eigenvalues and eigenfunctions. Clearly, there are eigenvalues with $k = n\pi, n \in \mathbb{Z}$; the corresponding eigenfunctions are antisymmetric with respect to the vertical axis, have zeros in all the vertices and are supported at the edges e_1, e_2, e_3 and e_4 . For these eigenvalues, Theorem 18.3 applies. Therefore, we will focus on the non-trivial eigenvalues with the eigenfunctions symmetric with respect to the vertical axis. The eigenfunctions must be zero at e_6 and e_7 , hence there is a zero at v_1 and v_2 . We will choose the ansatz

$$\begin{aligned} u_1(k, x) &= C_1 \sin kx, & u_4(k, x) &= -C_1 \sin kx, & u_2(k, x) &= C_2 \sin kx, \\ u_3(k, x) &= -C_2 \sin kx, & u_6(k, x) &= u_7(k, x) = 0, \\ u_5(k, x) &= C_3 \sin k \left(x - \frac{1}{2} \right) + C_4 \cos k \left(x - \frac{1}{2} \right). \end{aligned}$$

From the coupling condition at v_3 we have $C_2 = C_1$ (or $\sin k = 0$ which corresponds to already mentioned eigenvalues $k = n\pi$). Furthermore, we have from the coupling conditions at v_3 and v_4

$$\begin{aligned} -C_3 \sin \frac{k}{2} + C_4 \cos \frac{k}{2} &= C_1 \sin k, \\ C_3 \sin \frac{k}{2} + C_4 \cos \frac{k}{2} &= -C_1 \sin k, \end{aligned}$$

$$-2kC_1 \cos k + C_3k \cos \frac{k}{2} + C_4k \sin \frac{k}{2} = 0.$$

Adding the first two equations we find $C_4 = 0$ (or $\cos \frac{k}{2} = 0$ which leads again to eigenvalues as multiples of π , now with eigenvalues supported also at e_5). Hence we obtain

$$C_3 = -C_1 \frac{\sin k}{\sin \frac{k}{2}}$$

and hence

$$\tan k + 2 \tan \frac{k}{2} = 0.$$

From the last equation we find one of the eigenvalues $k_0 = \arccos(-\frac{1}{3}) \doteq 1.9106$. From normalization we find

$$1 = \|u\|^2 = 4|C_1|^2 \int_0^1 \sin^2 kx \, dx + \left| \frac{\sin k}{\sin \frac{k}{2}} \right|^2 |C_1|^2 \int_0^1 \sin^2 k \left(x - \frac{1}{2} \right) dx,$$

from which we have $C_1 \doteq 0.6124$.

Now we turn to generalized eigenfunction $e^s(k, x)$, $s = 1, 2$. (Do not confuse it with the notation for the edges, the generalized eigenfunctions have the superscript.) For the components of the first eigenfunction, we choose the ansatz

$$\begin{aligned} e_6^1(k, x) &= e^{-ikx} + s_{16} e^{ikx}, & e_7^1(k, x) &= s_{17} e^{ikx}, \\ e_j^1(k, x) &= A_j \sin kx + B_j \cos kx, & j &= 1, \dots, 4, \\ e_5^1(k, x) &= A_5 \sin k \left(x - \frac{1}{2} \right) + B_5 \cos k \left(x - \frac{1}{2} \right). \end{aligned}$$

From the coupling conditions at v_1 and v_2 we have

$$\begin{aligned} B_4 &= B_1 = 1 + s_{16}, & A_1 + A_4 + i(s_{16} - 1) &= 0, \\ B_3 &= B_2 = s_{17}, & A_3 + A_2 + is_{17} &= 0, \end{aligned}$$

and hence

$$A_4 = -A_1 - i(B_1 - 2), \quad A_3 = -A_2 - iB_2. \quad (18.33)$$

From the coupling conditions at the vertices v_3 and v_4 we obtain

$$A_1 \sin k + B_1 \cos k = -A_5 \sin \frac{k}{2} + B_5 \cos \frac{k}{2} = A_2 \sin k + B_2 \cos k, \quad (18.34)$$

$$-(A_1 + A_2) \cos k + (B_1 + B_2) \sin k + A_5 \cos \frac{k}{2} + B_5 \sin \frac{k}{2} = 0, \quad (18.35)$$

$$A_4 \sin k + B_4 \cos k = A_3 \sin k + B_3 \cos k = A_5 \sin \frac{k}{2} + B_5 \cos \frac{k}{2},$$

$$-(A_3 + A_4) \cos k + (B_3 + B_4) \sin k - A_5 \cos \frac{k}{2} + B_5 \sin \frac{k}{2} = 0.$$

Substituting from equation (18.33) to the last two equations we have

$$\begin{aligned} -A_1 \sin k + B_1(\cos k - i \sin k) + 2i \sin k &= -A_2 \sin k + B_2(\cos k - i \sin k) = \\ &= A_5 \sin \frac{k}{2} + B_5 \cos \frac{k}{2}, \end{aligned} \quad (18.36)$$

$$\begin{aligned} (A_1 + A_2) \cos k + (B_1 + B_2)(\sin k + i \cos k) - A_5 \cos \frac{k}{2} + B_5 \sin \frac{k}{2} &= \\ &= 2i \cos k. \end{aligned} \quad (18.37)$$

Equations (18.34), (18.35), (18.36) and (18.37) can be written as

$$M \cdot (A_1 \ B_1 \ A_2 \ B_2 \ A_5 \ B_5)^T = (0 \ 0 \ 0 \ -2i \sin k \ 0 \ 2i \cos k)^T$$

with

$$M = \begin{pmatrix} \sin k & \cos k & -\sin k & -\cos k & 0 & 0 \\ \sin k & \cos k & 0 & 0 & \sin \frac{k}{2} & -\cos \frac{k}{2} \\ -\cos k & \sin k & -\cos k & \sin k & \cos \frac{k}{2} & \sin \frac{k}{2} \\ -\sin k & \cos k - i \sin k & \sin k & -\cos k + i \sin k & 0 & 0 \\ 0 & 0 & \sin k & -\cos k + i \sin k & \sin \frac{k}{2} & \cos \frac{k}{2} \\ \cos k & \sin k + i \cos k & \cos k & \sin k + i \cos k & -\cos \frac{k}{2} & \sin \frac{k}{2} \end{pmatrix}$$

The matrix M is in k_0 not regular. However, we can find the coefficients as limits of solutions of the above equation for k approaching to k_0 . We find

$$\begin{aligned} A_1 = A_4 = \frac{1}{2}i, \quad B_1 = B_4 = 1, \quad A_2 = A_3 = -\frac{\sqrt{2}}{3} + \frac{1}{6}i, \\ B_2 = B_3 = -\frac{1}{3} - \frac{\sqrt{8}}{3}i, \quad A_5 = 0, \quad B_5 = -\frac{\sqrt{3}}{3} + \frac{\sqrt{6}}{3}i. \end{aligned}$$

For the inner product we find for $t = 0$ at k_0

$$\begin{aligned} k \langle \dot{a}u, e^1 \rangle &= k(\dot{a}_1 - \dot{a}_4) \left[C_1 \bar{A}_1 \int_0^1 \sin^2 kx \, dx + C_1 \bar{B}_1 \int_0^1 \sin kx \cos kx \, dx \right] + \\ &+ k(\dot{a}_2 - \dot{a}_3) \left[C_1 \bar{A}_2 \int_0^1 \sin^2 kx \, dx + C_1 \bar{B}_2 \int_0^1 \sin kx \cos kx \, dx \right] \doteq \\ &\doteq (\dot{a}_1 - \dot{a}_4)(0.2722 - 0.3406i) + (\dot{a}_2 - \dot{a}_3)(-0.4119 + 0.1431i) \end{aligned}$$

The term with \dot{a}_5 vanishes, because u_5 is antisymmetric with respect to the horizontal axis and e_5^1 is symmetric with respect to the horizontal axis.

The values at the vertices are

$$\begin{aligned} u(v_1) = 0, \quad \partial_\nu u_1(v_1) = -kC_1, \quad \overline{e_1^1(v_1)} = \bar{B}_1, \quad \partial_\nu \overline{e_1^1(v_1)} = -\bar{A}_1, \\ u(v_3) = C_1 \sin k, \quad \partial_\nu u_1(v_3) = kC_1 \cos k, \\ \overline{e_1^1(v_3)} = \bar{A}_1 \sin k + \bar{B}_1 \cos k, \quad \partial_\nu \overline{e_1^1(v_3)} = \bar{A}_1 k \cos k - \bar{B}_1 k \sin k, \\ u(v_2) = 0, \quad \partial_\nu u_2(v_2) = -kC_1, \quad \overline{e_2^1(v_2)} = \bar{B}_2, \quad \partial_\nu \overline{e_2^1(v_2)} = -\bar{A}_2, \\ u(v_3) = C_1 \sin k, \quad \partial_\nu u_2(v_3) = kC_1 \cos k, \\ \overline{e_2^1(v_3)} = \bar{A}_2 \sin k + \bar{B}_2 \cos k, \quad \partial_\nu \overline{e_2^1(v_3)} = \bar{A}_2 k \cos k - \bar{B}_2 k \sin k. \end{aligned}$$

The eigenfunction u is antisymmetric with respect to the horizontal axis and the generalized eigenfunction e^1 is symmetric with respect to the horizontal axis. From this follows that the contribution of the second term in F_1 from the edges e_4 and e_3 differs from the contribution of the edges e_1 and e_2 only in the sign before \dot{a}_j . The contribution of the edges e_5 from these reasons vanishes. To summarize, we have after rearranging the terms

$$\begin{aligned} & \frac{1}{k} \sum_{v \in \Gamma} \sum_{e_j \ni v} \frac{1}{4} \dot{a}_j (3 \partial_\nu u_j(v) \overline{e_j^s(k, v)} - u(v) \partial_\nu \overline{e_j^s(k, v)}) = \\ & (\dot{a}_1 - \dot{a}_4) \frac{1}{2} C_1 (\bar{A}_1 \sin k \cos k - \bar{B}_1 \sin^2 k) + (\dot{a}_2 - \dot{a}_3) \frac{1}{2} C_1 (\bar{A}_2 \sin k \cos k - \bar{B}_2 \sin^2 k) \doteq \\ & \doteq (\dot{a}_1 - \dot{a}_4)(-0.2722 + 0.0481i) + (\dot{a}_2 - \dot{a}_3)(0.1361 - 0.2406i) \end{aligned}$$

and for F_1

$$F_1 \doteq (\dot{a}_1 - \dot{a}_4)(-0.2925i) + (\dot{a}_2 - \dot{a}_3)(0.2758 - 0.0975i).$$

Since u is symmetric with respect to the vertical axis and the problem for e^2 is symmetric to the problem for e^1 with respect to the vertical axis, one can easily find F_2 .

$$F_2 \doteq (\dot{a}_1 - \dot{a}_4)(0.2758 - 0.0975i) + (\dot{a}_2 - \dot{a}_3)(-0.2925i).$$

For the imaginary part of \ddot{k} at k_0 we find from Theorem 18.1

$$\text{Im } \ddot{k} = - [(\dot{a}_1 - \dot{a}_4)^2 + (\dot{a}_2 - \dot{a}_3)^2] 0.1711 - (\dot{a}_1 - \dot{a}_4)(\dot{a}_2 - \dot{a}_3) 0.1141.$$

19 Topological resonances and tails of the integrated distribution for the mean intensity

In this section we will review the results of [GSS13] on so-called *topological* resonances. These resonances, studied also in Section 17, arise from eigenvalues, which can be obtained for some coupling conditions when there is a cycle with rationally related edges. Before we formulate the main theorem of the section, we begin with a definition.

Definition 19.1 *Let us assume a graph Γ with N internal edges and M half-lines with standard coupling at all the vertices. Let the functional values at the internal edges be*

$$f_j(x) = a_{j+}e^{ikx} + a_{j-}e^{-ikx}, \quad j = 1, \dots, N$$

with $x = 0$ at the middle of the edge. The mean intensity of the graph $\alpha(k)$ is defined as

$$\alpha(k) = \frac{1}{N} \sum_{j=1}^N (|a_{j+}|^2 + |a_{j-}|^2).$$

When one solves (numerically) the scattering problem with the incoming wave of unit flux and with (real) wave number k , one can find the coefficients a_{j+} , a_{j-} on the internal edges and subsequently also the mean intensity. Then one defines distribution

$$P(\alpha) = \lim_{K \rightarrow \infty} \frac{1}{K} \int^K \delta(\alpha - \alpha(k)) dk$$

and its cumulative form

$$I(\alpha) = \int_{\alpha}^{\infty} P(\alpha') d\alpha'.$$

We state the main result of this section, found both numerically and theoretically in [GSS13].

Theorem 19.2 *Let us assume a graph consisting of one cycle of C edges and let there be at all the vertices of the cycle exactly one half-line attached (see Figure 19.1). Let there be standard coupling at all the vertices. Then*

$$P(\rho) \sim \rho^{-\mu_C-1}, \quad I(\alpha) \sim \alpha^{-\mu_C}, \quad \mu_C = \frac{C+1}{2}$$

Proof: Now we present a sketch of the proof of the theorem following [GSS13]. First, we find the relation between the vector of the amplitudes of the incoming waves on the half-lines and the amplitudes of the waves on the internal edges. We construct the oriented graph Γ_2 similarly to Section 12, the only difference is that now there are two oriented bonds added also instead of the half-lines. Part of the oriented graph Γ_2 is shown in Figure 19.2; there are bonds corresponding to two adjacent edges and one half-line shown.

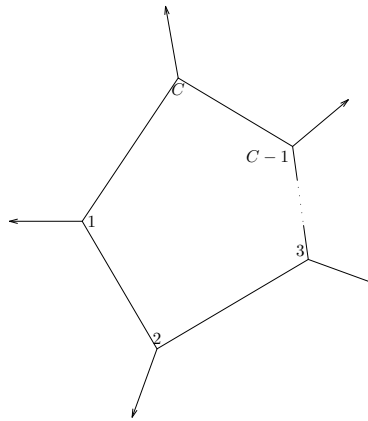


Fig. 19.1. Figure to Theorem 19.2 – graph with a cycle and attached half-lines.

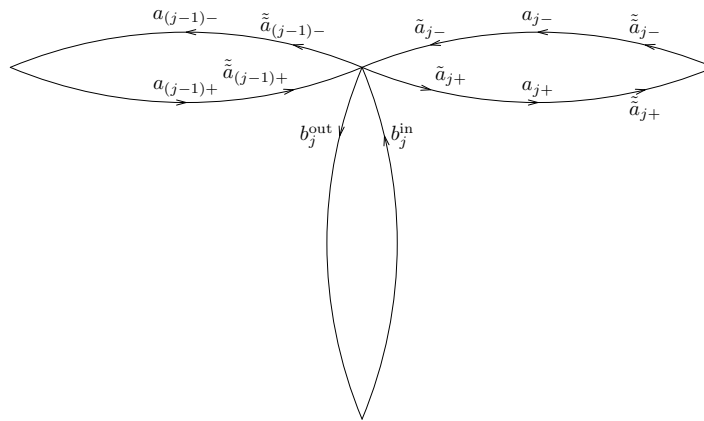


Fig. 19.2. Figure to Theorem 19.2 – part of the oriented graph.

The wavefunction on the j -th edge can be described by the following three possibilities.

$$\begin{aligned}
 f_j(x) &= a_{j+}e^{ikx} + a_{j-}e^{-ikx}, & x = 0 \text{ at the middle of the edge,} \\
 \tilde{f}_j(x) &= \tilde{a}_{j+}e^{ikx} + \tilde{a}_{j-}e^{-ikx}, & x = 0 \text{ at the middle vertex,} \\
 \tilde{\tilde{f}}_j(x) &= \tilde{\tilde{a}}_{j+}e^{ikx} + \tilde{\tilde{a}}_{j-}e^{-ikx}, & x = 0 \text{ at the right vertex.}
 \end{aligned}$$

From the relations

$$f_j(x - \ell_j(x)/2) = \tilde{f}_j(x), \quad f_j(x + \ell_j(x)/2) = \tilde{\tilde{f}}_j(x)$$

we have

$$\tilde{a}_{j+} = a_{j+} e^{-\frac{ik\ell_j}{2}}, \quad \tilde{a}_{j-} = a_{j-} e^{\frac{ik\ell_j}{2}}, \quad \tilde{a}_{j+} = a_{j+} e^{\frac{ik\ell_j}{2}}, \quad \tilde{a}_{j-} = a_{j-} e^{-\frac{ik\ell_j}{2}}. \quad (19.1)$$

From the definition of the vertex-scattering matrix (see Section 12) at the j -th vertex we obtain

$$\begin{pmatrix} \tilde{a}_{j+} \\ \tilde{a}_{(j-1)-} \\ b_j^{\text{out}} \end{pmatrix} = \sigma_j \begin{pmatrix} \tilde{a}_{j-} \\ \tilde{a}_{(j-1)+} \\ b_j^{\text{in}} \end{pmatrix}.$$

The vertex scattering matrix is $\sigma_j = \frac{2}{3}J_3 - I$. Using the previous equation and the relations (19.1) we obtain

$$\begin{aligned} e^{-\frac{ik\ell_j}{2}} a_{j+} &= -\frac{1}{3} e^{\frac{ik\ell_j}{2}} a_{j-} + \frac{2}{3} e^{\frac{ik\ell_{j-1}}{2}} a_{(j-1)+} + \frac{2}{3} b_j^{\text{in}} \\ e^{-\frac{ik\ell_{j-1}}{2}} a_{(j-1)-} &= \frac{2}{3} e^{\frac{ik\ell_j}{2}} a_{j-} - \frac{1}{3} e^{\frac{ik\ell_{j-1}}{2}} a_{(j-1)+} + \frac{2}{3} b_j^{\text{in}}, \end{aligned}$$

This can be rewritten as

$$\begin{pmatrix} I_C - \frac{2}{3} e^{ik\tilde{\ell}/2} P e^{ik\tilde{\ell}/2} & \frac{1}{3} e^{ik\tilde{\ell}} \\ \frac{1}{3} e^{ik\tilde{\ell}} & I_C - \frac{2}{3} e^{ik\tilde{\ell}/2} P^{-1} e^{ik\tilde{\ell}/2} \end{pmatrix} \mathbf{a} = \begin{pmatrix} \frac{2}{3} e^{ik\tilde{\ell}/2} P \mathbf{b}^{\text{in}} \\ \frac{2}{3} e^{ik\tilde{\ell}/2} \mathbf{b}^{\text{in}} \end{pmatrix},$$

where P is the permutation matrix of the cyclic permutation, I_C is $C \times C$ identity matrix, $\tilde{\ell} = \text{diag}(\ell_1, \ell_2, \dots, \ell_C)$ is $C \times C$ diagonal matrix, $\mathbf{a} = (a_{1-}, a_{2-}, \dots, a_{C-}, a_{1+}, a_{2+}, \dots, a_{C+})^T$ and $\mathbf{b}^{\text{in}} = (b_1^{\text{in}}, b_2^{\text{in}}, \dots, b_C^{\text{in}})^T$.

Hence we can find

$$\mathbf{a} = (I_{2C} - e^{ik\ell/2} \sigma_{CC} e^{ik\ell/2})^{-1} e^{ik\ell/2} \sigma_{CL} \mathbf{b}^{\text{in}},$$

where I_{2C} is $2C \times 2C$ identity matrix, $\ell = \begin{pmatrix} \tilde{\ell} & 0 \\ 0 & \tilde{\ell} \end{pmatrix}$ is $2C \times 2C$ diagonal matrix and

$$\sigma_{CL} = \frac{2}{3} \begin{pmatrix} P \\ I_C \end{pmatrix}, \quad \sigma_{CC} = \frac{1}{3} \begin{pmatrix} 2P & -I_C \\ -I_C & 2P^{-1} \end{pmatrix}.$$

The matrix σ_{CC} has eigenvalue 1 with eigenvector $(1, 1, \dots, 1, -1, -1, \dots, -1)^T$. The system has bound states if the matrix

$$\Sigma(k) = e^{ik\ell/2} \sigma_{CC} e^{ik\ell/2}$$

has eigenvalue 1, which can happen for $e^{ik\ell/2} = I_C$, e.g. when ℓ_j are integer multiples of ℓ_0 and $k = 4n\pi/\ell_0$. This cannot be satisfied for generic (rationally independent) lengths of the edges, but the point $e^{ik\ell/2} = I_C$ can be approached with arbitrary precision as k increases (see [BG00]).

Defining $\rho(k) := \frac{\mathbf{a}}{\mathbf{b}^{\text{in}}}$ we can write

$$P(\rho) = \langle \delta(\rho - \rho(k)) \rangle_k = \frac{1}{(2\pi)^C} \int \delta(\alpha - \alpha(\theta)) d^C \theta,$$

where we have replaced the matrix $k\ell$ by a diagonal matrix $\theta = \text{diag}(\theta_1, \dots, \theta_C, \theta_1, \dots, \theta_C)$. We focus on the contribution from the region close to $\theta = \mathbf{0}$. [GSS13] then claims that from the second order perturbation follows

$$\rho(\theta) \sim \frac{f^{(2)}(\hat{\theta})}{\bar{\theta}^2 + [g^{(2)}(\hat{\theta})]^2},$$

where $\bar{\theta} = \frac{1}{C} \sum_{j=1}^C \theta_j$, $\hat{\theta}_j = \theta_j - \bar{\theta}$ and the functions $f^{(2)}$ and $g^{(2)}$ should be described in an announced publication by the authors of [GSS13], which, unfortunately, has not been published yet. The above result implies that $P(\rho) \sim \rho^{\mu_C - 1}$ with $\mu_C = \frac{C+1}{2}$. The form of $I(\rho)$ follows from integration. Q.E.D.

From the numerical illustrations obtained in [GSS13] and the previous result, the authors come to the following conjecture.

Conjecture 19.3 *Let us assume a graph Γ with N internal and M external edges and standard coupling at all the vertices. Let there be at most one half-line attached at each vertex. We say that vertex v is on the boundary ∂H of the subgraph H if it is adjacent to at least one edge of H . Let L be the minimum of the size (cardinality) of ∂H over all connected subgraphs H that contain a cycle and that contain no lead. Let C be the number of edges in the shortest cycle. Let there be no loop (edge starting and ending at one vertex) and no vertices of degree 1.*

Then $I(\alpha) \sim \alpha^{-\mu}$ with

$$\mu = \begin{cases} \frac{L+2}{2} & \text{for } L \leq C - 1 \\ \frac{C+1}{2} & \text{for } L \geq C - 1 \end{cases}$$

The form of μ for $L \leq C - 1$ is consistent with predictions of random-matrix models for chaotic scattering.

The problem of topological resonances was also studied in [CdVT]. They divided the graphs into two sets: tree graphs with at most one vertex of degree 1 and all other graphs. For the former set, there are not eigenvalues with compactly supported eigenfunctions. They proved the following theorem which states that from this follows that the former set does not have resonances close to the real axis. This means (as stated in the introduction) that all the generalized eigenfunctions decay quickly.

Theorem 19.4 *Let us assume that the graph Γ is a tree with at most one vertex of degree 1. Let the length of its internal edges be ℓ_j , $j = 1, \dots, N$ and let $|L| = \sum_{j=1}^N \ell_j$. Then there exists a minimal finite number $h(\Gamma)$ so that for any choice of edge lengths for the set of resonances holds*

$$\text{Im } k^2 \leq -\frac{h(\Gamma)}{|L|}.$$

Acknowledgement: Support of the grant 15-14180Y of the Czech Science Foundation is acknowledged. The author thanks the referees for useful remarks.

A Appendix: Combinatorial and metric graphs

This appendix summarizes the basics of the graph theory. For more details we refer the reader e.g. to [Di06] or Appendix A of [BK13].

Definition A.1 Combinatorial graph G is a pair $G = (\mathcal{V}, \mathcal{E})$, where \mathcal{V} is the set of finitely or countably many points (vertices) and \mathcal{E} is the set of edges; each edge is identified with the pair $e = (v_i, v_j)$ of vertices $v_i, v_j \in \mathcal{V}$. Loops ($v_i = v_j$) and multiple edges are allowed.

Definition A.2 Metric graph Γ is a pair $\Gamma = (\mathcal{V}, \mathcal{E})$, where \mathcal{V} is the set of finitely or countably many points (vertices) and \mathcal{E} is the set of edges; each edge is identified with the pair $e = (v_i, v_j)$ of vertices $v_i, v_j \in \mathcal{V}$ and now length $\ell_k \in (0, \infty]$ is assigned to each edge. Again, loops and multiple edges are allowed.

With small abuse of notation we used \mathcal{E} for both the set of edges of a combinatorial graph and metric graph. The edges of a metric graph can be *finite* ($\ell_k < \infty$) or *(semi-)infinite* ($\ell_k = \infty$). The finite edges \mathcal{E}_f can be parametrized by intervals $x \in (0, \ell_k)$ with $x = 0$ corresponds to one end vertex and $x = \ell_k$ to another. The semi-infinite edges \mathcal{E}_i can be parametrized by intervals $x \in (0, \infty)$ with $x = 0$ corresponding to the vertex of the graph. The set $\Gamma \setminus \mathcal{E}_i$ is called compact part of a metric graph.

Definition A.3 Directed metric graph Γ_2 is a metric graph where to each edge (bond) orientation is assigned. One of the vertices of the bond b is called origin and denoted by $o(b)$ and the other terminus and denoted $t(b)$.

For both combinatorial and metric graphs, we define the following notions.

Definition A.4 The degree d_v of a vertex $v \in \mathcal{V}$ is the number of edges emanating from it. The graph is called *regular* if degree of all vertices is equal. The graph is called *complete* if each pair of vertices is connected by exactly one edge. Path is a non-empty subgraph $P = (\mathcal{V}_1, \mathcal{E}_1)$ of a graph G or Γ with $\mathcal{V}_1 = \{v_1, v_2, \dots, v_j\}$ and $\mathcal{E}_1 = \{(v_1, v_2), (v_2, v_3), (v_3, v_4), \dots, (v_{j-1}, v_j)\}$. If P is a path, then $C = P \cup \{(v_j, v_1)\}$ is called a cycle. The graph without cycles is a tree. The graph is *bipartite* if there exist two disjoint subsets of its vertices such that the edges of the graph do not connect vertices from same subset. Star graph is a graph with only one vertex in one of these subsets and other vertices in the other subset.

The following proposition on the bipartite graph is trivial.

Proposition A.5 The bipartite graph can be colored by only two colors such that no two vertices of the same color are connected by an edge.

Furthermore, we define *adjacency matrix*, for simplicity in the case with no loops and no multiple edges.

Definition A.6 The adjacency matrix A is $|\mathcal{V}| \times |\mathcal{V}|$ matrix (where $|\mathcal{V}|$ is the number of vertices of the graph) with entries $A_{ij} = 1$ if the vertex v_i is connected with the vertex v_j and $A_{ij} = 0$ otherwise. The degree matrix D is the diagonal $|\mathcal{V}| \times |\mathcal{V}|$ matrix with degrees of particular vertices on the diagonal. For a combinatorial graph we define a Laplacian matrix $L = D - A$.

B Appendix: L^p and Sobolev spaces

In this appendix we define L^p - and Sobolev spaces. For more details we refer the reader e.g. to [Ev98].

Let us define L^p -spaces and Sobolev spaces first in an open subset of \mathbb{R}^n and then for a graph.

Definition B.1 Let Ω denote open subset of \mathbb{R}^n and let $f : \Omega \rightarrow \mathbb{C}$ be a complex function of n variables on Ω . For a real number $1 \leq p < \infty$ we define the L^p norm of f as $\|f\|_p := (\int_{\Omega} |f(x)|^p dx)^{1/p}$ and for $p = \infty$ we define $\|f\|_{\infty} := \inf \{C \geq 0 : |f(x)| \leq C \text{ for almost every } x\}$. Function f belongs to $L^p(\Omega)$ iff $\|f\|_p < \infty$. Function f is locally integrable, i.e. belongs to $L^p(\Omega)_{\text{loc}}$, iff the above integral is finite for any compact subset $K \subset \Omega$.

In particular, for a metric graph and $p = 2$ we define in accordance with the previous definition square integrable functions on a graph.

Definition B.2 For a metric graph Γ with edges e_j of lengths $\ell_j \in (0, \infty]$ a function f with a components f_j on edges e_j belongs to $L^2(\Gamma)$ iff $\int_{e_j} |f_j(x)|^2 dx < \infty$ for all $j \in \{1, \dots, N+M\}$, where N is the number of finite edges and M the number of semi-infinite edges of the graph Γ .

Square integrable functions are important because of postulates of quantum mechanics. One of the postulates is that the wavefunction of a quantum particle is square integrable. The square of the wavefunction is interpreted as the probability density and thus square of the wavefunction should be normalizable.

To define the Sobolev space, we start by weakening the notion of partial derivative.

Definition B.3 The n -dimensional multiindex α is a n -tuple $\alpha = (\alpha_1, \alpha_2, \dots, \alpha_n)$ of non-negative integers. By the symbol D^{α} we denote $\partial_1^{\alpha_1} \partial_2^{\alpha_2} \dots \partial_n^{\alpha_n}$, where $\partial_j^{\alpha_j} \equiv \frac{\partial^{\alpha_j}}{\partial x_j^{\alpha_j}}$. By the symbol $|\alpha|$ we denote $|\alpha| = \alpha_1 + \alpha_2 + \dots + \alpha_n$.

Suppose that functions $f, g \in L^1_{\text{loc}}(\Omega)$ and α is a multiindex. We say that g is the α -th weak partial derivative of f (we write $D^{\alpha}f = g$) iff

$$\int_{\Omega} f D^{\alpha} \phi dx = (-1)^{|\alpha|} \int_{\Omega} g \phi dx$$

for all testfunctions $\phi \in C_c^{\infty}(\Omega)$, i.e. infinitely many times differentiable function with compact support in Ω .

Definition B.4 The Sobolev space $W^{k,p}(\Omega)$ consists of all locally integrable functions $f : \Omega \rightarrow \mathbb{R}$ such that for each multiindex α with $|\alpha| \leq k$, $D^{\alpha}f$ exists in the weak sense and belongs to $L^p(\Omega)$. The corresponding norm is $\|f\|_{k,p} = \left(\sum_{|\alpha| \leq k} \|D^{\alpha}f\|_p^p \right)^{1/p}$ for $1 \leq p < \infty$ and $\|f\|_{k,\infty} = \max_{|\alpha| \leq k} \|D^{\alpha}f\|_{\infty}$ for $p = \infty$.

Definition B.5 Let Γ be a metric graph with N internal and M external edges. By the symbol $W^{2,2}(\Gamma)$ we mean $W^{2,2}(\Gamma) = \oplus_{j=1}^{N+M} W^{2,2}(e_j)$, where e_j denotes j -th edge.

Let us note that the Sobolev space on the graph defined above also includes the functions which are not continuous at the vertices of the graph.

Sometimes one can find notation $H^k \equiv W^{k,2}$.

C Appendix: Self-adjoint extensions

In this section we recall basics of the theory of self-adjoint extensions; we give theorems without proofs. For a more detailed explanation we recommend e.g. the textbooks [BEH08, RS75b].

Definition C.1 Let L be operator from $D(L) \subset \mathcal{X}$ to \mathcal{Y} , where \mathcal{X} and \mathcal{Y} are Banach spaces. Then we call the set $\Gamma(L) := \{[x, Lx] : x \in D(L)\}$ the graph of the operator L . The operator L is closed if the set $\Gamma(L)$ is closed in the Banach space $\mathcal{X} \oplus \mathcal{Y}$.

Definition C.2 Let L be an operator in the Hilbert space \mathcal{H} with the scalar product (\cdot, \cdot) and let its domain $D(L)$ be dense in \mathcal{H} . By its adjoint we denote the operator L^* , which acts as $L^*y = y^*$, where $(y, Lx) = (y^*, x)$ for all $x \in D(L)$. The domain of L^* consists of all y for which the above relation holds. The operator is symmetric if $(y, Lx) = (Ly, x)$ and self-adjoint if $L = L^*$, i.e. the domains of L and L^* coincide. A self-adjoint operator L_1 is called self-adjoint extension of L if $D(L) \subset D(L_1)$ and $L = L_1$ on $D(L)$.

In the following text we omit the identity operator id in $L - \lambda \equiv L - \lambda \text{id}$.

Definition C.3 Let L be a linear operator in the Hilbert spaces \mathcal{H} . Then the regularity domain $\pi(L)$ is defined as those complex λ to which there exists positive constant c_λ such that $\|(L - \lambda)x\| \geq c_\lambda \|x\|$ holds for any $x \in D(L)$. The orthogonal complement of $\text{Ran}(L - \lambda)$ is called deficiency subspace of L with respect to λ . We denote its dimension by $\text{def}(L - \lambda)$.

Theorem C.4 It holds $\text{def}(L - \lambda) = \dim \text{Ker}(L^* - \bar{\lambda})$. The map $\lambda \mapsto \text{def}(L - \lambda)$ is constant on any connected components of the regularity domain $\pi(L)$.

Let us now consider a closed symmetric operator A in the Hilbert space \mathcal{H} and let us describe properties of its self-adjoint extensions.

Proposition C.5 For a closed symmetric operator A in the Hilbert space \mathcal{H} we have $\pi(A) \supset \mathbb{C} \setminus \mathbb{R}$, so it has at most two connected components.

Inspired by the previous proposition we define deficiency indices of the operator A .

Definition C.6 For a closed symmetric operator A we define deficiency indices $n_\pm(A) := \text{def}(A \mp i) = \dim \text{Ker}(A^* \pm i)$. We usually write the deficiency indices as the ordered pair $(n_+(A), n_-(A))$.

Proposition C.7 A symmetric operator A is self-adjoint iff it is closed and $n_\pm(A) = 0$.

Theorem C.8 (the first von-Neumann formula)

Let A be a closed symmetric operator. Then there is a unique decomposition $x = x_0 + x_+ + x_-$ of any $x \in D(A^*)$, where $x_0 \in D(A)$, $x_\pm \in \text{Ker}(A^* \pm i)$, and it holds

$$A^*x = Ax_0 - i(x_+ - x_-).$$

Definition C.9 A symmetric operator is maximal if it has no proper symmetric extensions, i.e. if from the relation $A \subset A'$ (for a symmetric operator A') follows that $A = A'$.

Theorem C.10 *A closed symmetric operator A has a non-trivial closed symmetric extension iff both $n_{\pm}(A) \neq 0$. The operator A has a self-adjoint extension iff $n_{+}(A) = n_{-}(A) \neq 0$. Let $n_{+}(A) = n_{-}(A) =: d$. If $d < \infty$ then any maximal extension of A is self-adjoint. If $d = \infty$ then there are no self-adjoint extensions.*

References

- [AC71] AGUILAR, J. AND COMBES, J.-M. A class of analytic perturbations for one-body Schrödinger operators. *Commun. Math. Phys.*, 1971. vol. 22, pp. 269–279.
- [ASW06a] AIZENMAN, M., SIMS, R., AND WARZEL, S. Absolutely continuous spectra of quantum tree graphs with weak disorder. *Commun. Math. Phys.*, 2006. vol. 264, pp. 371–389.
- [ASW06b] AIZENMAN, M., SIMS, R., AND WARZEL, S. Stability of the absolutely continuous spectrum of random Schrödinger operators on tree graphs. *Probab. Theory Related Fields*, 2006. vol. 136, pp. 363–394.
- [Ban14] BAND, R. The nodal count $\{0, 1, 2, 3, \dots\}$ implies the graph is a tree. *Phil. Trans. R. Soc. A*, 2007. vol. 372, pp. 20120504.
- [BBK01] BERKOLAIKO, G., BOGOMOLNY, E.B., AND KEATING J.P. Star graphs and Šeba billiards. *J. Phys. A: Math. Gen.*, 2001. vol. 34, pp. 335–350.
- [BC63] BELLMAN, R. AND COOK, K. L. *Differential-difference equations*. Academic Press, Inc., 1963, New York, 455 pp. ISBN 012410973X.
- [BC71] BALSLEV, E. AND COMBES, J.-M. Spectral properties of many body Schrödinger operators with dilatation-analytic interactions. *Commun. Math. Phys.*, 1971. vol. 22, pp. 280–294.
- [vBe01] V. BELOW, J. Can one hear the shape of a network? In *Partial differential equations on multistructures (Luminy, 1999)*, 2001. vol. 219 of *Lecture Notes in Pure and Appl. Math.*, pp. 19–36, Dekker, New York.
- [BEH08] BLANK, J., EXNER, P., AND HAVLÍČEK, M. *Hilbert-Space Operators in Quantum Physics*. Dordrecht, Springer, second (revised and extended) ed., 2008, 681 pp. ISBN 9781402088698.
- [BEG03] BRÜNING, J., EXNER, P., AND GEYLER, V.A. Large gaps in point-coupled periodic systems of manifolds. *J. Phys. A: Math. Gen.*, 2003. vol. 36, pp. 4890.
- [Ber13] BERKOLAIKO, G. Nodal count of graph eigenfunctions via magnetic perturbation. *Anal. PDE*, 2013. vol. 6, pp. 1213–1233.
- [BG00] BARRA, F. AND GASPARD P. On the level spacing distribution in quantum graphs *J. Stat. Phys.*, 2000. vol. 101, pp. 283–319.
- [BG03] BRÜNING, J. AND GEYLER, V. Scattering on compact manifolds with infinitely thin horns. *J. Math. Phys.*, 2003. vol. 44, pp. 371–405.
- [BHJ12] BAND, R., HARRISON J.M., AND JOYNER, C. H. Finite pseudo orbit expansions for spectral quantities of quantum graphs. *J. Phys. A: Math. Theor.*, 2012. vol. 45, pp. 325204.
- [BG95] BERENSTEIN, C. A. AND GAY, R. *Complex analysis and special topic in harmonic analysis*. Springer, 1995, New York, 482 pp. ISBN 0387944117.
- [BK13] BERKOLAIKO, G. AND KUCHMENT, P. *Introduction to Quantum Graphs*. Mathematical Surveys and Monographs 186. AMS, 2013, 270 pp. ISBN 9780821892114.
- [BPB09] BAND, R., PARZANCHEVSKI, O., AND BEN-SHACH G. The isospectral fruits of representation theory: Quantum graphs and drums. *J. Phys. A: Math. Theor.*, 2009. vol. 42, pp. 175202.
- [BW14] BERKOLAIKO, G. AND WEYAND, T. Stability of eigenvalues of quantum graphs with respect to magnetic perturbation and the nodal count of the eigenfunctions. *Phil. Trans. Roy. Soc. A.*, 2014. vol. 372, pp. 1471–2962.
- [CdVT] COLIN DE VERDIERE, Y. AND FRANCOISE TRUC, F. Topological resonances on quantum graphs. Preprint; <https://arxiv.org/abs/1604.01732>.
- [Chr08] CHRISTIANSEN, T.J. Resonances and balls in obstacle scattering with Neumann boundary conditions. *Inverse Probl. Imaging*, 2008. vol. 2, pp. 335–340.

- [DEL10] DAVIES, E. B., EXNER, P., AND LIPOVSKÝ, J. Non-Weyl asymptotics for quantum graphs with general coupling conditions. *J. Phys. A: Math. Theor.*, 2010. vol. 43, p. 474013.
- [DH12] DATCHEV, K., HEZARI, H. Resonant uniqueness of radial semiclassical Schrödinger operators *Appl Math Res Express*, 2012. vol. 2012, pp. 105–113.
- [Di06] DIESTEL, R. *Graph theory; 3rd ed.*. Graduate Texts in Mathematics, Springer, 2006, 411 pp.
- [DP11] DAVIES, E. B. AND PUSHNITSKI, A. Non-Weyl resonance asymptotics for quantum graphs. *Analysis and PDE*, 2011. vol. 4, no. 5, pp. 729–756.
- [DZ] DYATLOV, S. AND ZWORSKI, M. *Mathematical theory of scattering resonances*. Book in preparation; <http://math.mit.edu/~dyatlov/res/res.pdf>.
- [EL07] EXNER, P. AND LIPOVSKÝ, J. Equivalence of resolvent and scattering resonances on quantum graphs. In *Adventures in Mathematical Physics (Proceedings, Cergy-Pontoise 2006)*, vol. 447. Providence, R.I., 2007 pp. 73–81.
- [EL10] EXNER, P. AND LIPOVSKÝ, J. Resonances from perturbations of quantum graphs with rationally related edges. *J. Phys. A: Math. Theor.*, 2010. vol. 43, p. 1053.
- [EL11] EXNER, P. AND LIPOVSKÝ, J. Non-Weyl resonance asymptotics for quantum graphs in a magnetic field. *Phys. Lett. A*, 2011. vol. 375, pp. 805–807.
- [EL13] EXNER, P. AND LIPOVSKÝ, J. Resonances on hedgehog manifolds. *Acta Polytechnica*, 2013. vol. 53, pp. 416–426.
- [EL] EXNER, P. AND LIPOVSKÝ, J. Pseudo-orbit approach to trajectories of resonances in quantum graphs with general vertex coupling: Fermi rule and high-energy asymptotics. *Preprint*; <https://arxiv.org/abs/1608.03978>.
- [EM15] EXNER, P. AND MANKO, S. Spectra of magnetic chain graphs: coupling constant perturbations. *J. Phys. A: Math. Theor.*, 2015. vol. 48, pp. 125302.
- [EP05] EXNER, P. AND POST, O. Convergence of spectra of graph-like thin manifolds. *J. Geometry Phys.*, 2005. vol. 54, pp. 77–115.
- [EP07] EXNER, P. AND POST, O. Convergence of resonances on thin branched quantum wave guides. *J. Math. Phys.*, 2007. vol. 48, pp. 092104.
- [EP09] EXNER, P. AND POST, O. Approximation of quantum graph vertex couplings by scaled Schrödinger operators on thin branched manifolds. *J. Phys. A: Math. Theor.*, 2009. vol. 42, pp. 415305.
- [EP13] EXNER, P. AND POST, O. A general approximation of quantum graph vertex couplings by scaled Schrödinger operators on thin branched manifolds. *Comm. Math. Phys.*, 2013. vol. 322, pp. 207–227.
- [EŠ89] EXNER, P. AND ŠEBA, P. Bound states in curved quantum waveguides. *J. Math. Phys.*, 1989. vol. 30, pp. 2574–2580.
- [EŠ94] EXNER, P. AND ŠEREŠOVÁ, E. Appendix resonances on a simple graph. *J. Phys. A*, 1994. vol. 27, pp. 8269–8278.
- [EŠ97] EXNER, P. AND ŠEBA, P. Resonance statistics in a microwave cavity with a thin antenna. *Phys. Lett. A*, 1997. vol. 228, pp. 146–150.
- [ETV01] EXNER, P., TATER, M., AND VANĚK D. A single-mode quantum transport in serial-structure geometric scatterers. *J. Math. Phys.*, 2001. vol. 42, pp. 4050–4078.
- [Exn97] EXNER, P. Magneto-resonances on a lasso graph. *Found. Phys.*, 1997. vol. 27, pp. 171–190.
- [Exn07] EXNER, P. Leaky quantum graphs: a review. In *Analysis on Graphs and Applications*, 2007. vol. 77 of Proceedings of Symposia in Pure Mathematics, pp. 523–564.

- [Exn13] EXNER, P. Solvable models of resonances and decays in Proceedings of the conference *Mathematical Physics, Spectral Theory and Stochastic Analysis* (Goslar 2011; M.Demuth, W. Kirsch, eds.), Birkhäuser, Basel 2013; pp. 165–227.
- [Ev98] EVANS, L. C. *Partial differential equations*. Volume 19 of Graduate studies in mathematics. American Mathematical Society, 1998, 662 pp. ISBN 0821849743
- [FL90] FERNÁNDEZ, C. AND LAVINE, R. Lower bounds for resonance widths in potential and obstacle scattering. *Comm. Math. Phys.*, 1990. vol. 128, pp. 263–284.
- [FT00] FÜLÖP, T. AND TSUTSUI, I. A free particle on a circle with point interaction. *Phys. Lett. A*, 2000. vol. 264, pp. 366–374.
- [GG91] GORBACHUK, V.I. AND GORBACHUK, M.L. *Boundary value problems for operator differential equations* Kluwer, Dordrecht, 1991, 347 p. ISBN 978–94–010–5651–9
- [GG08] GOLDMAN N. AND GASPARD, P. Quantum graphs and the integer quantum Hall effect. *Phys. Rev. B*, 2008. vol. 77, p. 024302.
- [GS01] GUTKIN B. AND SMILANSKY U. Can one hear the shape of a graph? *J. Phys. A: Math. Gen.*, 2001. vol. 34, pp. 6061–6068.
- [GS06] GNUTZMAN S. AND SMILANSKY U. Quantum graphs: Applications to quantum chaos and universal spectral statistics. *Adv. Phys.*, 2006. vol. 55, pp. 527–625.
- [GSS13] GNUTZMANN, S, SCHANZ, H., AND SMILANSKY, U. Topological Resonances in Scattering on Networks (Graphs). *Phys. Rev. Lett.*, 2013. vol. 110, pp. 094101.
- [GSW04] GNUTZMANN, S, SMILANSKY, U., AND WEBER, J. Nodal counting on quantum graphs. *Waves in Random Media*, 2004. vol. 14, pp. S61–S73.
- [Har00] HARMER, M. Hermitian symplectic geometry and extension theory. *J. Phys. A: Math. Gen.*, 2000. vol. 33, pp. 9193–9203.
- [HBP⁺04] HUL, O., BAUCH, S., PAKOŃSKI, P., SAVYTSKYI, N., ZYCZKOWSKI, K., AND SIRKO, L. Experimental simulation of quantum graphs by microwave networks. *Phys Rev E Stat Nonlin Soft Matter Phys.*, 2004. vol. 69, p. 056205.
- [HLB⁺12] HUL, O., ŁAWNICZAK, M., BAUCH, S., SAWICKI, A., KUŚ, M., AND SIRKO, L. Are scattering properties of graphs uniquely connected to their shapes? *Phys. Rev. Lett.*, 2012. vol. 109, pp. 040402.
- [HŠS09] HUL, O., ŠEBA, P., AND SIRKO, L. Investigation of parameter-dependent properties of quantum graphs with and without time-reversal symmetry. *Phys. Scr.*, 2009. vol. T135, pp. 014048.
- [HTB⁺05] HUL, O., TYMOSHCHUK, O., BAUCH, S., KOCH, P. M., AND SIRKO, L. Experimental investigation of Wigner’s reaction matrix for irregular graphs with absorption. *J. Phys. A: Math. Gen.*, 2005. vol. 38, pp. 10489–10496.
- [Ivr80] IVRII, V. J. The second term of the spectral asymptotics for a Laplace–Beltrami operator on manifolds with boundary. *Funktsional. Anal. i Prilozhen*, 1980. vol. 14, no. 3, pp. 25–34.
- [Jin14] JIN, L. Scattering resonances of convex obstacles for general boundary conditions. *Comm. Math. Phys.*, 2014. vol. 335, pp. 759–807.
- [Kis97] KISELEV A. Some examples in one-dimensional ‘geometric’ scattering on manifolds. *J. Math. Anal. Appl.*, 1997. vol. 212, pp. 263–280.
- [KS97] KOTTOS, T. AND SMILANSKY, U. Quantum chaos on graphs. *Phys. Rev. Lett.*, 1997. vol. 79, pp. 4794–4797.
- [KS99a] KOTTOS, T. AND SMILANSKY, U. Periodic orbit theory and spectral statistics for quantum graphs. *Ann. Phys.*, 1999. vol. 274, pp. 76–124.
- [KS99b] KOSTRYKIN, V. AND SCHRADER, R. Kirchhoff’s rule for quantum wires. *J. Phys. A: Math. Gen.*, 1999. vol. 32, no. 4, pp. 595–630.

- [KS00] KOSTRYKIN, V. AND SCHRADER, R. Kirchhoff's rule for quantum wires. II: The inverse problem with possible applications to quantum computers. *Fortschritte der Physik*, 2000. vol. 48, pp. 703–716.
- [Kuc04] KUCHMENT, P. Quantum graphs I. Some basic structures. *Waves in Random Media*, 2004. vol. 14, pp. S107–S128.
- [Kuc05] KUCHMENT, P. Quantum graphs II. Some spectral properties of quantum and combinatorial graphs, 38 (2005), 4887–4900. *J. Phys. A: Math. Gen.*, 2005. vol. 38, pp. 4887–4900.
- [Kuc08] KUCHMENT, P. Quantum graphs: an introduction and a brief survey. In *Analysis on Graphs and its Applications*, Proc. Symp. Pure. Math. AMS, 2008 pp. 291–314.
- [Kur11] KURASOV, P. Inverse problems for quantum graphs: recent developments and perspectives. *Acta Phys. Pol. A*, 2011. vol. 120, pp. A-132–A-141.
- [Lan31] LANGER, R. On the zeros of exponential sums and integrals. *Bull. Amer. Math. Soc.*, 1931. vol. 37, pp. 213–239.
- [LBH⁺11] ŁAWNICZAK, M., BORKOWSKA, A., HUL, O., BAUCH, S., AND SIRKO, L. Experimental determination of the autocorrelation function of level velocities of microwave networks simulating quantum graphs. *Acta Phys. Pol. A*, 2011. vol. 120, pp. A185–A190.
- [LBH⁺12] ŁAWNICZAK, M., BAUCH, S., HUL, O., AND SIRKO, L. Experimental investigation of microwave networks simulating quantum chaotic systems: the role of direct processes. *Phys. Scr.*, 2012. vol. T147, pp. 014018.
- [LBS⁺13] ŁAWNICZAK, M., BAUCH, S., SAWICKI, A., KUŚ, M., AND SIRKO, L. Isoscattering microwave networks - The role of the boundary conditions. *Acta Phys. Pol. A*, 2013. vol. 124, pp. 1078–1081.
- [Lip15] LIPOVSKÝ, J. Pseudo-orbit expansion for the resonance condition on quantum graphs and the resonance asymptotics. *Acta Physica Polonica A*, 2015. vol. 128, no. 6, pp. 968–973.
- [Lip16] LIPOVSKÝ, J. On the effective size of a non-Weyl graph *J. Phys. A: Math. Theor.*, 2016. vol. 49, p. 375202.
- [LSB⁺14] ŁAWNICZAK, M., SAWICKI, A., BAUCH, S., KUŚ, M., AND SIRKO, L. Resonances and poles in isoscattering microwave networks and graphs. *Phys. Rev. E*, 2014. vol. 89, pp. 032911.
- [LV12] LAKSHITANOV, E. AND VAINBERG, B. A priori estimates for high frequency scattering by obstacles of arbitrary shape. *Comm. Part. Differ. Equat.*, 2012. vol. 37, pp. 1789–1804.
- [LZ16] LEE, M. AND ZWORSKI, M. A Fermi golden rule for quantum graphs. *J. Math. Phys.*, 2016. vol. 57, p. 092101.
- [Mel84] MELROSE, R.B. Polynomial bounds on the distribution of poles in scattering by an obstacle. *Journées “Équations aux Dérivées partielles”*, 1984. pp. 1–8.
- [Mus16] MUSSER, S. Weyl's law on Riemannian manifolds. Available at <http://math.uchicago.edu/~may/REU2016/REUPapers/Musser.pdf>.
- [OB12] OREN, I. AND BAND, R. Isospectral graphs with identical nodal counts. *J. Phys. A: Math. Theor.*, 2012. vol. 45, pp. 135203.
- [Pan06] PANKRASHKIN, K. Spectra of Schrödinger operators on equilateral quantum graphs. *Lett Math Phys.*, 2006. vol. 77, pp. 139–154.
- [Pau36] PAULING, L. The diamagnetic anisotropy of aromatic molecules. *J. Chem. Phys.*, 1936. vol. 4, pp. 673–677.
- [Pos12] POST., O. *Spectral analysis on graph-like spaces*. Lecture Notes in Mathematics, vol. 2039, Springer, Heidelberg, 2012., . ISBN 978–3–642–23839–0.
- [PS25] PÓLYA, G AND SZEGÖ, G. *Aufgaben und Lehrsätze aus der Analysis* Berlin, 1925. vol. 2, p. 49.

- [RS53] RUEDENBERG, K. AND SCHERR, C. Free-electron network model for conjugated systems, I. Theory. *J. Chem. Phys.*, 1953. vol. 21, pp. 1565–1581.
- [RS75a] REED, M. AND SIMON, B. *Methods of Modern Mathematical Physics, Vol. I: Functional Analysis*. Academic Press, 1972, 400 pp. ISBN 0125850506.
- [RS75b] REED, M. AND SIMON, B. *Methods of Modern Mathematical Physics, Vol. II: Fourier Analysis, Self-Adjointness*. Academic Press, 1975, 361 pp. ISBN 0125850026.
- [RS78] REED, M. AND SIMON, B. *Methods of Modern Mathematical Physics, Vol. IV: Analysis of operators*. Academic Press, 1978, 396 pp. ISBN 0125850042.
- [RS79] REED, M. AND SIMON, B. *Methods of Modern Mathematical Physics, Vol. III: Scattering theory*. Academic Press, 1979, 463 pp. ISBN 0125850034.
- [SAGE16] THE SAGE DEVELOPERS. *Sage Mathematics Software (Version 6.10)*, 2016. <http://www.sagemath.org>.
- [Sak94] SAKURAI, J. J. *Modern quantum mechanics*. Rev. ed., Addison-Wesley Publishing Company, 1994, 500 pp. ISBN 0201539292.
- [Šeb90] ŠEBA, P., Wave chaos in singular quantum billiard. *Phys. Rev. Lett.*, 1990. vol. 64, pp. 1855.
- [Si79] SIMON, B. The definition of molecular resonance curves by the method of exterior complex scaling. *Phys. Lett. A*, 1979. vol. 71, pp. 211-214.
- [SMC16] THE SAGE DEVELOPERS. *SageMath Cloud*, 2016. <https://cloud.sagemath.com>.
- [Wey11] WEYL, H. Über die asymptotische Verteilung der Eigenwerte. *Nachrichten von der Gesellschaft der Wissenschaften zu Göttingen, Mathematisch-Physikalische Klasse*, 1911. vol. 2, pp. 110–117.
- [Zwo99] ZWORSKI, M. Resonances in physics and geometry. *Notices of the AMS*, 1999. vol. 46, pp. 319–328.



Jiří Lipovský received his bachelor degree in general physics in 2006, his master degree in theoretical physics in 2008 and his PhD degree in theoretical physics in 2011, all from Charles University in Prague, Faculty of Mathematics and Physics. He was employed by the Nuclear Physics Institute of The Czech Academy of Sciences during his PhD studies. After a one-year postdoctoral stay in the group of prof. Pedro Freitas at the University of Lisbon, Portugal he returned to the Czech Republic and became an assistant professor at the University of Hradec Králové, Faculty of Science. He is interested in mathematical physics, mainly in the spectral and resonance properties of quantum graphs and damped wave equation.